KNEE JOINT LOADING MAGNITUDE, DISTRIBUTION,

AND ASYMMETRY WITH VEST-BORNE LOADS

By

Blake W. Jones

July, 2022

Director of Thesis: Paul DeVita, PhD

Major Department: Kinesiology

Abstract

INTRODUCTION: Chronic exposure to high tibiofemoral joint (TFJ) loads can be detrimental to knee joint health and lead to the onset of osteoarthritis (OA). Soldiers who carry heavy loads have greater risk for onset of OA. Load carriage increases TFJ contact forces, but it is unclear how the whole knee joint environment responds to incremental load carriage, relative to bodyweight. Furthermore, kinetic asymmetries between the dominant and nondominant limb are present during gait, but no studies have examined asymmetries in TFJ loading magnitude or distribution. We hypothesized vest-borne loads relative to bodyweight would cause an increase in TFJ contact forces and impulses in healthy young adults during gait, but the increase at the heavier condition would be attenuated by gait adaptations. We also hypothesized that TFJ contact forces and impulses would be greater in the dominant limb as compared to the non-dominant limb as vest-borne loads are added. **PURPOSE:** The purposes of this study were 1: to compare TFJ loads and walking patterns when walking on an instrumented treadmill while unloaded vs. loaded with a weighted vest at 15% and 30% bodyweight and 2: to compare the dominant and nondominant limbs' TFJ contact forces and impulses in correspondence with increasing load carriage.

METHODS: Young healthy adults (*n* = 24; 18-30 yrs.; 12 Females; 3 left legged; BMI 18 - 24.9) walked for five minutes per conditions of no load, 15% bodyweight load, and 30% bodyweight load on an instrumented treadmill while kinematic and ground reaction force data were recorded. Total, medial, and lateral first peak TFJ contact forces and impulses were calculated via an inverse-dynamics driven musculoskeletal model. One-way repeated measures ANOVAs ($\alpha = 0.05$) were used to investigate the loading conditions effect on the dependent variables. Orthogonal polynomial trend analysis was used to test for the present of quadratic trends ($\alpha = 0.05$) as evidence of disproportionate change in the dependent variable with increasing load carriage. 2 x 3 repeated measures ANOVAs ($\alpha = 0.05$) were used to test for interactions between limb dominance and load carriage. **RESULTS:** The 30% loading condition drove a disproportional increase in total and lateral TFJ impulses, whereas medial first peak TFJ contact forces and impulses responded in a linear fashion. There were no interactions between leg dominance and load carriage for TFJ contact forces or impulse. However, main effects revealed that the nondominant limb exhibited 6% greater peak medial TFJ contact forces and 9% greater medial impulses, while the dominant limb exhibited 21% greater peak lateral TFJ contact forces and 29% greater lateral impulses. **DISCUSSION:** These findings suggest that peak total TFJ impulses increased disproportionally at the 30% condition due to kinematic adaptations, such as a large decrease in leg stiffness. The medial knee compartment is not sensitive to increasing load carriage from 15% to 30% bodyweight, but the lateral compartment is sensitive. Lastly, there are variations in the distribution of knee joint contact forces when comparing the dominant and nondominant limb, with the lateral compartment being prominently different.

KNEE JOINT LOADING MAGNITUDE, DISTRIBUTION, AND ASYMMETRY WITH VEST-BORNE LOADS

Thesis

Presented to the Faculty of the Department of Kinesiology

East Carolina University

In Partial Fulfillment of the Requirements for

the Masters of Science in Kinesiology:

Biomechanics and Motor Control Concentration

By

Blake W. Jones

KNEE JOINT LOADING MAGNITUDE, DISTRIBUTION,

AND ASYMMETRY WITH VEST-BORNE LOADS

By

Blake W. Jones

APPROVED BY:

Director of Thesis _____

Paul DeVita, PhD

Committee Member _____

Ryan D. Wedge, PT, PhD

Committee Member _____

Nicholas Murray, PhD

Chair of the Department of Kinesiology _____

Joonkoo Yun, PhD

Dean of the Graduate School _____

Paul J. Gemperline, PhD

Table of Contents

List of Tables

List of Figures

List of Acronyms/Abbreviations

TFJ – Tibiofemoral Joint = Knee Joint

tTFJ Contact Force – Total Tibiofemoral Joint Contact Force

mTFJ Contact Force – Medial Tibiofemoral Joint Contact Force

tTFJ Contact Force – Lateral Tibiofemoral Joint Contact Force

Ham – Hamstrings

Quad – Quadriceps

Gastroc - Gastrocnemius

GRF – Ground Reaction Force

vGRF – Vertical Ground Reaction Force

mlGRF – Medial/Lateral Ground Reaction Force

mGRF – Medial Ground Reaction Force

apGRF – Anterior/Posterior Ground Reaction Force

bGRF – Breaking Ground Reaction Force = Posterior Ground Reaction Force

HEM – Internal Hip Extension Moment

KEM – Internal Knee Extension Moment

ADM – Internal Ankle Dorsiflexion Moment

HAM – Internal Hip Abduction Moment

HAM – Internal Knee Abduction Moment

KEAI – Internal Knee Extension Angular Impulse

KAAI – Internal Knee Abduction Angular Impulse

D – Dominant Limb

ND – NonDominant Limb

PCA – Physiological Cross-Sectional Area

Musculoskeletal model Equation Acronyms

- TS – Triceps Surae
- G – Gastrocnemius Muscle Force
- Q – Quadriceps Muscle Force
- H – Hamstrings Muscle Force
- TS PCA – Triceps Surae Physiological Cross Section Area
- GM PCA – Gluteus Maximus Physiological Cross Section Area

- Ham PCA – Hamstrings Physiological Cross Section Area
- Hd – Hamstrings Moment Arm
- GMd – Gluteus Maximus Moment Arm
- Qd – Quadriceps Moment Arm
- AT – Plantar Flexor Moment
- HT – Hip Extension Moment
- KT – Knee Extension Moment
- Ky – Horizontal Joint Reaction Force
- Kz – Vertical Joint Reaction Force
- KC – Tibiofemoral Compression Force
- KS – Anterior/Posterior Tibiofemoral Shear Force
- Lss – Lateral Support Structure

Chapter 1: Introduction

Joint loading, or force on the cartilage and bone of a weight bearing joint, is a major area of investigation in biomechanics due to an interest in maintaining joint health. A large portion of the literature examines knee joint loads, due to its relationship with osteoarthritis, as mechanical compressive forces alone can lead to cartilage tissue damage and chondrocyte death.[1] At the knee, the quadriceps and gastrocnemius muscle forces are the primary contributors to knee joint compressive forces.[2] Normal knee joint loads, 2-3 bodyweights (BW) during walking,[3,4] are necessary for joint health,[1,5–7] but chronic knee joint overloading can be detrimental to joint health and is a risk factor for the onset and progression of osteoarthritis.[1,8]

Due to the invasiveness of measuring in-vivo knee joint loads, no studies have directly examined how chronic knee joint loads impact articular cartilage integrity. However, studies in rabbits and bovines reveal that chronic joint overloading causes cartilage destruction.[9–11] Roemhildt et al. (2010)[11] found that chronic tibiofemoral compressive forces of 22% and 44% bodyweight on rabbit hind limbs led to surface lesions in the cartilage, increase in permeability, decrease in proteoglycan content, and a decrease in chondrocytes as compared to the 0% load group. In humans, lower extremity joints are overloaded when there is excessive weight.[12–18] Chronic excessive weight occurs in soldiers who carry heavy loads.

Military infantry are often required to carry loads upwards of 50 kg.[19] Noncombat injuries have increased over the past two decades with the primary musculoskeletal injuries coming from load carriage,[19,20] with 50% of these injuries occurring at the knee.[21] It has been hypothesized that these knee injuries are potentially caused by chronic overloading,[20] which could be contributing to the high incidence rate of OA in the military population.[22,23] Understanding how external loads

affect knee joint loads and how gait adaptations might attenuate these loads, is essential for understanding joint health in these populations.

Lower extremity gait mechanics change with load carriage,[15,17,18,20,24–28] with the knee being where most of the adaptations occur.[17,24,25,27] Knee range of motion during stance increases with load carriage due to an increase in peak knee flexion during early stance.[17,24,25,27] The increase in knee flexion has been attributed to the lower extremity increasing shock/energy absorption to mitigate the impact and peak vertical ground reaction forces.[25] Landing with a more flexed knee during load carriage would lengthen the ground reaction force's external lever arm,[29] which increases the internal knee extension moment,[17,29] and would disproportionately increase the total and medial knee joint forces.

Weight loss studies utilizing an inverse dynamics driven musculoskeletal models have demonstrated an approximate 2:1 ratio in reduced absolute peak TFJ contact forces and weight loss,[13] while a load carriage study by Willy et al.,[28] utilizing the same musculoskeletal model as the weight loss study, found a 2:1 ratio in increased absolute first peak medial TFJ contact forces and weight added.[28] However, when examining relative increase in weight and knee joint contact forces, load carriage of 20 kg resulted in a 26.0% increase in bodyweight but a 16.2% increase in peak medial joint contact forces. An incremental load carriage study, by Lenton et al.,[15] utilizing an EMG and optimization driven musculoskeletal model demonstrated a 0.9:1 and 0.8:1 increase in total TFJ contact forces to weight added during load carriage of 15 and 30 kg despite increases in peak knee flexion angle, indicating that the participants may have adapted to the heavier load carriage to attenuate the ratio at the heavier condition. Lenton et al.,[15] also demonstrated a 1.7:1 ratio increase in first peak medial TFJ contact forces to weight added for both loading conditions. When examining relative values, load carriage of 15 kg and 30 kg resulted in an 18% and 36% in

bodyweight, but only 10.1% and 19.9% in first peak medial joint contact forces.[15] The relative increase in external load was not proportional to the increase in relative medial TFJ contact forces,[15] and the ratio of increasing total TFJ load to weight added decreased at the heavier condition,[15] however, the previous load carriage studies both applied absolute external loads,[15,28] while their participants body mass varied by 13.4 kg[28] and 12.1 kg.[15] It is unclear if increasing loads that are relative to each participant's bodyweight will have a similar impact on TFJ contact forces, or if individuals might attenuate their increase in knee joint forces during load carriage via gait adaptations. Furthermore, only Willy et al.,[28] reported changes in medial tibiofemoral impulse with load carriage; it is unclear how increasing vest-borne loads will influence TFJ impulse magnitude and distribution.

Lastly, there have been no investigations on dominant vs nondominant tibiofemoral joint loads during gait. A lack of studies on this topic is partially due to assumptions of gait symmetry for simplicity, with symmetry being defined as no statistically significant difference between the dominant and nondominant limbs.[30] However, a review by Sadeghi et al.[31] revealed that the lower limbs have natural differences that are referred to as functional asymmetry, such as one limb acting as the primary stabilizer and the other limb acting as the primary propulsor.[32] Functional asymmetry is present in mechanical power and energy with the dominant leg exhibiting greater positive work, making it the muscle power generator, while the nondominant leg exhibits greater negative works, making it the muscle power absorber, throughout the gait cycle.[31] The dominant leg has also been shown to exhibit a greater peak knee extension moment than the nondominant leg indicating that the dominant does slightly more weight bearing at the knee.[33] Functional asymmetry can be altered by changing external variables during gait,[34] such as adding load carriage. The kinetic functional differences between the dominant and nondominant limb may

impact the magnitude and distribution of knee joint loads between the limbs during load carriage.

Hypothesis

Based on previous literature, we hypothesized vest-borne loads relative to bodyweight will cause an increase in tibiofemoral joint contact forces and impulses in healthy young adults during gait, but the increase at the 30% condition will be attenuated by gait adaptations. We also hypothesized that tibiofemoral joint contact forces and impulses will be greater in the dominant limb as compared to the non-dominant limb as vest-borne loads are added.

Purpose

The purposes of this study were 1: to compare tibiofemoral joint loads and walking patterns when walking on an instrumented treadmill while unloaded vs. loaded with a weighted vest at 15% and 30% bodyweight and 2: to compare the dominant and nondominant limbs tibiofemoral joint contact forces and impulses in correspondence with increasing load carriage.

Delimitations

1. Participants will be between the ages of 18-30
2. Participants will be able to perform load carriage
3. Participants will have a BMI between 18 and 25 kg/m^2
4. Participants will have no previous major lower extremity injuries or surgery
5. Leg dominance determined via self-report
6. 1.4 m/s walking speed will be used during the trials
7. 15% and 30% bodyweight will be the load carriage conditions.

Operational Definitions

Biomechanical Plasticity – Natural adaptations in gait in response to a condition, such as external loads, that can attenuate increases in knee joint loads

Knee Joint Loads – Tibiofemoral Contact Forces

Functional Asymmetry – Functional differences between the dominant and non-dominant leg

Chapter 2: Review of Literature

Introduction

The purposes of this study were 1: to compare tibiofemoral joint loads and gait patterns when walking on an instrumented treadmill while unloaded vs. loaded with a weighted vest at 15% and 30% bodyweight, and 2: to compare the dominant and nondominant limb's tibiofemoral joint contact forces and impulses in correspondence with increasing load carriage. We hypothesized 1: vest-borne loads relative to bodyweight will cause an increase in total, medial, and lateral tibiofemoral joint contact forces and impulses in healthy young adults during gait, but this increase will be attenuated at the 30% condition due to gait adaptations, and 2: tibiofemoral joint contact forces and impulses will be greater in the dominant limb as compared to the non-dominant limb as vest-borne loads are added. This review of literature will inspect healthy joint loading, unhealthy joint loading, knee joint load modeling, obesity effects on locomotion and knee joint loads, load carriage effects on locomotion and knee joint loads, and asymmetry between dominant and nondominant limbs. These topics will provide the necessary information for the background and rational of the present study.

Healthy Joint Loading

The knee is a weight bearing joint that is comprised of the patellofemoral joint and the tibiofemoral joint.[3] The knee also consists of various soft tissues including ligaments, articular cartilage, and menisci which are responsible for stability, proprioception, and fluid knee movement.[35] More importantly, these structures are responsible for transmitting load during weight bearing activities and for attenuating shock impulses that occur during locomotion.[35] Vertical ground reaction forces (vGRF) are applied to the body contributing to a portion of knee

joint contact force; the other portion comes from muscles forces via muscle contractions, specifically the gastrocnemius, quadriceps, and hamstrings.[36–38] Normal physiological joint loading from daily activities like walking and climbing stairs is good for joint health. During knee joint loading, water and synovial fluid is squeezed out of the articular cartilage to lubricate the knee joint and to adapt to compression by acting as a cushion.[1] The chondrocytes, which are the cells in the cartilage, respond to loading via mechanical transduction triggering a cascade of pathways that regulate the extra cellular matrix, induce cell differentiation, circulate nutrients, and promote repair.[1,5–7]

Physiological loading is also responsible for stimulating mechanical transduction pathway that activate anti-inflammatory cytokines which down regulate the transcription of the mRNA of cartilage degradation enzymes such as matrix metalloproteinases (MMPs), as seen in **Figure 1.**[8] Bone health is maintained and regulated via physiological loading,[39] and external loads in moderation can also be beneficial to bone health.[39] Snow et al.[40] demonstrated that postmenopausal women who exercised with an approximately 5 kg weighted vest for five years maintained significantly more bone density at the hip and greater trochanter than the controls, while also increasing bone density at the femoral neck. It is evident that normal weight bearing activities and moderate load carriage is necessary for maintaining joint and bone health of the lower extremity.

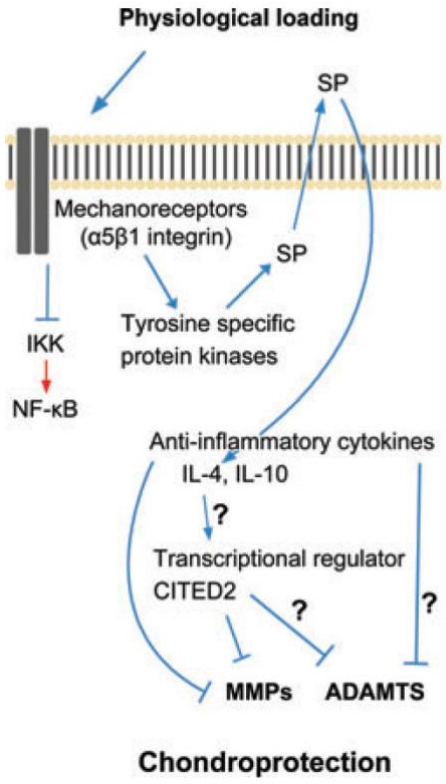

Figure 1: Mechanical Transduction Pathway for Chondroprotection of Articular Cartilage[8]

Unhealthy Joint Loading

Chronic joint overloading can be detrimental to joint health and is a risk factor for the onset of osteoarthritis. Chronic overloading can lead to the activation of inflammatory pathways that lead to the production of cytokines, such as interleukin-1B,[41] that can trigger cascade of reactions that activate MMP and aggrecanases (ADAMT) enzymes which participate in cartilage degradation as seen in **Figure 2.**[8] Excessive chronic mechanical compressive forces alone can lead to cartilage tissue damage and chondrocyte death.[8] Various animal studies in rabbits and bovines have demonstrated that chronic overloading causes cartilage destruction.[9–11] Roemhildt et al.[11] found that chronic tibiofemoral compressive forces of 22% and 44% bodyweight on rabbit hind

limbs lead to surface lesions in the cartilage as seen in image B of **Figure 3**, an increase in permeability, decrease in proteoglycan content, and a decrease in chondrocytes as compared to the 0% load group as see in image D of **Figure 3.** Cell death of chondrocytes is responsible for the decrease/alteration in the extracellular matrix properties and the loss of the ability of the cartilage to resist compressive forces potentially leading to cartilage degradation and the onset of OA.[10] It is evident that excessive chronic overloading of the joint is detrimental to cartilage health. In humans, lower extremity joints are overloaded when there is excessive weight. Two populations that experience chronic excessive weight are individuals with obesity and soldiers who carry heavy loads.

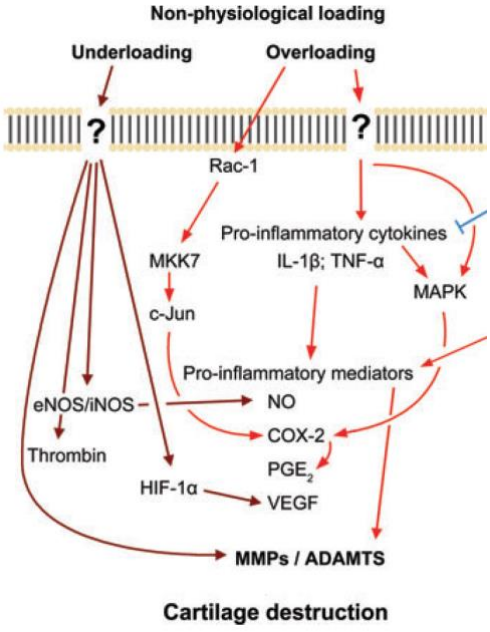

Figure 2: Mechanical Transduction Pathway for Chondroprotection of Cartilage Degradation[8]

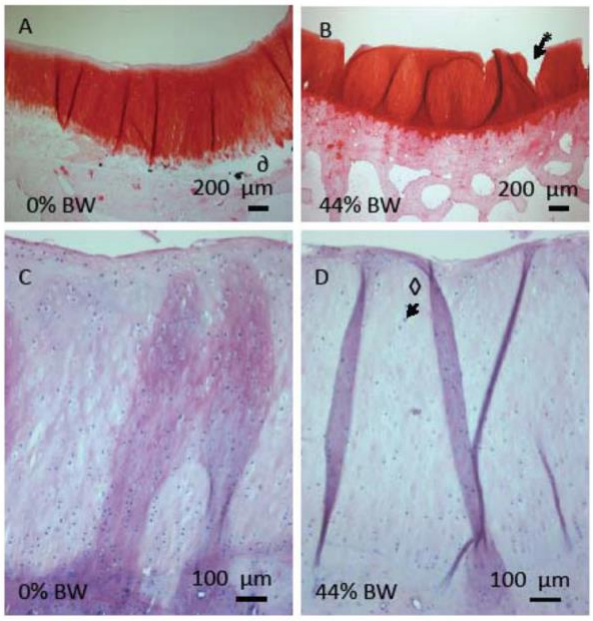

Figure 3: Cartilage Surface Damage and Chondrocyte Loss in Rabbits Tibiofemoral Joint: Before and after 44% chronic bodyweight load[11]

As of 2020, 40.3% of males and 39.7% of females have obesity.[42] Class III obesity numbers increased 70% from 2000 to 2010 with approximately 15.5 million U.S. adults having class III obesity [43]. Obesity has been shown to be related to the prevalence of knee osteoarthritis.[44] Obesity

also contributes to the occurrence and progression of OA at the knee[45] with A dose response relationship existing between BMI and incidence rates of knee OA.[46] It has been hypothesized that this relationship might exist because of changes in loading patterns and increases in absolute loads[47]

Load carriage is common in military population. Modern soldiers are often required to carry loads upwards of 50 kg.[19] However, soldiers of various different sizes are often required to carry the same magnitude of load. Noncombat injuries have increased over past two decades with the primary musculoskeletal injuries coming from load carriage.[19,20] Approximately 50% of these noncombat musculoskeletal overuse injuries are occurring at the knee.[21] It has been hypothesized that these knee injuries are potentially from chronic overloading.[20] Also, the incidence rate of OA in the military population is much higher incidence rate for OA per 1000 people as compared to the general population.[22,23] At the age of 40 and up the incidence rate in the military for OA is 26.91 per 1,000 person-years[22] while the incidence rate at the same age for the general population is 12.40 per 1,000 person-years.[22,23] These data combined with what is known about military load carriage leads the notion that heavy military loads are altering the knee joint environment and potentially leading to noncombat overuse injuries and potentially OA.

Knee Joint Load Modeling

To understand how these forces might affect the knee joint environment during locomotion, the knee joint contact forces must first be calculated or estimated by using the individuals' physical parameters, kinetics, and kinematics as inputs into a musculoskeletal model. Knee joint loads have been estimated via two-dimensional and three-dimensional musculoskeletal models.[36] The reduction approach to musculoskeletal knee models involves the use of kinematic and kinetic data

to compute inverse dynamics to estimate knee joint forces, as seen in **Figure 4**, which break down these components of the approach.[3,48–52] These models often use collected subject anthropometric data and segmental parameters recorded by Dempster[53] to individualize the data. Many of these models require several assumptions and simplifications such as, treating the quadriceps as one muscle force, not including co-contracting muscles at various joints, and modeling the segments as rigid bodies.[48,49]

The reduction approach, and specifically the musculoskeletal model by DeVita and Hortobágyi,[48] has been compared to in-vivo tibiofemoral contact force data set from Fregly et al.[4] by Dumas et al..[49] The DeVita and Hortobágyi (2001)[48] model's proximal-distal and musculo-tendon force curve pattern were similar to in-vivo patterns from Fregly et al.[4] and to the CAMS knee sample from Taylor et al,[54] as seen in **Figure 5.** with r^2 from 0.71 to 0.92.[49] Further modifications of the DeVita and Hortobágyi model[48] by Willy et al.[55] (2016) incorporates medial and lateral compartmental loading, which is the edition of the model used in this study as described in Chapter 3 ***Musculoskeletal Model***. The models estimates of peak total TFJ contact force and impulse estimates from this model were within 3% and 7%, respectively, of *in-vivo* gait data from an individual with an instrumented knee prosthesis, while peak medial TFJ contact force and impulse are within 7% and 4% *in-vivo* gait data as seen in **Figure 6**.[56] This reduction approach can successfully model in-vivo tibiofemoral contact forces and is appropriate for theoretical and pedagogical purposes when the user is aware of the its limitations, such as the previously mentioned assumptions and simply moment arms, and line of pull depending on only one angle.[49] It is important to calculate these loads in order to better understand the knee loading environment during locomotion and when diseases or external conditions are evident/applied, such as osteoarthritis and load carriage.

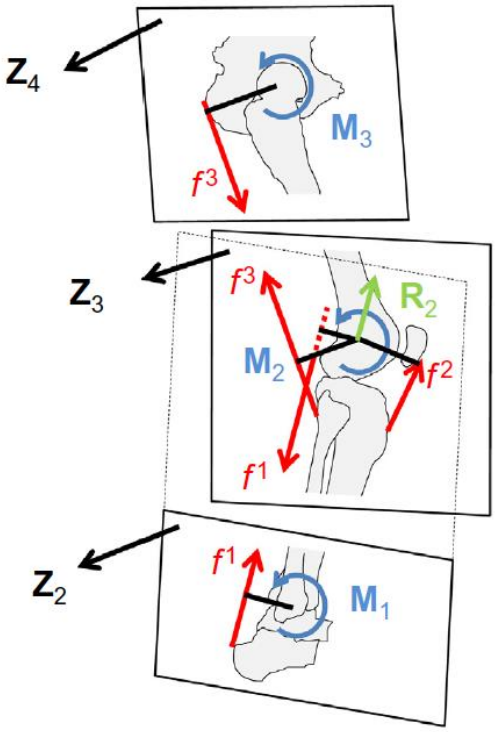

Figure 4: Reduction Approach: Muscle forces in red, joint torques in blue and the knee joint contact force in green[49]

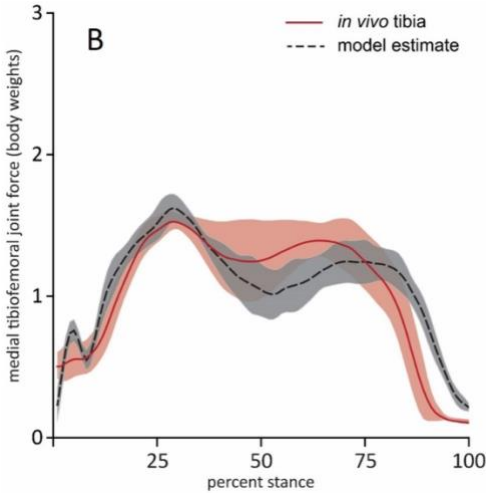

Figure 5: Comparison of In-Vivo Contact Force to Estimated Forces from Willy et al. (2016) Model[56]

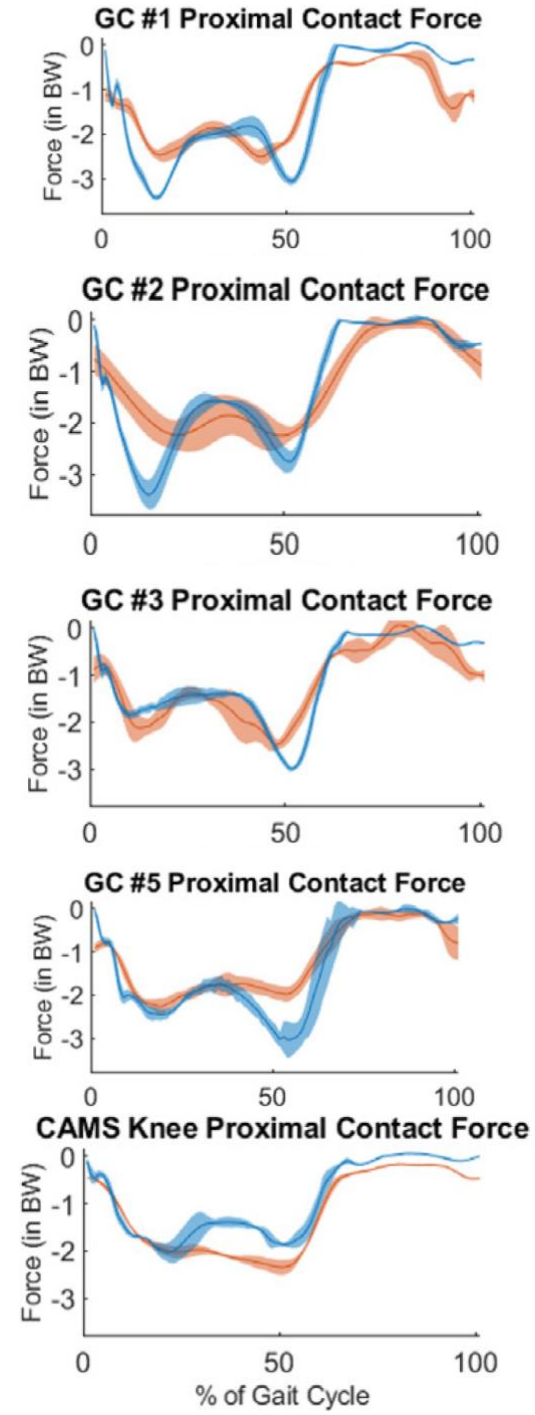

Figure 6: Comparison of In-Vivo Contact Force to Estimated Forces from DeVita's (2001) model[49]

Obesity Effects on Locomotion and Knee Joint Loads

A dose response relationship exist between BMI and incidence rates of knee OA.[46] Chronic knee joint overloading is one of the factors contributing to this relationship, with knee joint loads being partially influenced by kinematic changes.[13] Obese individuals exhibit gait adaptations such as, walking with a much larger step width, shorter stride length, greater abduction of the hip throughout the gait cycle, greater average dorsiflexion, less average plantar flexion, more time in double support, and less time in swing as compared to normal weight individuals.[12,57–59] These studies consisted of individuals who were moderately obese and did not stratify subjects based on class of obesity, but they do provide evidence that individuals with moderate obesity do demonstrate alterations in gait. There is also evidence that moderately obese individuals walk with a generally more extended knee,[12,29,60] however, moderately obese individuals only walked with a significantly more extended knee when walking at a quick pace of 1.5 m/s.[60] When individuals have class 3 obesity, they walk with a significantly more extended knee.[29] Therefore, individuals with class 3 obesity might exhibit different or increased gait adaptations as compared to moderately obese individuals. The reason for these gait adaptations in both moderately obese and severely obese adults has been attributed to reductions in energy expenditure.[13,57] This is important because obese individuals expend significantly more energy during gait,[61] therefore adaptations that reduce energy expenditure allow them to move more efficiently. Furthermore, these gait adaptations also play a role in muscle forces, joint torques, and ultimately knee joint loading.[13,16,60,62,63]

Browning and Kram (2007)[12] found that moderately obese individuals had 60% greater absolute GRF when compared to normal weight individuals. Absolute sagittal plane moments, and peak extensor moments were also greater in the obese group than the normal weight group, with

peak extensor knee moments being 51% greater for the obese group at 1.5 m/s indicating changes in loads at the knee. Furthermore, absolute knee joint compression and shear forces of obese individuals were significantly greater than lean individuals, but when normalized by bodyweight and lean body mass there was no difference.[14] This does not mean that absolute loads are not important because articular cartilage does not necessarily adapt to large increases in weight.[64] This increase in absolute knee loading can attributed to the significant increase in absolute GRF and changes in kinematics instead of quadriceps force because there is some evidence that there is no increase in quadriceps muscle force in individuals with obesity.[13,60,63] Another approach that assist in confirming the observations of increasing knee loads with obesity are massive weight loss studies in individuals with obesity, which have found that significant weight loss can lead to significant reductions in knee joint loads indicating the role of bodyweight on the knee joint.[13,16,63,65] Furthermore, absolute knee extension moment have been shown to increase with increasing BMI,[12] which is consistent with Harding et al. (2016)[14]; however, DeVita & Hortobágyi (2003)[62] found that class 3 obese individuals did not demonstrate an increase in absolute joint torques as compared to lean individuals.

This phenomena of can be attributed to a decrease in gait speed and a decrease in stride length, which leads to a more extended knee during heel strike, as previously mentioned, ultimately leading to a decrease in knee joint torque due to the shortened lever arm.[62] An explanation for these differences in the findings of the two studies has been provided by Browning & Kram[12]; the differences are potentially due to 50% of the DeVita & Hortobágyi[62] sample having a BMI greater than 40, while the sample from Browning and Kram[12] consisted of individuals with an average BMI of 33. It could be that individuals who exhibit class III obesity have different walking patterns

than individuals with class I obesity indicating that there is potentially a BMI threshold for biomechanical plasticity to be induced. This establishes that it is possible to adapt to extra weight.

Load Carriage Effects on Locomotion and Knee Joint Loads

Load carriage is known to lead to alterations in locomotion biomechanics with respect to kinematics. There is a consensus that body-borne loads cause an increase in overall stance phase and double support.[26,28,66,67] Seay et al.[17] demonstrated that hip and ankle range of motion (ROM) during stance increased with symmetrical 15 kg vest-borne loads and further increased with 55 kg loads. Knee ROM also increased with 15 and 55 kg loads as compared to the unloaded condition but there was no difference between the two loaded conditions. Attwells et al.[27] also found that knee ROM increased as backpack loads increased from 8, 16, 40, to 50 kg. These results are consistent with Kinoshita[25] who explained that the increase in knee flexion occurs to absorb more shock and mitigate the impact forces. However, these studies contradict Birell & Haslam[26] who found knee ROM to decrease at backpack loads of 24 and 32 kg indicating that there is not a clear consensus on knee ROM during load carriage.

It should be noted that these previously mentioned studies that examined load carriage and locomotion were primarily comprised of male soldiers. However, Martin & Nelson[67] compared both men and women while walking with no load, 9 kg, 17 kg, 29 kg, and 36 kg backpack loads. It was found that there were significant differences between men and women in the various spatiotemporal parameters as the load increased, such as women decreasing their stride length and increasing their double support time; the women also demonstrated more significant alteration in the parameters as the load increased. The study largely attributed this to the difference in body mass coupled with the practically identical absolute load values that were applied to the men and

women which resulted in load relative to lean body mass values of .8 for men and 1.08 for women in the 36 kg condition. Slider et al.[68] conducted a similar study but used relative loads at 10%, 20%, and 30% of bodyweight and found no significant differences between men and women in spatiotemporal parameters, kinematics, or muscle activity indicating the importance of the use of relative loads when examining women and men.

Load carriage during gait can cause an increase in magnitude and change in the distribution of moments and forces at the knee. Seay et al.[17] found that during stance, peak knee extension torque was greater in both the 15 kg loading condition at .53 Nm/kg and the 55 kg loading condition at .87 Nm/kg as compared to the unloaded condition at .40 Nm/kg, and that the 55 kg condition knee extension torque was significantly greater than the 15 kg condition knee extension torque; furthermore, ankle plantarflexion and hip extension torques were both increased significantly as the load increased. Knee flexion torque during early stance was increased as the load increased, but knee flexion torque during late stance only saw a significant difference with the 55 kg load, with there being no difference between no load and the 15 kg load. It is evident that there are changes in the lower extremity during load carriage, but based on the literature and the conclusion by Seay et al,[17] it is the knee where most of these mechanical adaptation are occurring in response to increasing external loads.

Knee joint loads respond differently to varying absolute magnitude or varying relative percent bodyweight of external loads.[15,18] There is a significant main effect for load carriage of 15 and 30 kg on joint contact forces in first medial peak and second total peak as seen in **Figure 7**.[15] Load carriage of a 15 kg and 30 kg vest results in an 18.3 and 36.4% increase in bodyweight but only a 11% and 18% increase in total knee joint contact forces indicating that increase in load carriage is not proportional to increase in total and medial knee joint contact forces.[15] This lack of

proportionality with increasing weight and increasing knee load is similar to the lack of proportionality weight loss in individuals with obesity and decrease in knee joint loads. This leads to the notion that individuals during load carriage may attenuate increasing knee joint forces at heavier loads via gait adaptations, i.e., they display biomechanical plasticity. However, how this happens is unclear.

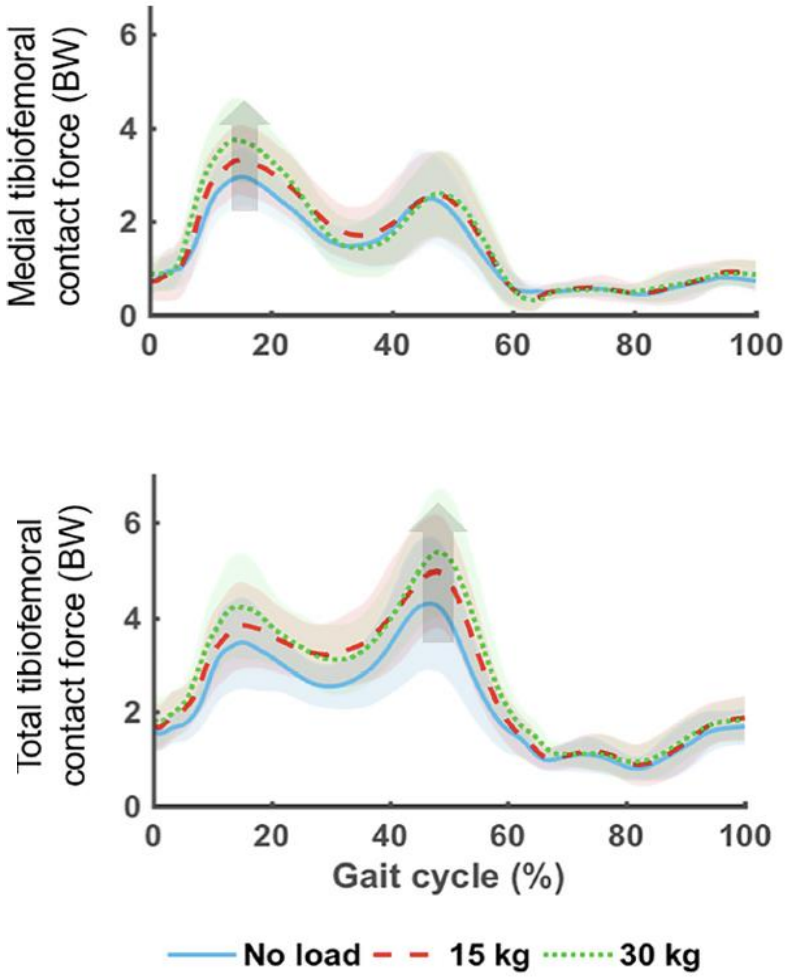

Figure 7: Medial and Total Tibiofemoral Joint Contact Forces when Carrying No Load vs 15 kg vs 30 kg[15]

Dominant vs. Nondominant Limb

Gait symmetry is often assumed partially due to simplicity,[31] with symmetry being defined as no statistically significant difference between the dominant and nondominant limbs.[30] Furthermore, it has been difficult to test gait asymmetries via consecutive gait cycles due to lack of recent technology, such as split belt treadmills. However, the lower limbs do exhibit natural gait differences that can be referred to as functional asymmetry,[31] such as one limb acting as the primary stabilizer and the other limb acting as the primary propulsor.[32] Functional asymmetry between the dominant and nondominant limb may be attributed to various biomechanical and physiological factors.[31]

Functional asymmetry is present in mechanical power and energy with the dominant leg exhibiting greater positive work, making it the muscle power generator, while the nondominant leg exhibits greater negative works, making it the muscle power absorber, throughout the gait cycle.[31] The dominant leg has been shown to exhibit a greater peak knee extension moment than the nondominant leg indicating that the dominant does slightly more weight bearing at the knee.[33] There is also evidence that there is medial-lateral ground reaction force asymmetry while walking, as the dominant leg exhibits greater peak lateral GRF and lesser peak medial GRF than the nondominant, suggesting that leg dominance may play a role in medial-lateral balance during gait.[69] Furthermore, it has been demonstrated that from a muscle strength perspective, the dominant limb has been reported to exhibit greater peak quadriceps strength but lesser peak hamstring strength. There are also differences in fatiguability with the dominant limb having greater aerobic capacity than the nondominant limb.[70] Lastly, there are motor control differences with dominant limb often taking the primary role in functional task, such as kicking a ball,[32] which has been attributed to skill acquisition[71,72] and potentially lower limb motor neuron connection

differences as it has been shown that there are large motor neuron asymmetries between the left and right side in the third sacral region.[31,73] It is difficult to specify what causes lower limb asymmetries, but it is evident that lower limb asymmetry exist, nonetheless.

Functional asymmetry can be altered by changing external variables during gait.[34] Adding load carriage during walking could alter kinetic and kinematic asymmetries through shifting of weight to the dominant side or relying on the dominant limb to make to adapt the increased load. However, no studies have examined TFJ contact force and impulse magnitude and distribution asymmetries with or without load carriage. Based on the asymmetry literature, kinematic, kinetic, and muscle force differences between the dominant and nondominant limb may impact the magnitude and distribution of knee joint loads between the limbs.

Chapter 3: Methods

Introduction

The purposes of this study were 1: to compare tibiofemoral joint loads and gait patterns when walking on an instrumented treadmill while unloaded vs. loaded with a weighted vest at 15% and 30% bodyweight, and 2: to compare the dominant and nondominant limb's tibiofemoral joint contact forces and impulses in correspondence with increasing load carriage. We hypothesized 1: vest-borne loads relative to bodyweight will cause an increase in total, medial, and lateral tibiofemoral joint contact forces and impulses in healthy young adults during gait, but this increase will be attenuated at the 30% condition due to gait adaptations, and 2: tibiofemoral joint contact forces and impulses will be greater in the dominant limb as compared to the non-dominant limb as vest-borne loads are added. To test the first hypothesis, each participant complete walking trials with a weighted vest at 0%, 15%, and 30% bodyweight on an instrumented split-belt treadmill during motion capture. The knee joint loads and kinematics were compared across each condition to determine if there is a difference in knee joint loads and if kinematics play a role in attenuating the potential increase in knee joint loads. For the second hypothesis, the knee joint loads and kinematics will be compared between the participants' dominant and nondominant limb across all external loading conditions to determine if there is a difference in the way the limbs respond to external load. This methods section will contain details on the participants, instruments, design and procedures, musculoskeletal model, and analysis.

Participants

This study included a convenience sample of 24 healthy young adults, 12 females and 12 males, approximately 18 - 30 years old, and BMI from 18 - 24.9 kg/m^2, **Table 1**. Participants were recruited via flyers, in-person recruitment, and through word of mouth. Their participation was

voluntary with no incentives, and they provided written consent as approved by the University Internal Review Board, **Appendix A**, before they took part in the study. Potential participants were informed about the details of the study and were told that they have the power to end their participation in the study at any point.

Participants were excluded if they do not fall within the 18 – 30 year age range. Participants were excluded if they have experienced any major lower extremity injuries or surgery. It has been shown that traumatic lower limb injuries, such as ACL ruptures can lead to altered knee joint loads, which could confound the results.[48,74] Participants were excluded if they have a leg length discrepancy greater than 2 cm. Participants were also excluded if they have a BMI that is less than 18 $kg \cdot m^{-2}$ or greater than or equal to 25 $kg \cdot m^{-2}$.

Table 1: Participant Demographics, Mean (SD)

	Females (n = 12)	Males (n = 12)	Total (n = 24)
Age (Years)	22.7 (1.6)	22.7 (3.0)	22.7 (2.3)
Height (m)	1.70 (0.06)	1.80 (0.10)	1.75 (0.09)
Mass (kg)	60.0 (6.6)	73.0 (7.0)	66.5 (9.4)
Mass (N)	589 (64)	716 (69)	652 (92)
BMI ($kg \cdot m^{-2}$)	20.6 (1.5)	22.4 (1.3)	21.5 (1.6)

m: meters. kg: kilograms.

Instruments

The Health Survey, **Appendix B**, will determine if the participant meets the criteria for the study, and the Physical Activity and Readiness Questionnaire (PAR-Q), **Appendix C,** determined if the participant was able to perform the activity without consulting a physician. A height and weight mechanical beam physician scale was used to measure height and weight. Leg length from greater trochanter to lateral malleolus was measured via tape measure. Leg dominance was self-

reported. If the participant is unsure of their leg dominance they were asked which leg they would kick a kickball with.[75] A reflective marker system applied by the principal investigator was used to mark the 66 bony landmarks and segments of interest listed in **Appendix D.** Gait data was obtained via three-dimensional motion capture, which consist of a 17-camera motion capture system (Qualisys, Göteburg, Sweden) collected at 240 hz. The gait and lower extremity force data, sampled at 2000 hz, was collected on an instrumented dual belt treadmill with two embedded force plates (Bertec, Columbus, Ohio). Raw gait data was cleaned and organized in Qualisys Track Manager software (QTM). A custom program[55] in LabVIEW (National Instruments, Austin, Texas) called a costume pipeline in Visual 3-D (C-Motion, Germantown, Maryland) to build the static model and to calculate joint angles and moments from the motion files, which were then used as inputs to an axial musculoskeletal model by DeVita & Hortobágyi (2001)[48] including the later additions described in Messier et al. (2011)[63] and Willy et al. (2016)[55] to compute tibiofemoral joint contact forces (the model is described in detail under *Musculoskeletal Model*). Output variables were organized in excel via LabVIEW and MATLAB 2021b (MathWorks, Natick Massachusetts) compiler software. Statistics were conducted in SPSS v.28 (IBM, Chicago, Illinois), and figure were constructed in MATLAB.

Design and Procedures

The design of this study was experimental in nature. For the first hypothesis, the independent variable was application of an external vest-borne load, no load vs 15% load vs 30% load. The dependent variables were the first peak tibiofemoral joint contact forces and impulses. For the second hypothesis, the independent variables were the application of external load and the distinction between the dominant and nondominant limb. The dependent variables were the first

tibiofemoral joint contact forces and impulses. For both hypotheses, various components of the musculoskeletal model were also investigated.

Over the phone, the researcher marked participant responses to the Health Survey and Physical Activity and Readiness questionnaire to determine if they met the criteria for the study. Participants were then scheduled to visit the Human Movement Analysis Lab (HMAL) in the Department of Physical therapy which is located in the Health Science Building at East Carolina University in Greenville, North Carolina. There was one data collection day for each participant that was completed within a 120-minute period. The participants were asked to wear tight fitting spandex; if a participant did not have adequate clothing for motion capture, then the lab provided the spandex. Upon arrival, participants read and signed the informed consent, **Appendix E**, and were then given a chance to ask any questions about the study. Anthropometric measures including height, mass, and leg length from greater trochanter to lateral malleolus were obtained along with self-reported leg dominance. An unloaded Mir Pro or Mir Women's adjustable weighted vest (Mir, San Jose, California) was fitted to the participant, followed by the use hypoallergenic tape and elastic wraps to attach 66 retroreflective markers to bony landmarks on the participants' upper and lower extremities, trunk, and pelvis for the collection of 3-D motion capture data.

Participants then stood on an instrumented split-belt treadmill and with their arms out for static motion capture. The start of the unloaded trial began with the participants being instructed to walk on the treadmill at 1.4 $m \cdot s^{-1}$ for 5-minutes. During this time, motion and force data were recorded in 10 second intervals, via Qualisys Track Manager (QTM). Afterwards, the participant was allowed a 5-minute break. The weighted vest was loaded at 15% participants' bodyweight via 1.36 kg steel bricks that were individually placed in the vest's brick pouches, **Table 2**. The weight of the vest plus participant was recorded in kilograms. Another static trial was then recorded,

followed by the participant being instructed to walk at 1.4 $m \cdot s^{-1}$ for 5-minutes. The same procedure as the unloaded and 15% bodyweight trials was repeated for the 30% bodyweight load trial, **Table 2**. After the last weighted condition, markers were removed from the participant, and they were dismissed from the study.

Table 2: Load and Impulse Added, Mean (SD)

	Females (n = 12)	Males (n = 12)	Total (n = 24)
15% Load (kg)	9.3 (1.4)	10.9 (1.1)	10.1 (1.5)
30% Load (kg)	18.1 (2.0)	22.1 (2.0)	20.1 (2.8)
15% Load (N)	91.7 (13.5)	107.1 (10.6)	99.2 (14)
30% Load (N)	177.2 (19.8)	216.5 (20.0)	197.4 (28)
Baseline Impulse (N·s)	370 (42)	474 (47)	422 (69)
15% Impulse (N·s)	427 (48)	556 (64)	491 (86)
30% Impulse (N·s)	489 (54)	637 (73)	563 (98)

Baseline impulse was determined by taking the participants mass in N and multiplying it by their mean stance time based on the no load condition.15% and 30% impulse were determined in the same fashion as the baseline impulse but incorporated the added mass from the external load and the mean stance time for that condition.
kg: kilograms. N: Newtons. s: Seconds

Musculoskeletal Model

A reduction musculoskeletal model of axial tibiofemoral joint contact force, created by DeVita and Hortobágyi (2001),[48] modified by Messier et al., (2011)[63] and further modified by Willy et al. (2016),[55] was used in a custom LabVIEW program[55] to calculate the tibiofemoral joint forces during walking with and without load. Ground reaction forces and kinematics were used along with the participant's individualized anthropometrics, moments of inertia and mass centers determined by Hanavan's mathematical model,[76] and segment masses by Dempster et al[53] to do inverse dynamics consisting of linear and angular Newtonian equations to calculate joint moment and joint reaction forces at the ankle, knee, and hip. Afterwards, hamstring, quadriceps, and

triceps-surae (assumed to be only gastrocnemius and soleus) musculo-tendon forces were calculated.

Triceps-Surae (TS) muscle force was calculated using **Equation 1**,[48] the quotient of the calculated ankle joint plantar flexor moment (AT) and the determined Achilles tendon moment arm from Klein et al.[77] assumed that there is no co-contraction of tibialis anterior. The gastrocnemius force (G) was then calculated using **Equation 2**, which is the product of the TS muscles force and the gastrocnemius proportion of the physiological cross-sectional area Gastroc PCA) of the triceps-surae.[55,78] The gastrocnemius force relative to the tibia was 3° posterior to the long axis of the shank.[48] Hamstrings muscle force (H) was calculated via the hip extensor moment (HEM) (Hamstring and Gluteus Maximus only). The hamstrings moment proportion (HTP) of the hip extension moment (HEM) was calculated by **Equation 3**,[48] which is the hamstrings PCA (HAM PCA)[78] divided by the sum of the HAM PCA and gluteus maximus PCA (GM PCA)[78]. This quotient is then multiplied by the average hamstrings moment arm (Hd) at the hip joint and the average gluteus maximus moment arm (GMd) at the hip joint as a function of hip flexion angle based on data from Németh and Ohlsén.[79] This is under the assumption that hamstrings muscle force is parallel with the femur segment, and was therefore applied to the tibia as a function of knee flexion angle.[48] Finally, hamstring force was calculated from **Equation 4**,[48] which is the quotient of hamstrings torque and hamstrings moment arm at the hip.

$$TS = AT / ATd \qquad \textbf{Equation 1}$$

$$G = TS\ (Gastroc\ PCA) \qquad \textbf{Equation 2}$$

$$HTP = [Ham\ PCA/ (Ham\ PCA + GM\ PCA)]\ (Hd/GMd) \qquad \textbf{Equation 3}$$

$$H = HTP(HEM)/Hd \qquad \textbf{Equation 4}$$

Quadriceps muscle force (Q) was determined by taking the previously calculated knee extensor torque (KT) from inverse dynamics and adding it to the hamstring force times the

hamstring moment arm plus the gastrocnemius force times the gastrocnemius moment arm; the hamstring and gastrocnemius values make up the knee flexor torque which accounts for co-contraction.[80–83] This net knee toque is then divided by the quadriceps moment arm (Qd),[84] as seen in **Equation 5**,[48] to compute the quadriceps force. The quadriceps force is a function of the knee flexion angle.[48,55,63,80]

$$Q = (Kt + H(Hd) + G(Gd)) / Qd \qquad \textbf{Equation 5}$$

The external loads from the ground reaction forces generate an external adductor moment on the knee that is resisted by abductor moments from the quadriceps and lateral support structure (Lss).[63] The Lss force was determined by the remaining torque that is necessary to balance the external adductor torque at the knee;[55,63,86,87] **Figure 8.** by Andriacchi,[87] provides a schematic overview the role of the external adductor moment and the Lss. The tibiofemoral joint compression force (Kc) was calculated via **Equation 6**,[48,63] which took the sum of the hamstrings, gastrocnemius, and quadriceps force, and the vertical (Kz) and horizontal (Ky) knee joint reaction forces that run parallel along long axis of the shank, and this was added to the Lss force; **Figure 9.** by Messier et al. (2011)[63] provides a schematic overview of the model and how the muscle forces, joint reaction forces, and lateral stability create the compressive and shear forces that comprise the tibiofemoral joint contact forces.

$$Kc = G \cos \alpha + H \cos \beta + Q \cos \phi - Kz \cos \lambda + Ky \sin \lambda + Lss \qquad \textbf{Equation 6}$$

The tibiofemoral compression force (Kc) was then applied perpendicularly at an 8.8° posterior tibial slope.[88] The medial tibiofemoral compressive force was estimated via the methods of Schipplein and Andriacchii[87] as a function off knee joint width and frontal plane moments, and based on the assumptions that TFJ compression force act only at the medial and lateral plateau and that the plateaus follow a sagittal path.[55,86,87] Subject specific knee joint width was used to

determine the medial (25% of width) and lateral (75% of width) contact points.[86] The total axial tibiofemoral joint contact force acting through 25% of the subject specific knee width generated a frontal plane moment that is subtracted from the knee's internal abduction moment[55,86] The total TFJ contact force required to account for the knee's internal abduction moment is considered part of the force acting on the medial contact point; the negative remainder moment is then divided by the medial compartment moment arm to acquire the remaining total TFJ force, which is then equally parsed to the medial and lateral contact points. This ultimately provides the medial and lateral knee joint compartment compressive forces.[55]

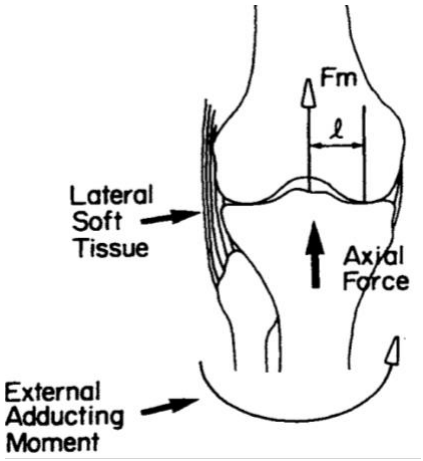

Figure 8: Schematic of Balancing the External Adduction Moment at the Knee[87]

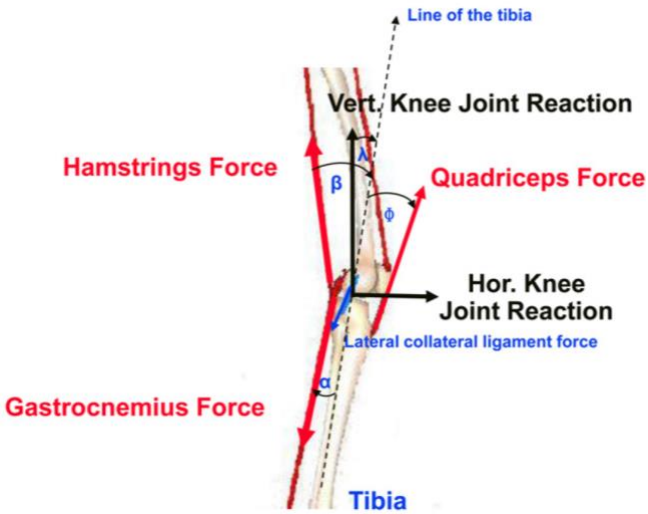

Figure 9: Schematic of the DeVita & Hortobágyi Musculoskeletal Model[63]

Data Processing and Analysis

During data collection, markers were identified in QTM, and an AIM model was generated for each participant after their first walking trial; this model was subsequently applied to the participant's later trials for automatic marker identification. After data collection, each 10 second QTM capture was trimmed to first right heel strike to the end of the file and exported as two separate .tsv files, one for the right force plate and one for the left. Then 5 individual stance phases

(heel strike to toe off) were trimmed in QTM for both the left and right leg of each 10 second capture for each participant at each condition. The trimmed files were exported as .c3d files.

A custom LabVIEW program by Willy et al.[55] took inputs of the participant's mass in kg and height in meters, the participants sex, the walking speed of 1.4 $m \cdot s^{-1}$, a 50 frame static calibration, the two .tsv files, and the 5 individual stance phases of the right or left leg from the .v3d files. When ran, LabVIEW software called a custom V3D pipeline that built an 8-segment model, with each segment being model as a cylinder, which was applied to the motion files. Marker and ground reaction force data were filtered with a 15-Hz cutoff frequency via a 4th order, zero-lag, low pass, Butterworth filter.[55,89,90] The software then used motion and force data to do inverse dynamics in visual 3D to compute hip, knee, and ankle moments and powers in the sagittal, frontal, and transverse planes. The software then used the lower extremity kinematic data and the computed moments as inputs to the musculoskeletal model as described above. Joint reaction forces, gastrocnemius, quadriceps, hamstrings forces, total tibiofemoral joint compressive forces, along with medial and lateral tibiofemoral compartment compressive forces, were calculated throughout each individual stance phase. Spatiotemporal parameters were calculated from for the right and left leg from the two .tsv files.

The software then exported the results for each individual stance into multiple .txt files. For each group of 5 stance phases, data from the .txt files were organized into 402 variables per stance along with an average and standard deviation of the 5 stances, and then exported into a Microsoft excel spreadsheet. A compiler program in LabVIEW was then used to pull the variables of interest for the right or left limb at the given condition at the values for each of the participants 5 stance phases, along with the average and standard deviation for each participant and compile them into an excel spreadsheet. Time series data was compiled in the same software in a similar

fashion where the average of the 5 stance phases at each percent stance (out of 100% stance) were put into an excel spreadsheet. Further compiler software in MATLAB compiled all of the data of interest for each condition into one spreadsheet and took an overall average across all participants, and then created time series plots for the right limb. The software also converted data into absolute and normalized forms, and further organized right and left participate data into dominant and nondominant, compiled dominant and nondominant data via overall averages, and created dominant vs nondominant time series plots.

To answer the hypotheses, only the 5 stance phases taken from the last 2 minutes of each condition for both the left and right leg were used for the analyses. Ground reaction force, joint angles, lower extremity moments, and knee joint contact forces over stance time figures, along D vs ND bar graphs were computed in MATLAB. To test the first hypothesis a one-way repeated measures analysis of variance (ANOVA; $\alpha = 0.05$), was used to compare tibiofemoral joint contact forces in the right limb across the three external loading conditions (0%, 15%, 30%). Further one-way repeated measures ANOVAs were used to analyze other components and outputs from the musculoskeletal model that contribute to the first peak of TFJ contact force and help answer the hypothesis. These variables were the following: peak ground reaction forces, ground reaction force impulses, peak estimated quadriceps and hamstrings forces and impulses, peak lower extremity internal sagittal plane moments and angular impulses, peak lower extremity internal frontal plane moments and angular impulses, peak power at K1, step length, stance time, peak lower extremity sagittal and frontal plane joint angles, and leg stiffness defined as the maximum vertical force divided by change in vertical leg length, subsequently modeling the leg as a spring . Boxplots were generated for each dependent variable across the three loading conditions to determine the presence of outliers. An outlier being defined as 1.5 box plot lengths from the edge of the box,

denoted as a ° in SPSS. Extreme outliers were defined as 3 box plot lengths from the edge of the box, denoted as a * in SPSS. If extreme outliers were present, we probed the data for potential data entry or measurement errors. If the extreme outliers were due to truly unusual data and did not affect the results for the repeated measures ANOVA, then the data were not excluded. To confirm if the within-subjects factors had equal variance, Mauchly's test of sphericity was used ($\alpha = 0.05$). If the data passed the sphericity test ($p > 0.05$) then the results of repeated measures ANOVA within subject effects were interpreted with no corrections. If sphericity was violated ($p < 0.05$) then Greenhouse-Geisser corrections results were made to the degrees of freedom of the dependent variables to enable interpretation of the repeated measures ANOVAs.[91] Partial eta squared (η_p^2) within-subject effect sizes[92–94] were determined for each ANOVA effect. Effect sizes were considered small (0.02), medium (0.06), or large (0.14).[21,92–94] Bonferroni corrected pairwise comparisons were used for post-hoc analysis ($\alpha = 0.05$). Polynomial orthogonal trends were used to determine the presence of linear and quadratic trends ($\alpha = 0.05$), along with partial eta squared within-subject effect sizes of the trends.

To answer the second hypothesis a 2 x 3 repeated measures ANOVA was used to compare knee joint contact forces between the dominant and nondominant knee limb across the three external loading conditions. The same extra variables as the first hypothesis were also analyzed withing the scope of the second hypothesis. The same outlier test, sphericity test, and corrections, as mentioned above, were applied to the results of the 2 x 3 ANOVA. Furthermore, the same effect size tests were applied to the main effects and the interactions. Significant interactions ($\alpha = 0.05$) between load and dominant vs nondominant limb were probed to uncover simple main effects. Paired samples two-tailed T-tests were used to investigate differences between the dominant and nondominant limbs at each separate loading condition, along with Cohen's d (*d)* effect sizes, which

were considered small (0.2), medium (0.5) or large (0.8).[93,95] One-way repeated measures ANOVAs were used to investigate the effect of the loading condition on the dominant limb and separately the effect of load carriage on the nondominant limb, along partial eta squared effect sizes.

Chapter 4: Results

Introduction

The purposes of this study were 1: to compare tibiofemoral joint loads and gait patterns when walking on an instrumented treadmill while unloaded vs. loaded with a weighted vest at 15% and 30% bodyweight, and 2: to compare the dominant and nondominant limb's tibiofemoral joint contact forces and impulses in correspondence with increasing load carriage. We hypothesized 1: vest-borne loads relative to bodyweight will cause an increase in total, medial, and lateral tibiofemoral joint contact forces and impulses in healthy young adults during gait, but this increase will be attenuated at the 30% condition due to gait adaptations, and 2: tibiofemoral joint contact forces and impulses will be greater in the dominant limb as compared to the non-dominant limb as vest-borne loads are added. The sections for purpose 1 are the following: load carriage effects on first peak TFJ contact force magnitude and distribution, load carriage effects on TFJ impulse magnitude and distribution, load carriage effects on peak muscle forces and impulses, load carriage effects on knee sagittal and frontal plane moments, and load carriage effects on spatiotemporal parameters and kinematics. The sections for purpose 2 are the following: load carriage effects on dominant vs nondominant first peak TFJ contact force magnitude and distribution, load carriage effects on dominant vs nondominant TFJ impulse magnitude and distribution, load carriage effects on dominant vs nondominant peak muscle forces and impulses, load carriage effects on dominant vs nondominant knee sagittal and frontal plane moments and knee power, load carriage effects on dominant vs nondominant ground reaction force peaks and impulses, and load carriage effects on spatiotemporal parameters and kinematics.

Load Carriage Effects on First Peak TFJ Contact Force Magnitude and Distribution

First peak total, medial and lateral TFJ forces increased directly with increased load carriage (tTFJ $p < .001$, $\eta_p^2 = .853$; mTFJ $p < .001$, $\eta_p^2 = .842$ lTFJ $p < .001$, $\eta_p^2 = .779$), **Table 3** & **Figure 10**. From 0% load to 15% (99 $\pm$ 14 N), and from 0% to 30% (197 $\pm$ 28 N), peak tTFJ increased on average 315 N (16.0%) and 708 N (35.7%); peak mTFJ increased 195 N (13.2%) and 403 N (27.7%), and peak lTFJ increased 108 N (14.3%) and 263 N (35.1%), respectively, **Table 3**. All peak TFJ forces were described by linear trends (tTFJ $p < .001$, $\eta_p^2 = .890$; mTFJ $p < .001$, $\eta_p^2 = .884$; lTFJ $p < .001$, $\eta_p^2 = .834$), but no quadratic trends (tTFJ $p = .189$, $\eta_p^2 = .074$; mTFJ $p = .602$, $\eta_p^2 = .012$; lTFJ $p = .127$, $\eta_p^2 = .098$).

TFJ impulses responded similarly, with load carriage increasing tTFJ impulse ($p < .001$, $\eta_p^2 = .863$), mTFJ impulse ($p < .001$, $\eta_p^2 = .833$), and LTFJ impulse ($p < .001$, $\eta_p^2 = .789$), **Table 3** & **Figure 10**. From 0% load to 15% (69 N·s), and from 0% to 30% (141 N·s), tTFJ impulse increased 123 N·s (14.5%) and 278 N·s (32.7%); mTFJ impulse increased 83 N·s (14.6%), and 169 N·s (29.8%), and lTFJ impulse increased 41 N·s (14.2%) and 110 N·s (38.2%), respectively, **Table 3**. All peak TFJ forces were described by significant linear trends (tTFJ $p < .001$, $\eta_p^2 = .874$; mTFJ $p < .001$, $\eta_p^2 = .884$; lTFJ $p < .001$, $\eta_p^2 = .825$). No quadratic trend component was evident in mTFJ impulse ($p = .705$, $\eta_p^2 = .006$). However, tTFJ and lTFJ impulse both exhibited quadratic trends components with large effect sizes (tTFJ $p = .014$, $\eta_p^2 = .233$; lTFJ $p = .009$, $\eta_p^2 = .262$).

Table 3: Tibiofemoral Joint Forces and Impulses, Mean (SD)

Variable	No Load	15% Load	30% Load	Main Effects	Trend Quadratic
				p	*p*
				η_p^2	η^2
First Peak tTFJ (N)	1978 (501)	2294 (550) **	2685 (692) **, ‡	**< .001** **.853**	.189 .074
First Peak mTFJ (N)	1462 (329)	1655 (374) **	1867 (430) **, ‡	**< .001** **.842**	.602 .012
First Peak lTFJ (N)	725 (242)	833 (271) **	988 (330) **, ‡	**< .001** **.779**	.108 .108
TFJ Impulse (N·s)	851 (184)	974 (221) **	1129 (278) **, ‡	**< .001** **.863**	**.014** **.233**
mTFJ Impulse (N·s)	563 (132)	645 (162) **	731 (187) **, ‡	**< .001** **.833**	.705 .006
lTFJ Impulse (N·s)	288 (108)	329 (122) **	398 (154) **, ‡	**< .001** **.789**	**.009** **.262**

Averages (SD) for first peak and impulses of the tibiofemoral joint. Repeated measures ANOVA results for main effects, Bonferroni pairwise comparisons, and post-hoc quadratic trend analysis. Post-hoc linear trend analysis all at $p < .001$

0% load is walking with an unloaded weighted vest, 15% load is walking with the weighted vest loaded at 15% bodyweight, and 30% load is walking with the weighted vest loaded at 30% bodyweight. First peak total, medial, and lateral tibiofemoral joint contact forces and impulse increased significantly with load and exhibited linear trends.

η_p^2: Partial eta. Squared. N: Newtons. s: seconds.

*$p < 0.05$ compared with No-Load, **$p \leq 0.005$ compared with No-Load.

†$p \leq 0.05$ compared with 15% Load, ‡$p \leq 0.005$ compared with 15% Load.

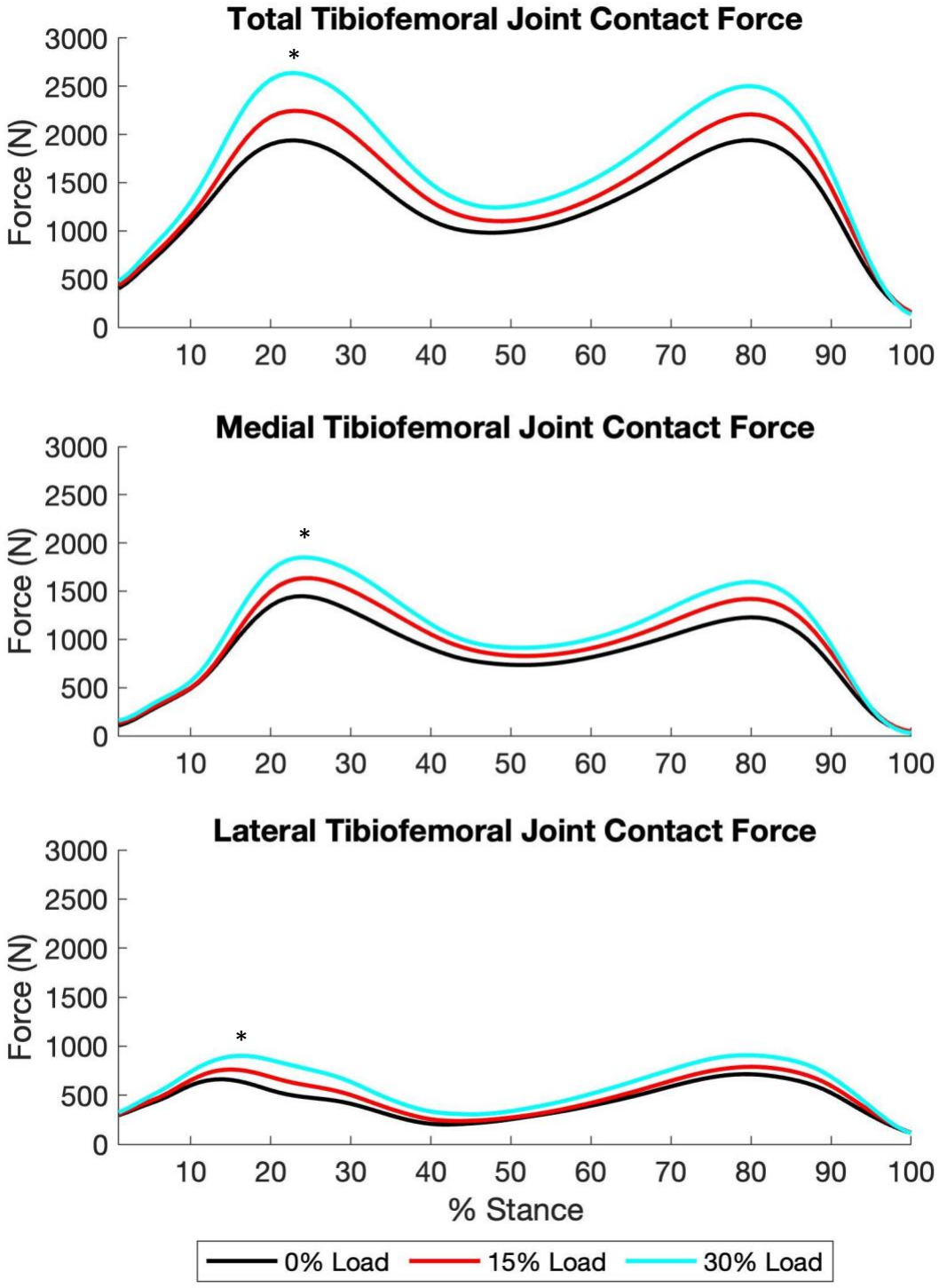

Figure 10: Tibiofemoral Joint Contact Forces Across Loading Conditions
Total, medial, and lateral tibiofemoral contact forces over percent stance during load carriage of 0% BW, 15% BW, and 30% BW. Bold line represents the mean across all participants. The first peak of total, medial, and lateral tibiofemoral joint contact forces increased across condition ($p < .001$). Impulse determined over nonnormalized time. * $p < 0.05$ for load effect

Load Carriage Effects on Muscle Forces

First peak hamstring and quadriceps force increased directly with load carriage (Ham $p < .001$, $\eta_p^2 = .586$; Quad $p < .001$, $\eta_p^2 = .708$), **Table 4** & **Figure 11**. From 0% load to 15%, and from 0% to 30%, peak hamstring force increased 34 N (7.6%) and 104 N (23.2%), and peak quadriceps force increased 164 N (16.5%) and 407 N (40.8%), **Table 4**. Peak Hamstring force and quadriceps force both demonstrated linear trends (Peak Ham $p < .001$, $\eta_p^2 = .664$; Peak Quad $p < .001$, $\eta_p^2 = .758$) and no quadratic trends (Peak Ham $p = .060$, $\eta_p^2 = .145$; Pk Quad $p = .102$, $\eta_p^2 = .112$). Hamstrings, quadriceps, and gastrocnemius impulse increased with increased load carriage (Ham $p < .001$, $\eta_p^2 = .463$; Quad $p < .001$, $\eta_p^2 = .793$; Gastroc; $p < .001$, $\eta_p^2 = .758$), **Table 4** & **Figure 11**. From 0% load to 15% load, and from 0% to 30%, hamstring impulse increased 10 N·s (12.1%), and 27 N·s (32.5%), quadriceps impulse increased 42 N·s (16.2%) and 96 N·s (38.1%), and gastrocnemius impulse increased 29 N·s (13.7%) 68 N·s and (31.8%). **Table 4**. Hamstring, quadriceps, and gastrocnemius impulse all demonstrated linear trends (Ham $p < .001$, $\eta_p^2 = .543$; Quad $p < .001$, $\eta_p^2 = .820$; Gastroc $p < .001$, $\eta_p^2 = .771$). There were no quadratic trends for Hamstrings or quadriceps impulse (Ham $p = .264$, $\eta_p^2 = .054$; Quad $p = .093$, $\eta_p^2 = .118$), but there was a significant quadratic trend for the gastrocnemius ($p = .015$, $\eta_p^2 = .229$) **Table 4**.

Table 4: Muscle Forces and Impulses, Mean (SD)

Variable	No Load	15% Load	30% Load	Main Effects	Trend Quadratic
				p	p
				η_p^2	η_p^2
First Peak Ham (N)	448 (165)	482 (183) *	552 (220) **, ‡	< **.001** **.586**	.060 **.145**
First Peak Quads (N)	996 (353)	1160 (413) **	1403 (510) **, ‡	< **.001** **.708**	.102 .112
Hamstring Impulse (N·s)	83 (49)	93 (58) **	119 (71) **, ‡	< **.001** **.463**	.264 .054
Quadriceps Impulse (N·s)	252 (73)	294 (87) **	348 (109) **, ‡	< **.001** **.793**	.093 .118
Gastrocnemius Impulse (N·s)	211 (47)	240 (61) **	278 (78) **, ‡	< **.001** **.758**	**.015** **.229**

Averages (SD) for first peak forces and impulses for the hamstrings and quadriceps, along with gastrocnemius impulse. Repeated measures ANOVA results for main effects ($p < .05$), Bonferroni pairwise comparisons, and post-hoc quadratic trend analysis. Post-hoc linear trend analysis all at $p < .001$

0% load is walking with an unloaded weighted vest, 15% load is walking with the weighted vest loaded at 15% bodyweight, and 30% load is walking with the weighted vest loaded at 30% bodyweight.

Peak hamstrings and quadriceps force along with impulse increased significantly with load.

η^2: Partial eta. Squared. N: Newtons. s: seconds.

*p < 0.05 compared with No-Load, **p ≤ 0.005 compared with No-Load.

†p ≤ 0.05 compared with 15% Load, ‡p ≤ 0.005 compared with 15% Load.

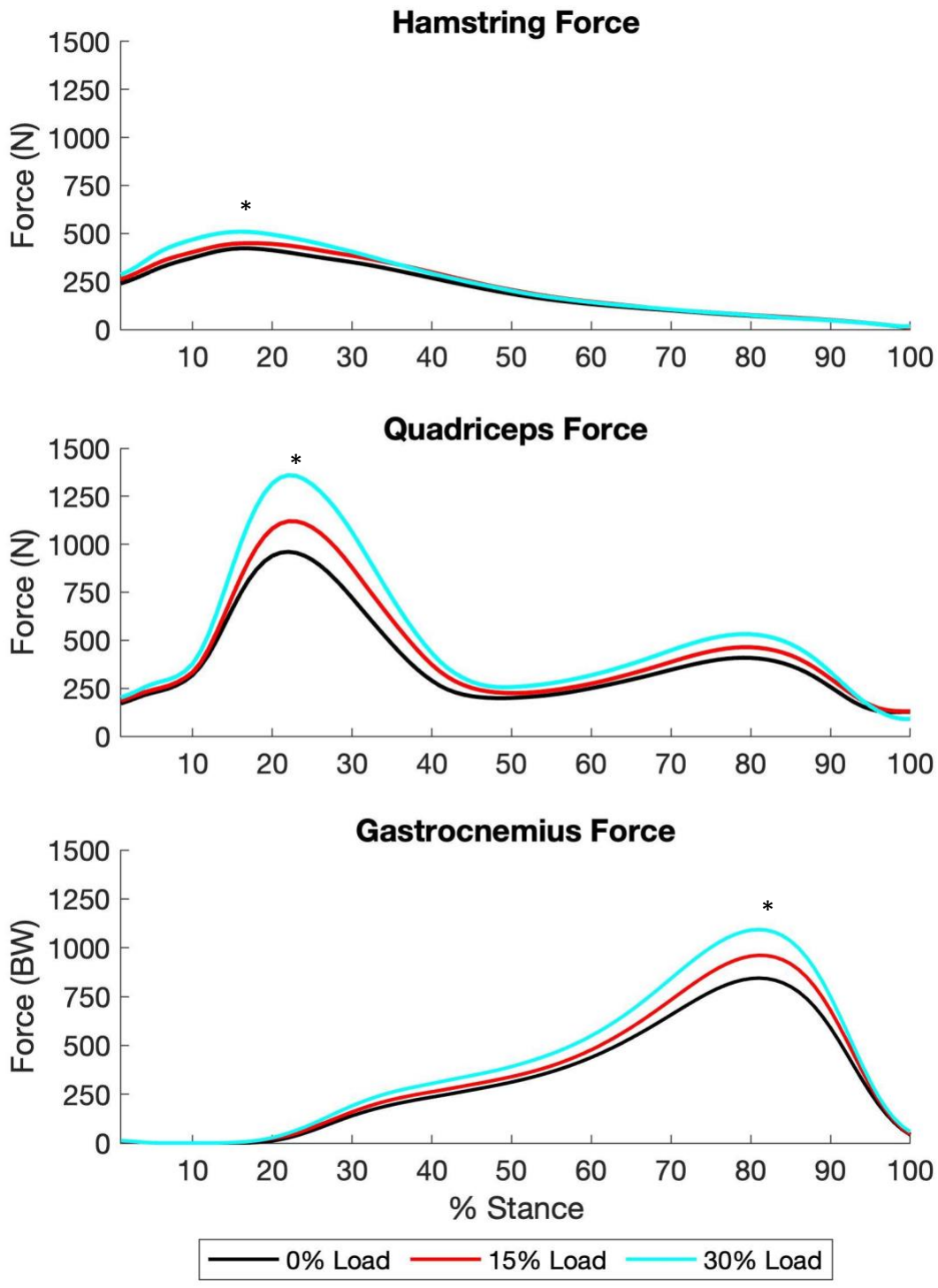

Figure **11: Muscle Forces Across Loading Conditions**
Hamstring, quadriceps, and gastrocnemius forces over percent stance during load carriage of 0% BW, 15% BW, and 30% BW. Bold line represents the mean across all participants. The first peak of quadriceps and hamstrings force increased across condition $p < .001$. Impulse determined over nonnormalized time. * $p < 0.05$ for load effect

Load Carriage Effects on Sagittal and Frontal Plane Moments

Lower extremity peak internal knee sagittal and frontal plane moments increased with increasing load (KEM $p < .001$, $\eta_p^2 = .614$; KAM $p < .001$, $\eta_p^2 = .469$) **Table 5** & **Figure 12**. From 0% load to 15%, and from 0% to 30%, peak knee extension moment increased on average 0.10 N·m/kg (17.2%) and 0.24 N·m/kg (41.4%), and peak knee abduction moment increased 0.05 N·m/kg (11.9%) and 0.07 N·m/kg (16.7%) **Table 5**. Both peak internal sagittal and frontal plane moments were described by linear trends (KEM $p < .001$, $\eta_p^2 = .670$; KAM $p < .001$, $\eta_p^2 = .614$), but no quadratic trends (KEM $p = .227$, $\eta_p^2 = .063$; KAM $p = .183$, $\eta_p^2 = .076$). Lower extremity internal sagittal and frontal plane angular impulses increased with increasing load (KEAI $p < .001$, $\eta_p^2 = .547$; KAAI $p < .001$, $\eta_p^2 = .526$), **Table 5** & **Figure 12.** Knee extension and abduction angular impulses were described by linear trends (KEAI $p < .001$, $\eta_p^2 = .608$; KAAI $p < .001$, $\eta_p^2 = .618$), and no quadratic trends (KEAI $p = .739$, $\eta_p^2 = .005$; KAAI $p = .116$, $\eta_p^2 = .082$).

Table 5: Internal Knee Sagittal and Frontal Plane Moments and Angular Impulses, Mean (SD)

Variable	No Load	15% Load	30% Load	Main Effects	Trend Quadratic
				p	*p*
				η_p^2	η^2
Peak Knee Extension Moment (N·m/kg)	0.58 (0.25)	0.68 (0.30) **	0.82 (0.36) **, ‡	**< .001** **.614**	.227 .063
Peak Knee Abduction Moment (N·m/kg)	-0.42 (0.14)	-0.47 (0.16) **	0.49 (0.16) **	**< .001** **.469**	.183 .076
Knee Extension Angular Impulse (N·m·s/kg)	0.07 (0.04)	0.08 (0.05) **	0.10 (0.05) **, ‡	**< .001** **.547**	.739 .005
Knee Abduction Angular Impulse (N·m·s/kg)	-0.12 (0.05)	-0.14 (0.06) **	-0.15 (0.07) **,†	**< .001** **.526**	.166 .082

Averages (SD) for peak knee extension and knee abduction moments, and knee extension and knee abduction angular impulses at each loading conditions. Repeated measures ANOVA results for main effects, Bonferroni pairwise comparisons, and post-hoc quadratic trend analysis. 0% load is walking with an unloaded vest, 15% load is the vest loaded at 15% bodyweight, and 30% load is the vest loaded at 30% bodyweight. η_p^2: Partial eta. Squared. N: Newtons. m: meters. kg: kilograms*$p < 0.05$ compared with No-Load, **$p \leq 0.005$ compared with No-Load.
†$p \leq 0.05$ compared with 15% Load, ‡$p \leq 0.005$ compared with 15% Load.

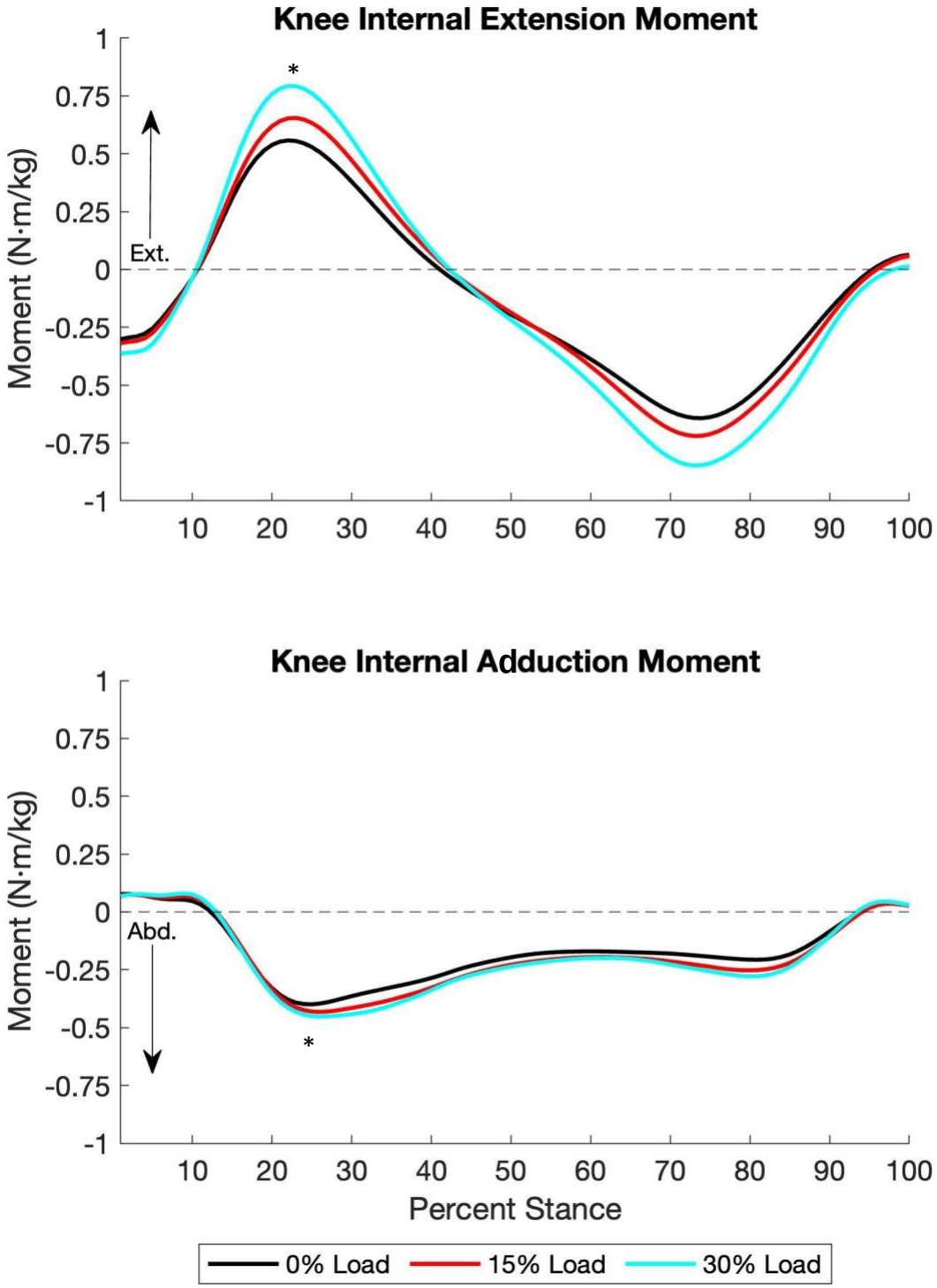

Figure 12: **Lower Extremity Sagittal Plane Moments Across Loading Conditions**
Peak knee extension and knee abduction moments over percent stance during load carriage of 0% BW, 15% BW, and 30% BW. Bold line represents the mean across all participants. The peak of the sagittal plane moments increased across condition $p < .005$. Angular impulse determined over nonnormalized time. * $p < 0.05$ for load effect

Load Carriage Effects on Spatiotemporal Parameters and Kinematics

Step length did not significantly change with load carriage (p = .259, η_p^2= .057), however, stance time increased with increasing load carriage (p < .001, η_p^2= .359), **Table 6**. From 0% load to 15%, and from 0% to 30%, average stance time increased 5 ms (0.7%) and 14 ms (2.2%). Stance time exhibited a linear trend (p < .001, η_p^2= .416), but no quadratic trend (p = .217, η_p^2= .066).

There were significant but small increases in peak hip flexion angle (p = .010, η_p^2= .211), peak knee flexion angle (p < .001, η_p^2= .355), and first peak ankle plantar flexion angle (p < .001, η_p^2= .380) during early stance with increasing load, **Table 6 & Figure 13**. From 0% load to 15%, and from 0% to 30%, peak hip flexion exhibited mean increased 1.3° (5.0%) and 2.0° (7.4%) peak knee flexion increased 0.8° (4.2%), and 2.0° (10.5%), and peak ankle plantar flexion increased 0.8° (11.0%) and 1.3° (17.8%), **Table 6**. Peak hip flexion, knee flexion, and ankle plantar flexion exhibited linear trends (Hip Flexion p = .013, η_p^2= .240; Knee Flexion p < .001. η_p^2= .479; Ankle Plantar Flexion p < .001, η_p^2= .625) and no quadratic trends (Hip Flexion p = .257, η_p^2= .055; Knee Flexion p = .608, η_p^2= .012; Ankle Plantar Flexion p = .699, η_p^2= .007). Leg stiffness decreased with increasing load carriage (p < .001, η_p^2= .853), **Table 6** & **Figure 13**. From 0% to 15% load, and from 0% to 30%, leg stiffness decreased 0.58 $N \cdot mm^{-1}$ (8.2%) and 1.93 $N \cdot mm^{-1}$ (27.3%). Linear (p < .001, η_p^2= .870) and quadratic trends (p < .001, η_p^2= .624) were both present with large effect sizes.

Table 6: Spatiotemporal Parameters and Kinematics, Mean (SD)

Variable	No Load	15% Load	30% Load	Main Effects	Trend Quadratic
				p η_p^2	p η_p^2
Step Length (m)	0.73 (0.03)	0.73 (0.03)	0.73 (0.03)	.374 .039	.440 .026
Stance Time (ms)	646 (.03)	651 (.03) *	660 (0.03) *,‡	**< .001** **.359**	.217 .066
Peek Hip Flexion Angle (°)	25.8 (10.4)	27.1 (11.3) *	27.71 (12.6) *	**.010** **.211**	.257 .055
Peak Knee Flexion Angle (°)	-19.1 (4.7)	-19.9 (4.5)	-21.1 (5.5) **,†	**< .001** **.335**	.608 .012
First Peak Plantar Flexion Angle (°)	-7.3 (3.8)	-8.1 (3.5) **	-8.6 (3.6) **	**< .001** **.380**	.699 .007
Leg Stiffness ($N \cdot mm^{-1}$)	7.08 (1.27)	6.50 (1.02) **,	5.14 (0.80) **, ‡	**< .001** **.853**	**< .001** **.624**

Averages (SD) for step length, peak hip flexion, peak knee flexion, first peak plantar flexion, and leg stiffness. Repeated measures ANOVA results for main effects, Bonferroni pairwise comparisons, and post-hoc quadratic trend analysis. Post-hoc linear trend analysis all spatiotemporal parameters, sagittal plane angles, and leg stiffness at $p < .005$

0% load is walking with an unloaded weighted vest, 15% load is walking with the weighted vest loaded at 15% bodyweight, and 30% load is walking with the weighted vest loaded at 30% bodyweight.

Step length was not affected by load carriage. Peak hip and knee flexion, and first peak plantar flexion increased significantly. Leg stiffness decreased significantly with load carriage. Peak knee flexion, peak hip flexion, first peak ankle plantar flexion, and leg stiffness exhibited linear trends. Leg stiffness also exhibited a quadratic trend.

η_p^2: Partial eta. Squared. m: meters. °: degrees. N: Newtons. mm: millimeters. ms: milliseconds.

*$p < 0.05$ compared with No-Load, **$p \leq 0.005$ compared with No-Load.

†$p \leq 0.05$ compared with 15% Load, ‡$p \leq 0.005$ compared with 15% Load.

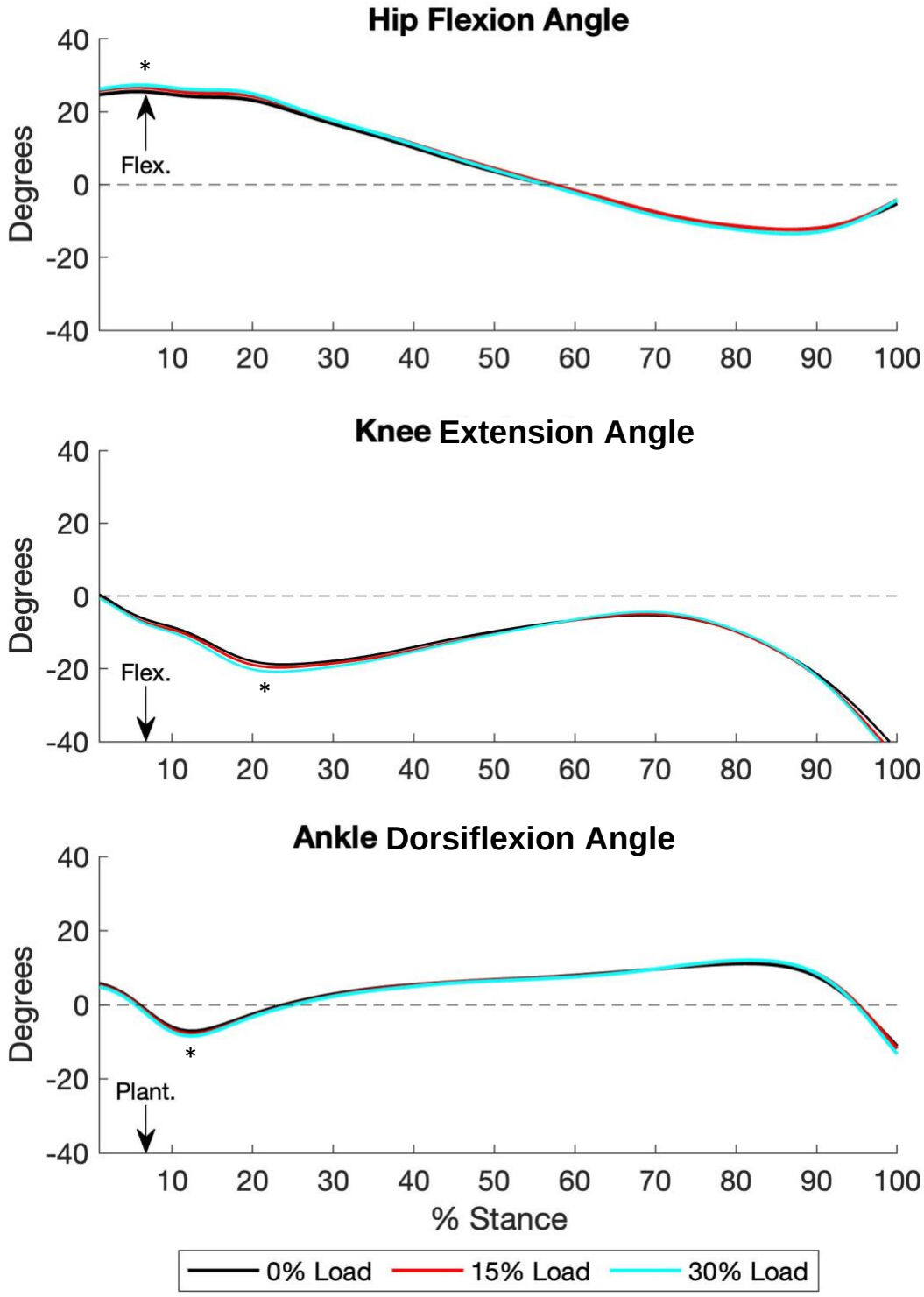

Figure 13: Lower Extremity Sagittal Plane Kinematics Across Loading Conditions
Knee flexion, hip flexion, and ankle plantar flexion over percent stance during load carriage of 0% BW, 15% BW, and 30% BW. Bold line represents the mean across all participants. The peak angles increased across condition. * $p < 0.05$ for load effect

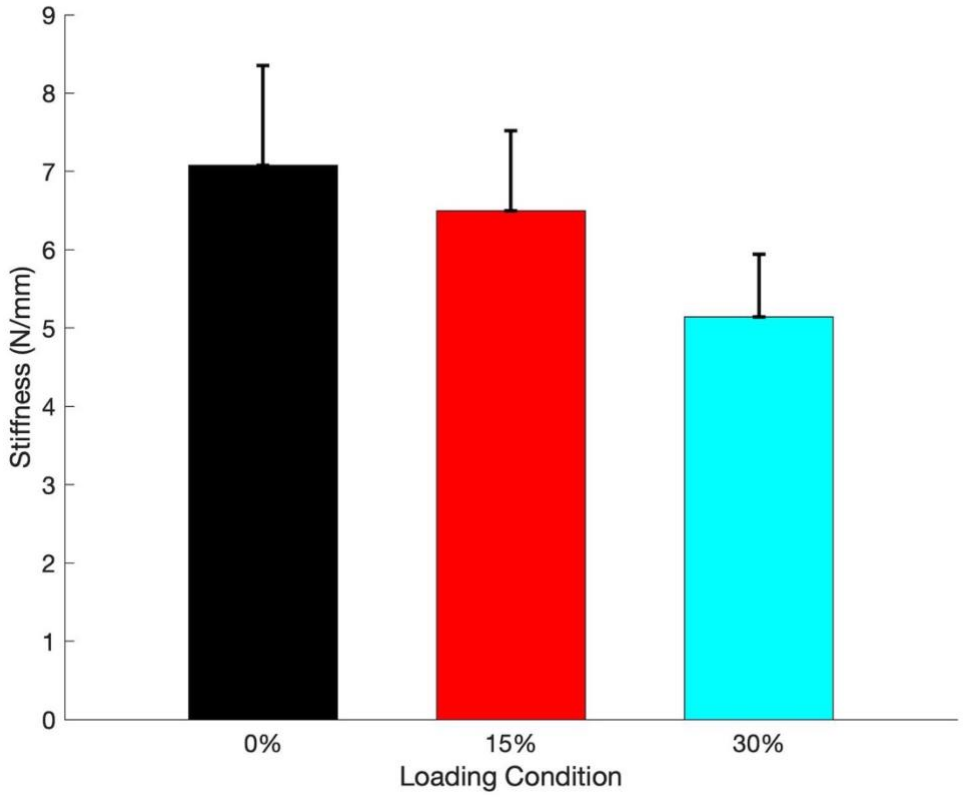

Figure 14: Leg Stiffness Across Loading Conditions
Leg Stiffness during load carriage of 0% BW, 15% BW, and 30% BW. Each bar is the average leg stiffness of the participants at the corresponding load carriage condition. The error bar is one standard deviation above the mean. Leg stiffness decreased significantly with load $p < .001$

Load Carriage Effects on Dominant vs NonDominant TFJ Magnitude and Distribution

No interaction was present for first peak total, medial, and lateral TFJ contact forces (tTFJ $p = .265$, $\eta_p^2 = .056$; mTFJ $p = .828$, $\eta_p^2 = .008$; lTFJ $p = .358$, $\eta_p^2 = .039$), **Table 7** & **Figure 15**. First peak total, medial, and lateral TFJ forces increased directly with increased load carriage (tTFJ $p < .001$, $\eta_p^2 = .903$; mTFJ $p < .001$, $\eta_p^2 = .910$; lTFJ $p < .001$, $\eta_p^2 = .776$). There was no difference between dominant and nondominant peak tTFJ contact force ($p = .088$, $\eta_p^2 = .121$), but nondominant peak mTFJ contact force was greater than dominant ($p = .026$, $\eta_p^2 = .198$), while dominant peak lTFJ contact force was greater than nondominant ($p < .001$, $\eta_p^2 = .369$), **Table 7** & **Figure 15** & **16**. At 0%, 15%, and 30% load carriage, nondominant peak mTFJ force was 107 N (7.0%), 93 N (5.4%), and 107 N (5.5%) greater than dominant; dominant peak lTFJ force was 140 N (21.5%), 167 N (22.7%), and 177 N (20.3%) greater than nondominant.

No significant interaction was present between load and limb dominance for total, medial, and lateral TFJ impulses (tTFJ $p = .498$, $\eta_p^2 = .027$; mTFJ $p = .768$, $\eta_p^2 = .074$; lTFJ $p = .058$, $\eta_p^2 = .133$), **Table 7** & **Figure 17**. Total, medial and lateral TFJ impulses increased with increasing load carriage (tTFJ $p < .001$, $\eta_p^2 = .889$; mTFJ $p < .001$, $\eta_p^2 = .890$; lTFJ $p < .001$, $\eta_p^2 = .759$) **Table 7** & **Figure 16** & **17**. No significant difference was present between dominant and nondominant tTFJ impulse ($p = .070$, $\eta_p^2 = .135$), but nondominant mTFJ impulse was greater than dominant ($p = .005$, $\eta_p^2 = .298$), while dominant lTFJ impulses was greater than nondominant ($p < .001$, $\eta_p^2 = .400$), **Table 7** & **Figure 17**. At 0%, 15%, and 30% load carriage, nondominant mTFJ impulse was 57 N·s (9.5%), 57 N·s (8.3%) 71 N·s (9.1%) greater than dominant; dominant lTFJ impulse was 72 N·s (29.9%), 80 N·s (28.8%), and 94 N·s (28.1%) greater than nondominant.

Table 7: Dominant and NonDominant Peak Tibiofemoral Joint Forces and Impulses, Mean (SD)

Variable		0%	15%	30%	Load	D vs ND	Interaction
Peak tTFJ (N)	D	1955 (487)	2291 (543)	2678 (685)	***p* < .001**	*p* = .088	*p* = .265
	ND	1885 (517)	2178 (547)	2558 (656)	**η_p^2= .903**	η_p^2= .121	η_p^2= .056
Peak mTFJ (N)	D	1467 (334)	1682 (397)	1898 (455)	***p* < .001**	***p* = .026**	*p* = .828
	ND	1574 (387)	1775 (438)	2005 (469)	**η_p^2= .910**	**η_p^2= .198**	η_p^2= .008
Peak lTFJ (N)	D	720 (245)	818 (292)	961 (358)	***p* < .001**	***p* < .001**	*p* = .358
	ND	580 (173)	651 (183)	784 (255)	**η_p^2 = .776**	**η_p^2 = .369**	η_p^2 = .039
tFJF Impulse (N·s)	D	847 (183)	975 (221)	1124 (278)	***p* < .001**	*p* = .070	*p* = .498
	ND	832 (202)	952 (236)	1101 (275)	**η_p^2 = .889**	η_p^2 = .135	η_p^2 = .027
mTFJ Impulse (N·s)	D	570 (138)	657 (172)	742 (195)	***p* < .001**	***p* = .005**	*p* = .181
	ND	627 (176)	714 (205)	813 (221)	**η_p^2= .890**	**η_p^2= .298**	η_p^2= .074
lTFJ Impulse (N·s)	D	277 (118)	318 (135)	382 (171)	***p* < .001**	***p* < .001**	*p* = .058
	ND	205 (80)	238 (86)	288 (124)	**η_p^2 = .759**	**η_p^2 = .400**	η_p^2 = .133

Averages (SD) for first peak and impulses of the tibiofemoral joint. 2x3 repeated measures ANOVA results for main effects and interactions.
0% load is walking with an unloaded weighted vest, 15% load is walking with the weighted vest loaded at 15% bodyweight, and 30% load is walking with the weighted vest loaded at 30% bodyweight. First peak medial and lateral tibiofemoral joint contact forces and tTFJ, mTFJ, and lTFJ impulses increased significantly with load.
η_p^2: Partial eta. Squared. N: Newtons. s: seconds.

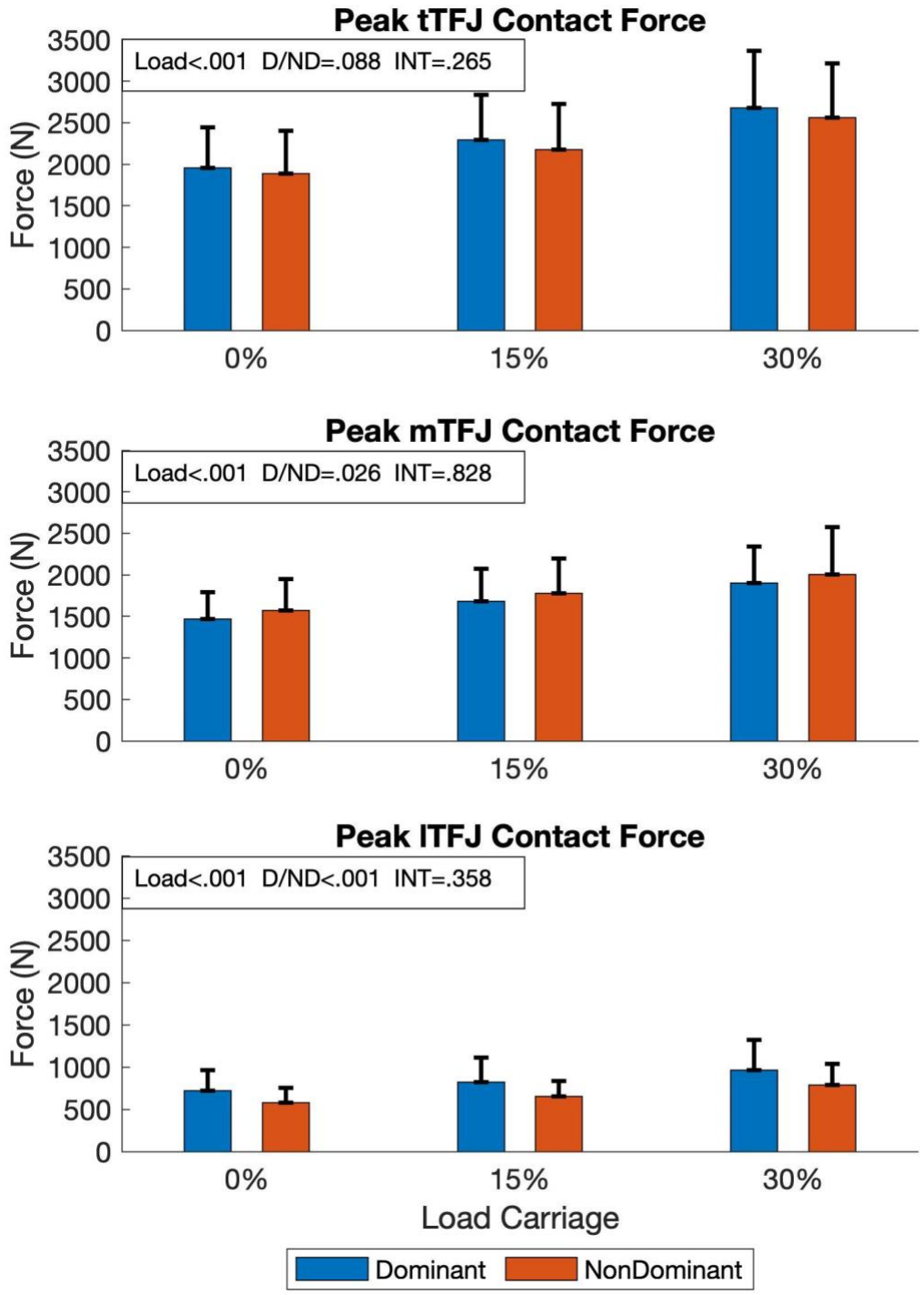

Figure 15: Dominant and NonDominant TFJ Contact Forces Across Loading Conditions
First peak total, medial and lateral dominant and nondominant TFJ forces during load carriage of 0% BW, 15% BW, and 30% BW. Each bar represents mean peak TFJ force at the corresponding load carriage condition. The error bar is one standard deviation above the mean.
Probing interaction through paired t-tests: *$p < 0.05$ between Dominant and NonDominant.
N: Newtons.

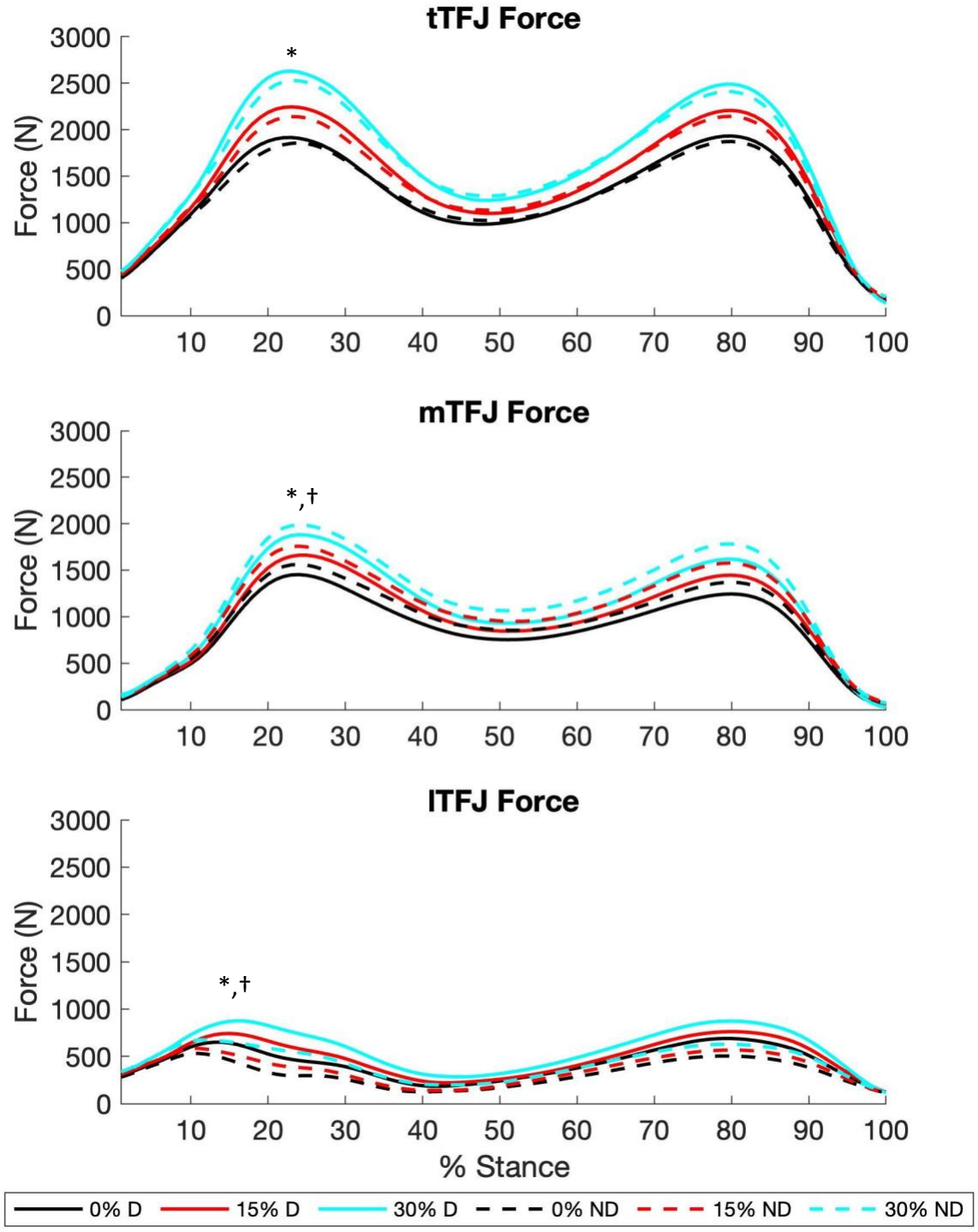

Figure 16: Time Series Dominant and NonDominant TFJ Force Across Loading Conditions Total, medial, and lateral tibiofemoral contact forces over percent stance during load carriage of 0% BW, 15% BW, and 30% BW. Lines represent the means across all participants. Impulse determined over nonnormalized time. #$p < 0.05$ for Interaction, *$p < 0.05$ for load effect, †$p < 0.05$ for leg dominance effect.

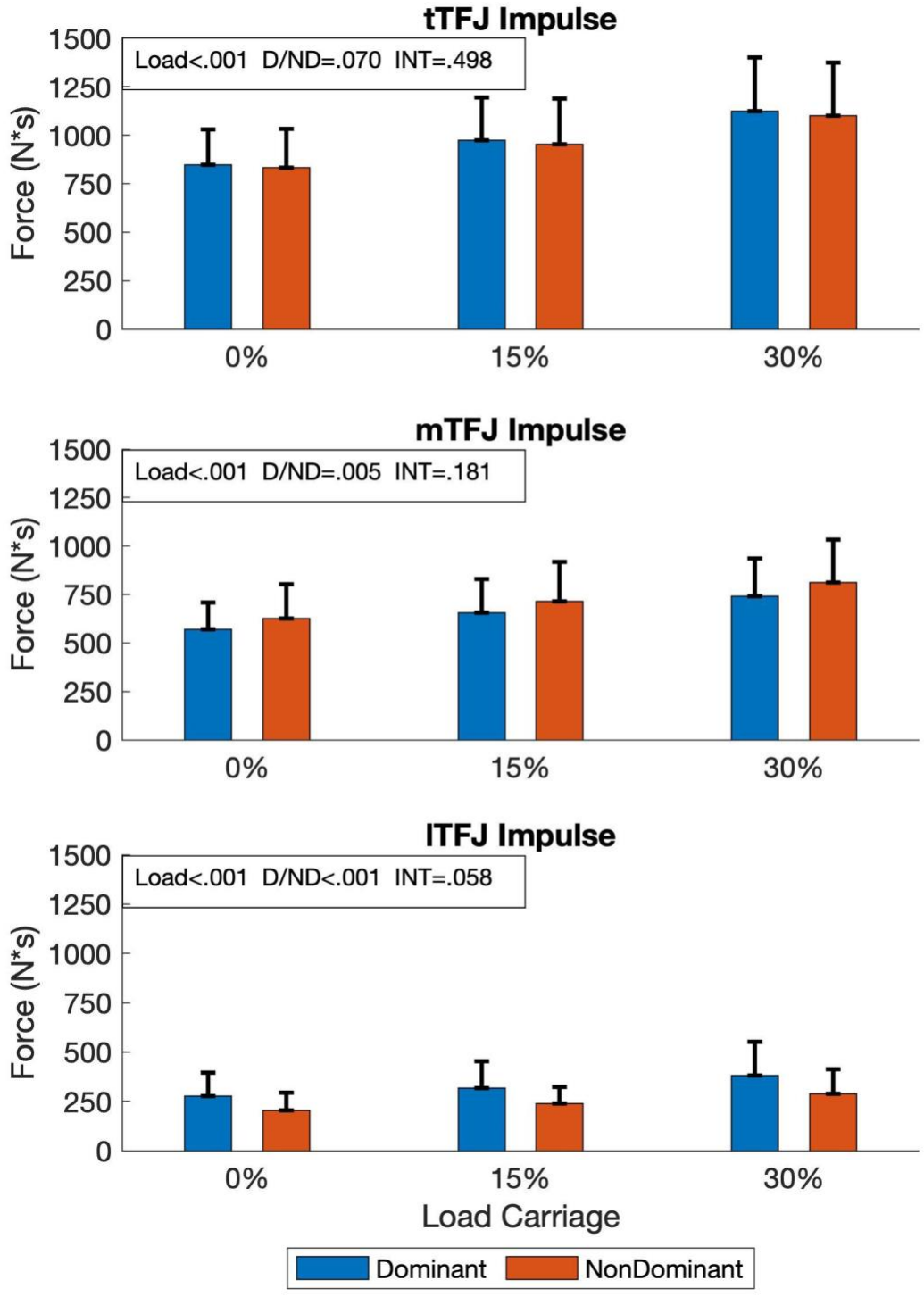

Figure 17: Dominant and NonDominant TFJ Impulse Across Loading Conditions
Total, medial and lateral dominant and nondominant TFJ impulses during load carriage of 0% BW, 15% BW, and 30% BW. Each bar represents mean peak TFJ force at the corresponding load carriage condition. The error bar is one standard deviation above the mean.
N: Newtons. s: seconds.

Load Carriage Effects on Dominant vs NonDominant Muscle Forces

An interaction between load and limb dominance with a medium effect size was present for first peak hamstring force (p = .046, η_p^2= .125). Probing the interaction between the dominant and nondominant limb at each loading condition via two-tailed paired t-tests revealed that there was no significant difference between limbs at 0% and 15% load (0% p = .745, d = .067; 15% p = .126, d = .325), but the nondominant limb experienced significantly greater tTFJ forces at 30% load (p = .027, d = .475) as compared to the dominant, **Table 8** & **Figure 18**. Probing the interaction on the effect of load carriage on dominant peak hamstrings force and nondominant peak hamstrings force via one-way repeated measures ANOVAs revealed that dominant and nondominant peak hamstrings force increased with increasing load (D p < .001, η_p^2= .595; ND p < .001, η_p^2 = .798), **Table 8**. No interaction was present for peak quadriceps force (p = .134, η_p^2= .084), **Table 9**. Peak quadriceps force increased with increasing load carriage (p < .001, η_p^2 = .782) with dominant being greater than nondominant (p = .011, η_p^2= .249), **Table 9 & Figure 18 & 19**. At 0%, 15%, and 30% load carriage, nondominant peak hamstring force was 4 N (0.9%), 20 N (4.0%), and 33 N (5.8%) greater than dominant; dominant peak quadriceps force was 130 N (14.5%), 169 N (16.0%), and 194 N (15.1%) greater than nondominant.

No significant interaction was present between load and limb dominance for hamstrings, quadriceps, or gastrocnemius impulses (Ham p = .197, η_p^2 = .070; Quad p = .138, η_p^2 = .086; Gastroc p = .645, η_p^2 = .018), **Table 9 & Figure 19 & 20**. Hamstring, quadriceps, and gastrocnemius impulses all increased with load carriage (Ham p < .001, η_p^2 = .547; Quad p = .181, η_p^2 = .890; Gastroc p < .001, η_p^2 = .786) with no significant differences between dominant and nondominant hamstring or gastrocnemius impulse (Ham p = .084, η_p^2= .124; Gastroc p = .312, η_p^2 = .044), but dominant quad impulse was greater than nondominant (p = .030, η_p^2 = .190, **Table 9**

& Figure 19 & 20. At 0%, 15%, and 30% load carriage, the dominant and quadriceps impulse was 16 N·s (6.7%), 24 N·s (8.6%) 24 N·s (7.2%).

Table 8: D vs. ND Peak Hamstrings Force Across Load Interaction, Mean (SD)

Variable		0%	15%	30%	$\underline{p}$ η_p^2
Peak Ham Force (N)	D	458 (161)	495 (178)	557 (216)	**$\underline{p < .001}$** **$\eta_p^2 = .595$**
	ND	462 (174)	515 (192)	591 (213)	**$\underline{p < .001}$** **$\eta_p^2 = .708$**
					Interaction
	$\underline{p}$ d	$\underline{p = .745}$ $d = .067$	$\underline{p = .126}$ $d = .325$	**$\underline{p = .026}$** $d = .484$	**$\underline{p = .027}$** **$\eta_p^2 = .483$**

Averages (SD) for first peak total hamstrings force. 2x3 repeated measures ANOVA results for main effects and interactions. Two-tailed paired samples t-tests results for dominant vs nondominant peak hamstrings force at each loading condition, and one-way repeated measures ANOVA results for dominant peak hamstrings force across each loading condition and nondominant peak hamstrings force across each loading condition.
0% load is walking with an unloaded weighted vest, 15% load is walking with the weighted vest loaded at 15% bodyweight, and 30% load is walking with the weighted vest loaded at 30% bodyweight.
η_p^2: Partial eta. Squared. *d*: Cohen's d. N: Newtons.

Table 9: Dominant and NonDominant Peak Muscle Forces and Impulses, Mean (SD)

Variable		0%	15%	30%	Load	D vs ND	Interaction
Peak Quad Force (N)	D	964 (335)	1143 (404)	1384 (499)	**$p < .001$**	**$p = .011$**	$p = .134$
	ND	834 (359)	974 (363)	1190 (479)	**$\eta_p^2 = .782$**	**$\eta_p^2 = .249$**	$\eta_p^2 = .084$
Ham Impulse (N·s)	D	85 (49)	96 (57)	111 (70)	**$p < .001$**	$p = .084$	$p = .197$
	ND	89 (48)	102 (57)	120 (68)	**$\eta_p^2 = .547$**	$\eta_p^2 = .124$	$\eta_p^2 = .070$
Quad Impulse (N·s)	D	248 (71)	291 (86)	344 (108)	**$p < .001$**	**$p = .030$**	$p = .127$
	ND	232 (76)	267 (83)	320 (105)	**$\eta_p^2 = .836$**	**$\eta_p^2 = .190$**	$\eta_p^2 = .086$
Gastroc Impulse (N·s)	D	211 (46)	240 (60)	276 (78)	**$p < .001$**	$p = .312$	$p = .653$
	ND	208 (56)	235 (66)	270 (79)	**$\eta_p^2 = .786$**	$\eta_p^2 = .044$	$\eta_p^2 = .018$

Averages (SD) for peak quadriceps forces and hamstrings and quadriceps impulses, along with gastrocnemius impulse. 2x3 repeated measures ANOVA results for main effects and interactions. 0% load is walking with an unloaded weighted vest, 15% load is the weighted vest loaded at 15% bodyweight, and 30% load is the vest loaded at 30% bodyweight.
η_p^2: Partial eta. Squared. N: Newtons. s: seconds.

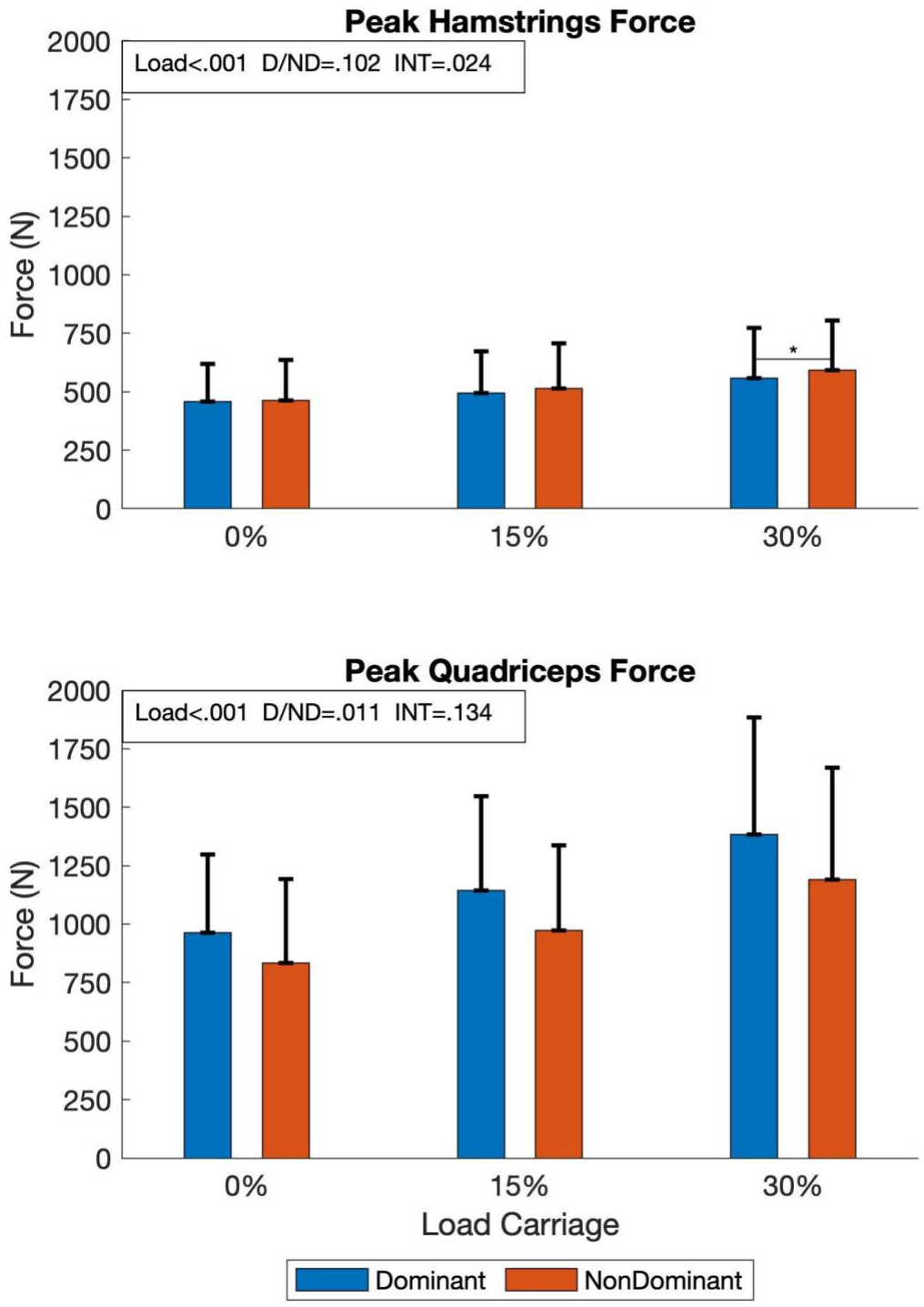

Figure 18: Dominant and NonDominant Peak Muscle Forces Across Loading Conditions
Hamstrings and quadriceps dominant and nondominant forces during load carriage of 0% BW, 15% BW, and 30% BW. Each bar represents mean peak TFJ force at the corresponding load carriage condition. The error bar is one standard deviation above the mean.
N: Newtons. s: seconds.

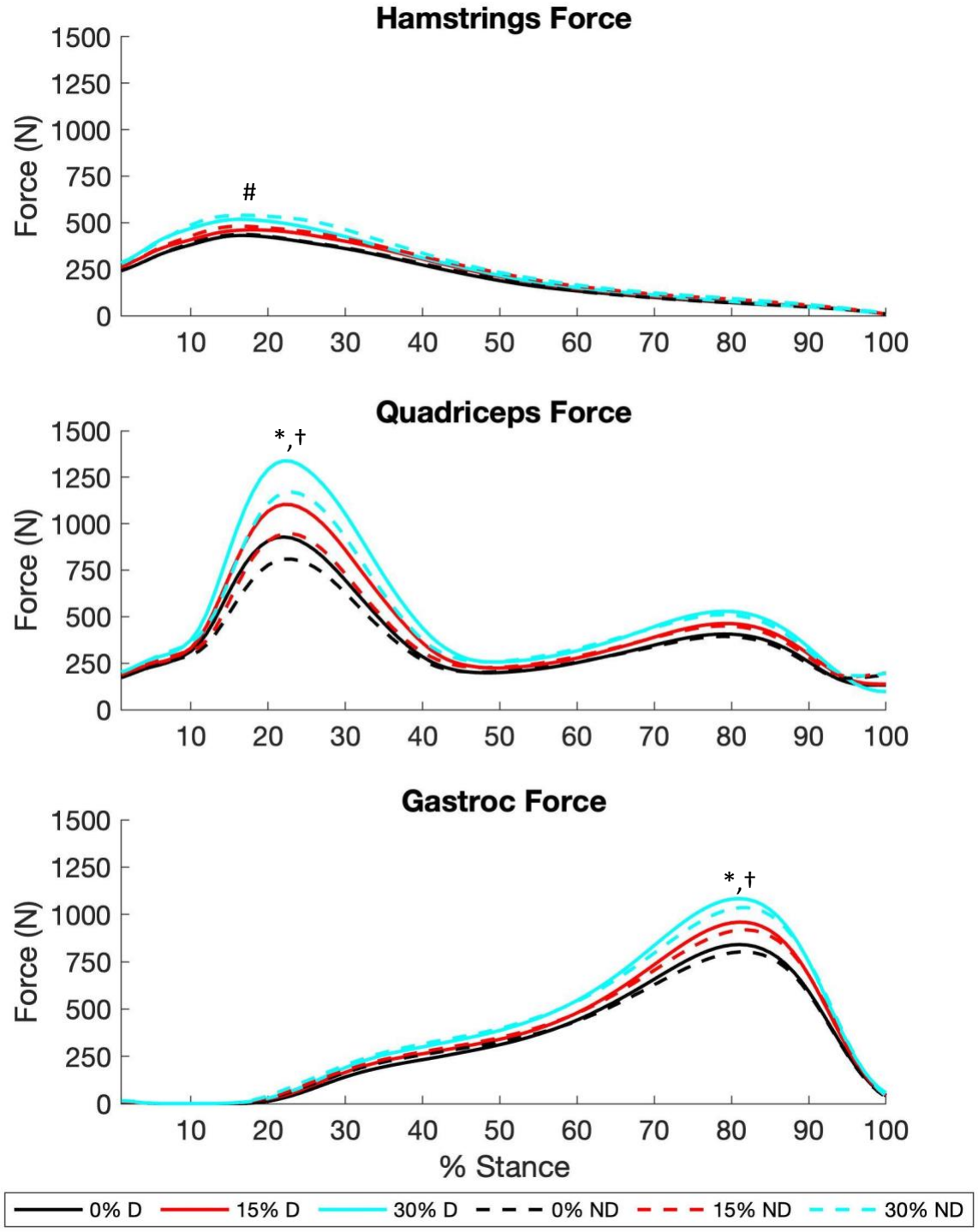

Figure 19: Time Series Dominant and NonDominant TFJ Force Across Loading Conditions Hamstrings and Quadriceps forces over percent stance during load carriage of 0% BW, 15% BW, and 30% BW. Lines represent the means across all participants. Impulse determined over nonnormalized time. Impulse determined over nonnormalized time. #$p < 0.05$ for Interaction, *$p < 0.05$ for load effect, †$p < 0.05$ for leg dominance effect.

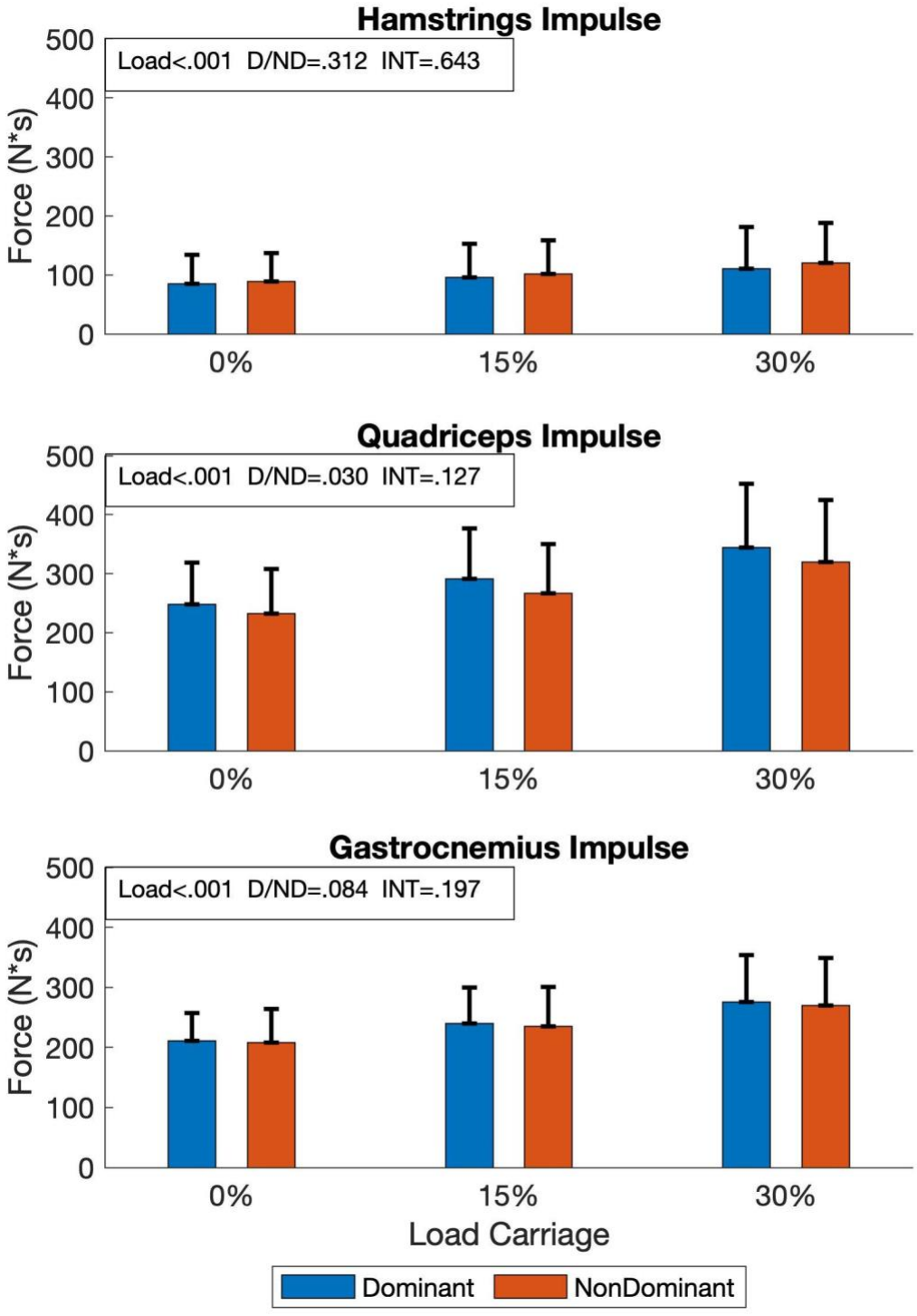

Figure 20: Dominant and NonDominant Muscle Impulses Across Loading Conditions
Hamstrings, quadriceps, and gastrocnemius dominant and nondominant impulses during load carriage of 0% BW, 15% BW, and 30% BW. Each bar represents mean peak TFJ force at the corresponding load carriage condition. The error bar is one standard deviation above the mean. N: Newtons. s: seconds.

Load Carriage Effects on Dominant vs NonDominant Sagittal and Frontal Plane Moments

No interactions were present for peak internal knee extension moment or peak knee abduction moment (KEM $p = .198$, $\eta_p^2 = .068$; KAM $p = .286$, $\eta_p^2 = .052$), **Table 10 & Figure 21**. Peak knee extension and abduction moments increased directly with increased load carriage (KEM $p < .001$, $\eta_p^2 = .659$; KAM $p < .001$, $\eta_p^2 = .712$) with dominant knee extension moment being greater than nondominant ($p = .016$, $\eta_p^2 = .226$), and nondominant peak knee abduction moment being greater than dominant ($p = .005$, $\eta_p^2 = .299$) **Table 10** & **Figure 21** & **22**. At 0%, 15%, and 30%; dominant peak knee extension moment was 0.11 N·m/kg (22.2%), 0.13 N·m/kg (21.8%), and 0.15 N·m/kg (20.7%) greater than nondominant, while nondominant peak abduction moment was 0.11 N·m/kg (20.8%), 0.10 N·m/kg (16.8%), and 0.12 N·m/kg (19.1%) greater than dominant.

No interactions between load and limb dominance were present for knee extension or abduction angular impulse (KEAI $p = .442$, $\eta_p^2 = .035$; KAAI $p = .072$, $\eta_p^2 = .127$), **Table 10 & Figure 23**. Peak knee extension and abduction angular impulses increased with increasing load carriage (KEAI $p < .001$, $\eta_p^2 = .615$; KAAI $p < .001$, $\eta_p^2 = .556$). Dominant knee extension angular impulse was greater than dominant ($p = .011$, $\eta_p^2 = .248$), while nondominant knee abduction angular impulse was greater than ($p = .003$, $\eta_p^2 = .320$), **Table 10** & **Figure 22** & **23**. At 0%, 15%, and 30%; dominant knee extension angular impulse was 0.02 N·m·s/kg (33.0%), 0.02 N·m·s/kg (28.0%), and 0.02 N·m·s/kg (22.0%) greater than nondominant, and nondominant peak abduction moment was 0.03 N·m·s/kg (20.7%), 0.05 N·m·s/kg (28.8%), and 0.06 N·m·s/kg (31.6%) greater than dominant.

Table 10: Dominant and NonDominant Peak Sagittal and Frontal Plane Moments Mean (SD)

Variable		0%	15%	30%	Load	D vs ND	Interaction
Peak Knee Extension Moment (N·m/kg)	D	0.55 (0.24)	0.66 (0.30)	0.80 (0.35)	***p* < .001**	***p* = .016**	p = .198
	ND	0.44 (0.25)	0.53 (0.26)	0.65 (0.36)	**η_p^2= .659**	**η_p^2= .226**	η_p^2= .068
Peak Knee Abduction Moment (N·m/kg)	D	-0.43 (0.16)	-0.49 (0.19)	-0.52 (0.20)	***p* < .001**	***p* = .005**	p = .286
	ND	-0.54 (0.12)	-0.59 (0.14)	-0.64 (0.17)	**η_p^2 = .712**	**η_p^2 = .299**	η_p^2 = .052
Knee Extension Angular Impulse (N·m·s/kg)	D	0.07 (0.03)	0.08 (0.04)	0.10 (0.05)	***p* < .001**	***p* = .011**	p = .442
	ND	0.05 (0.03)	0.06 (0.04)	0.08 (0.05)	**η_p^2= .615**	**η_p^2= .248**	η_p^2= .035
Knee Abduction Angular Impulse (N·m·s/kg)	D	-0.13 (0.06)	-0.15 (0.08)	-0.16 (0.08)	***p* < .001**	***p* = .003**	p = .072
	ND	-0.16 (0.07)	-0.20 (0.06)	-0.22 (0.07)	**η_p^2 = .556**	**η_p^2 = .320**	η_p^2 = .127

Averages (SD) for first peak and impulses of the tibiofemoral joint. 2x3 repeated measures ANOVA results for main effects and interactions.
0% load is walking with an unloaded weighted vest, 15% load is walking with the weighted vest loaded at 15% bodyweight, and 30% load is walking with the weighted vest loaded at 30% bodyweight.
η_p^2: Partial eta. Squared. N: Newtons. s: seconds. m: meters kg: kilograms

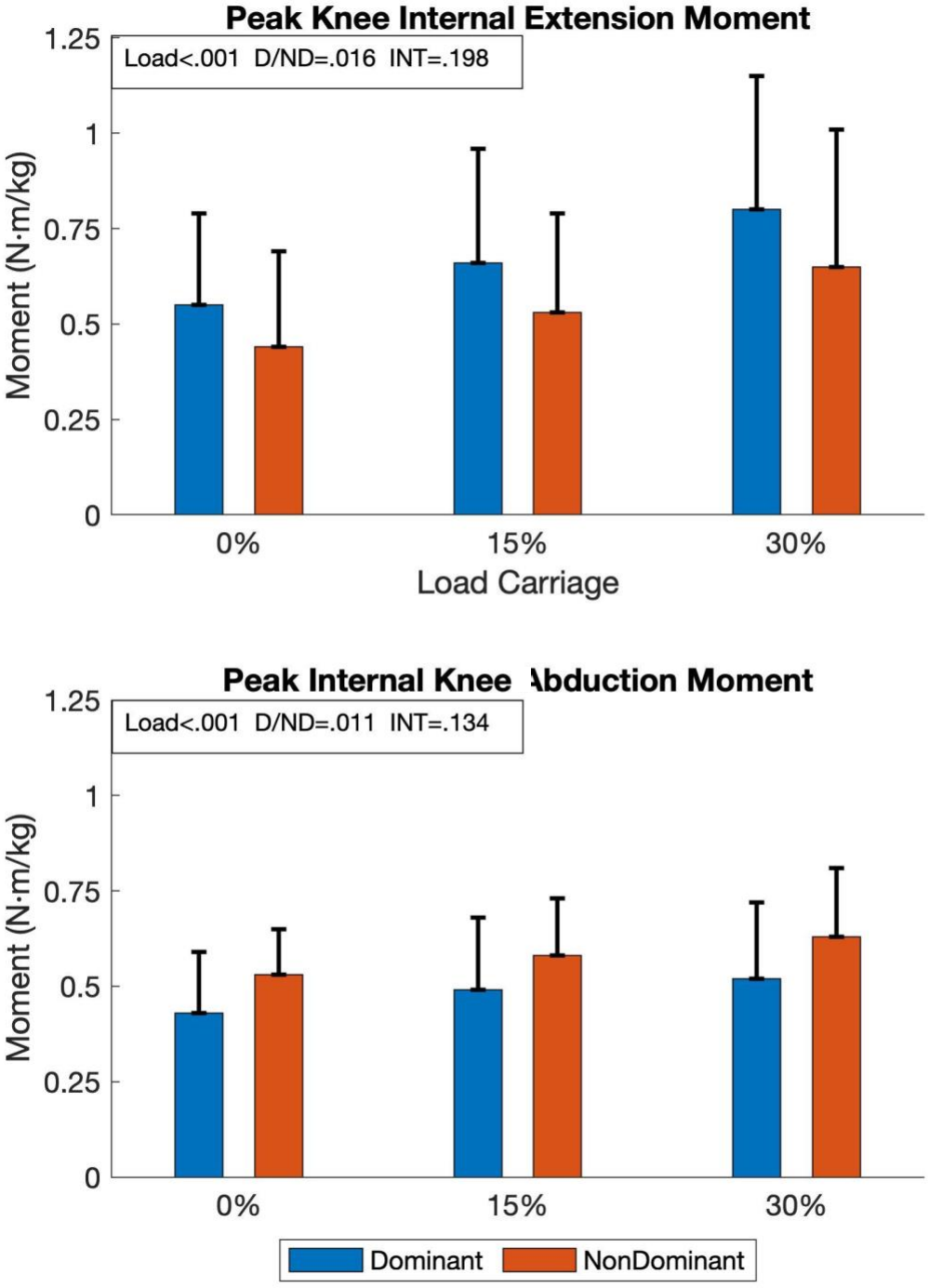

14

Figure 21: Dominant and NonDominant Muscle Impulses Across Loading Conditions
Dominant and nondominant peak internal, peak internal knee extension and abduction moments during load carriage of 0% BW, 15% BW, and 30% BW. Each bar represents mean knee moment at the corresponding load carriage condition. The error bar is one standard deviation above the mean. N: Newtons. m: meters. kg: kilograms

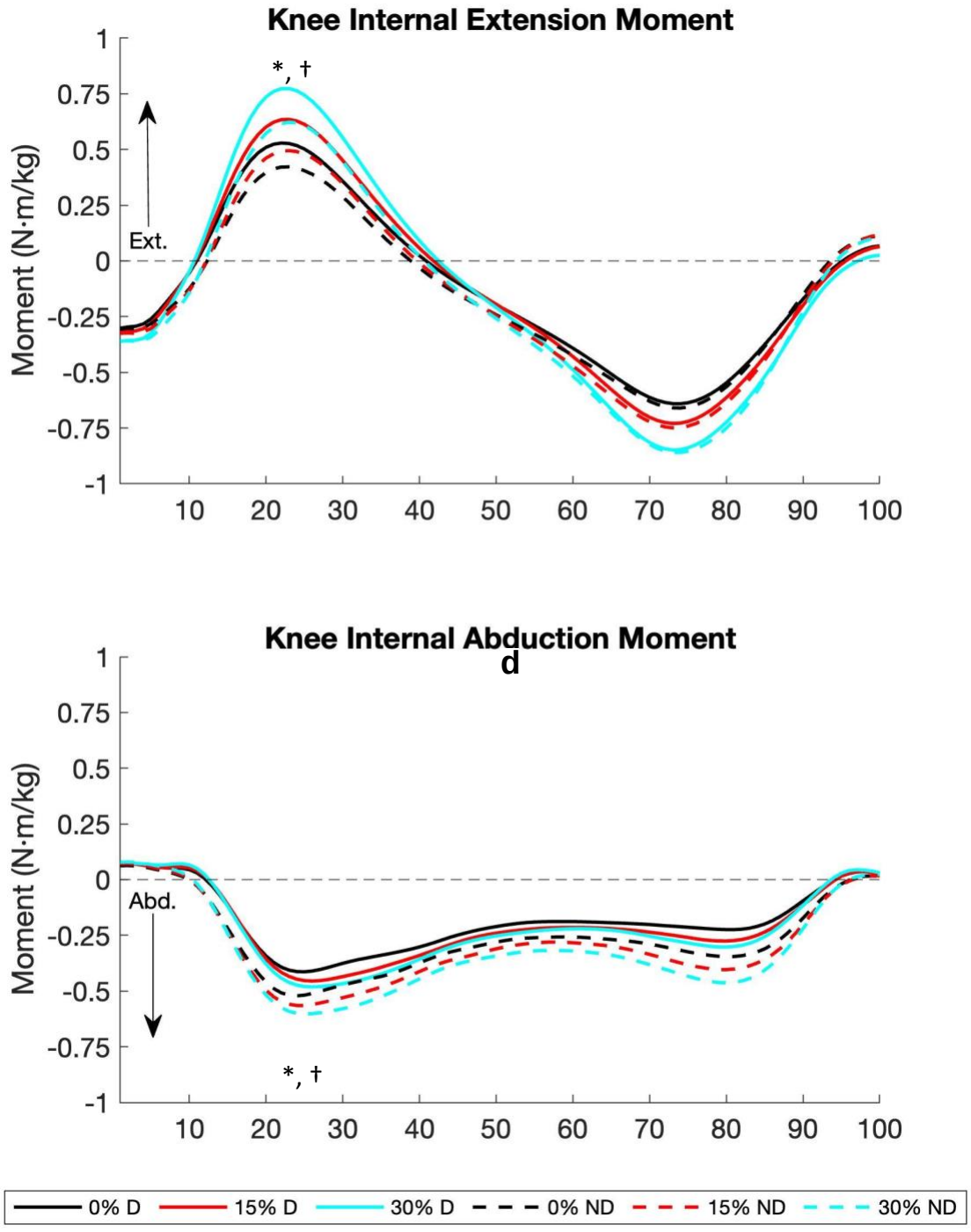

Figure 22: Time Series D vs ND Sagittal Moments Across Loading Conditions
Dominant and nondominant internal peak internal knee extension and abduction moments over percent stance during load carriage of 0% BW, 15% BW, and 30% BW. Lines represent the means across all participants. #$p < 0.05$ for Interaction, *$p < 0.05$ for load effect, †$p < 0.05$ for leg dominance effect.

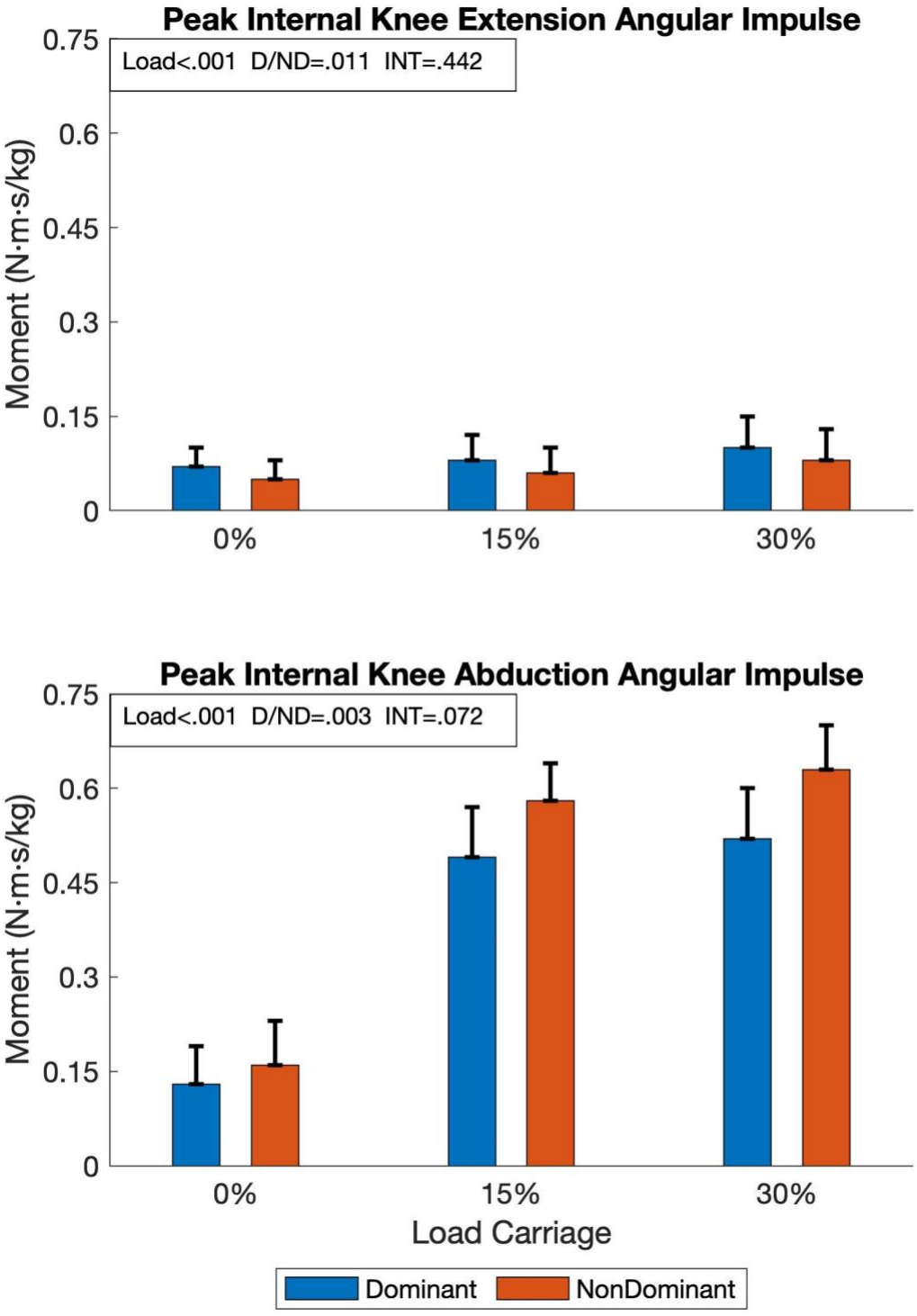

Figure 23: Dominant and NonDominant Frontal Moments Across Loading Conditions
Dominant and nondominant internal knee extension and abduction angular impulses during load carriage of 0% BW, 15% BW, and 30% BW. Each bar represents mean frontal plane moment at the corresponding load carriage condition. The error bar is one standard deviation above the mean. N: Newtons. m: meters. kg: kilograms

Load Carriage Effects on Dominant vs NonDominant Ground Reaction Forces

No interactions were present between load and limb dominance for first peak vGRF, first peak mGRF or peak bGRF (vGRF p = .130, η_p^2 = .085; mGRF p = .908, η_p^2 = .004; bGRF p = .447, η_p^2 = .034), **Table 11** & **Figure 24**. First peak vGRF, mGRF and bGRF increased with increasing load carriage (vGRF p < .001, η_p^2= .959; mGRF p < .001, η_p^2 = .586; bGRF p < .001, η_p^2 = .952). There was no difference between dominant and nondominant first peak vGRF and peak bGRF (vGRF p = .177, η_p^2 = .078; bGRF p = .946, η_p^2 < .001), but nondominant mGRF was greater than dominant (p = .004, η_p^2 = .314), **Table 11** & **Figure 24** & **25**. At 0%, 15%, and 30% load carriage; nondominant peak mGRF force was 7 N (10.2%), 5 N (6.6%), and 7 N (8.2%) greater than dominant.

No significant interaction was present between load and limb dominance for vGRF impulse (p = .869, η_p^2 = .006), mGRF impulse (p = .534, η_p^2 = .055) or bGRF impulse (p = .066, η_p^2 = .112), **Table 11** & **26**. vGRF, mGRF, and bGRF impulse all increased with increasing load carriage (p < .001, η_p^2 = .955), medial TFJ impulse (p < .001, η_p^2 = .677), and lateral TFJ impulse (p < .001, η_p^2 = .759) increased with increasing load carriage. Dominant vGRF impulses were greater than nondominant (p = .032, η_p^2 = .185), but nondominant mGRF impulse was greater than dominant (p = .002, η_p^2 = .358), **Table 11** & **Figure 25** & **26**. At 0%, 15%, and 30% load carriage, dominant vGRF impulse was 4 N·s (1.1%), 3 N·s (0.7%) 5 N·s (1.1%) greater than nondominant, and nondominant mGRF impulse was 1 N·s (4.4%), 1 N·s (3.9%), and 1 N·s (3.5%) greater than dominant.

Table 11: Dominant and NonDominant Peak GRF and Impulses, Mean (SD)

Variable		0%	15%	30%	Load	D vs ND	Interaction
Peak vGRF (N)	D	804 (113)	927 (124)	1042 (153)	***p* < .001**	*p* = .177	*p* = .130
	ND	802 (124)	913 (139)	1025 (158)	**η_p^2 = .959**	η_p^2 = .078	η_p^2 = .085
Peak mGRF (N)	D	65 (11)	73 (14)	81 (16)	***p* < .001**	***p* = .004**	*p* = .908
	ND	72 (14)	78 (17)	88 (19)	**η_p^2 = .586**	**η_p^2 = .311**	η_p^2 = .004
Peak bGRF (N)	D	143 (22)	170 (30)	197 (29)	***p* < .001**	*P* = .946	*p* = .447
	ND	146 (29)	170 (29)	196 (34)	**η_p^2 = .952**	η_p^2 = .000	η_p^2 = .034
vGRF Impulse (N·s)	D	355 (54)	402 (65)	453 (75)	***p* < .001**	***p* = .032**	*p* = .869
	ND	351 (58)	399 (69)	448 (75)	**η_p^2 = .955**	**η_p^2 = .185**	η_p^2 = .006
mGRF Impulse (N·s)	D	22 (4)	25 (5)	28 (6)	***p* < .001**	***p* = .002**	*p* = .534
	ND	23 (5)	26 (5)	29 (6)	**η_p^2 = .677**	**η_p^2 = .358**	η_p^2 = .055
bGRF Impulse (N·s)	D	22 (4)	26 (5)	30 (5)	***p* < .001**	*p* = .195	*p* = .066
	ND	22 (4)	26 (5)	30 (5)	**η_p^2 = .932**	**η_p^2 = .400**	η_p^2 = .112

Averages (SD) for first peak and impulses of vGRF, mGRF, and bGRF. 2x3 repeated measures ANOVA results for main effects and interactions.

0% load is walking with an unloaded weighted vest, 15% load is walking with the weighted vest loaded at 15% bodyweight, and 30% load is walking with the weighted vest loaded at 30% bodyweight.

η_p^2: Partial eta. Squared. N: Newtons. s: seconds.

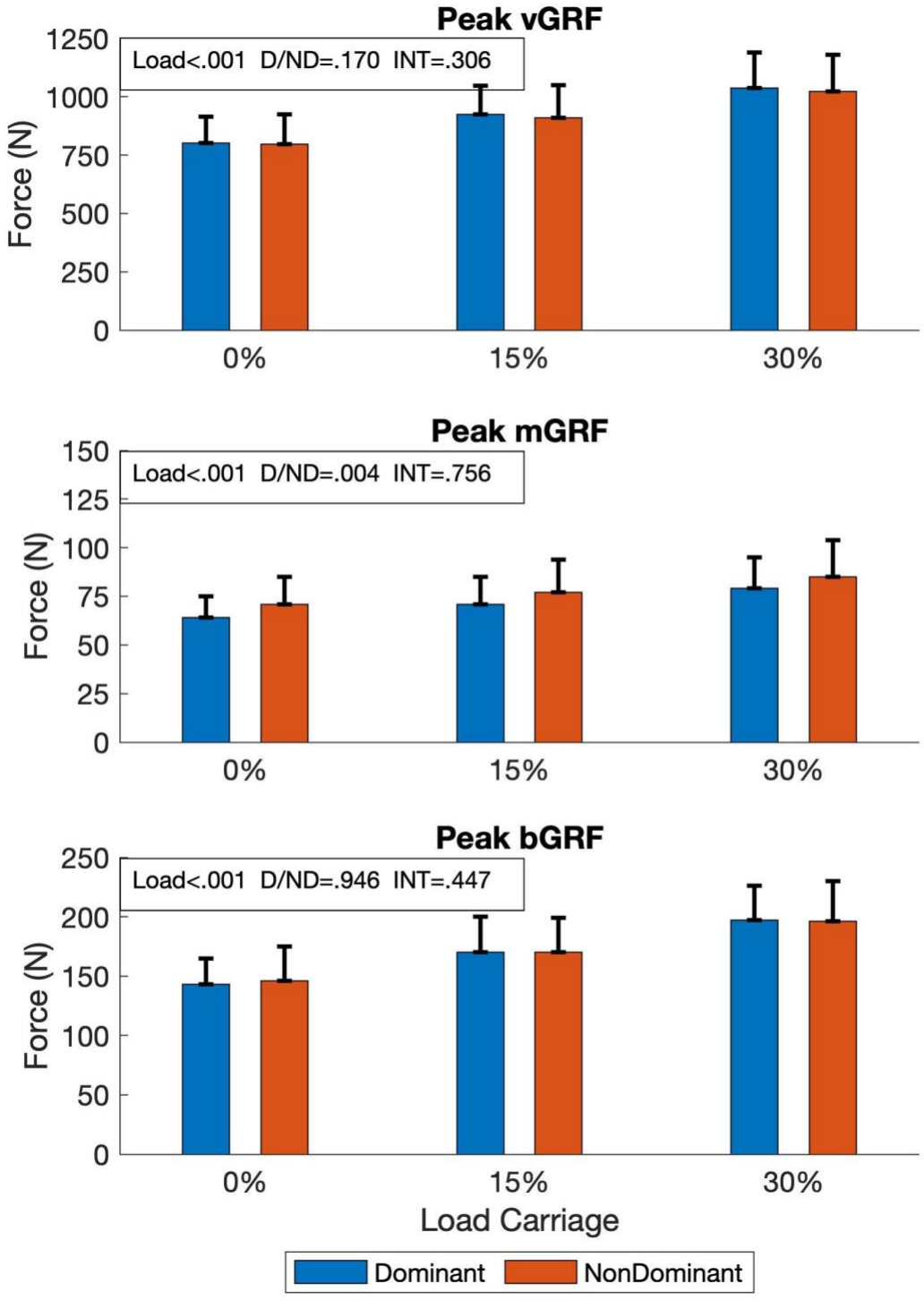

Figure 24: Dominant and NonDominant Peak GRF Across Loading Conditions
Peak vertical, medial, and breaking dominant and nondominant ground reaction forces during load carriage of 0% BW, 15% BW, and 30% BW. Each bar represents mean peak GRF at the corresponding load carriage condition. The error bar is one standard deviation above the mean. N: Newtons. s: seconds.

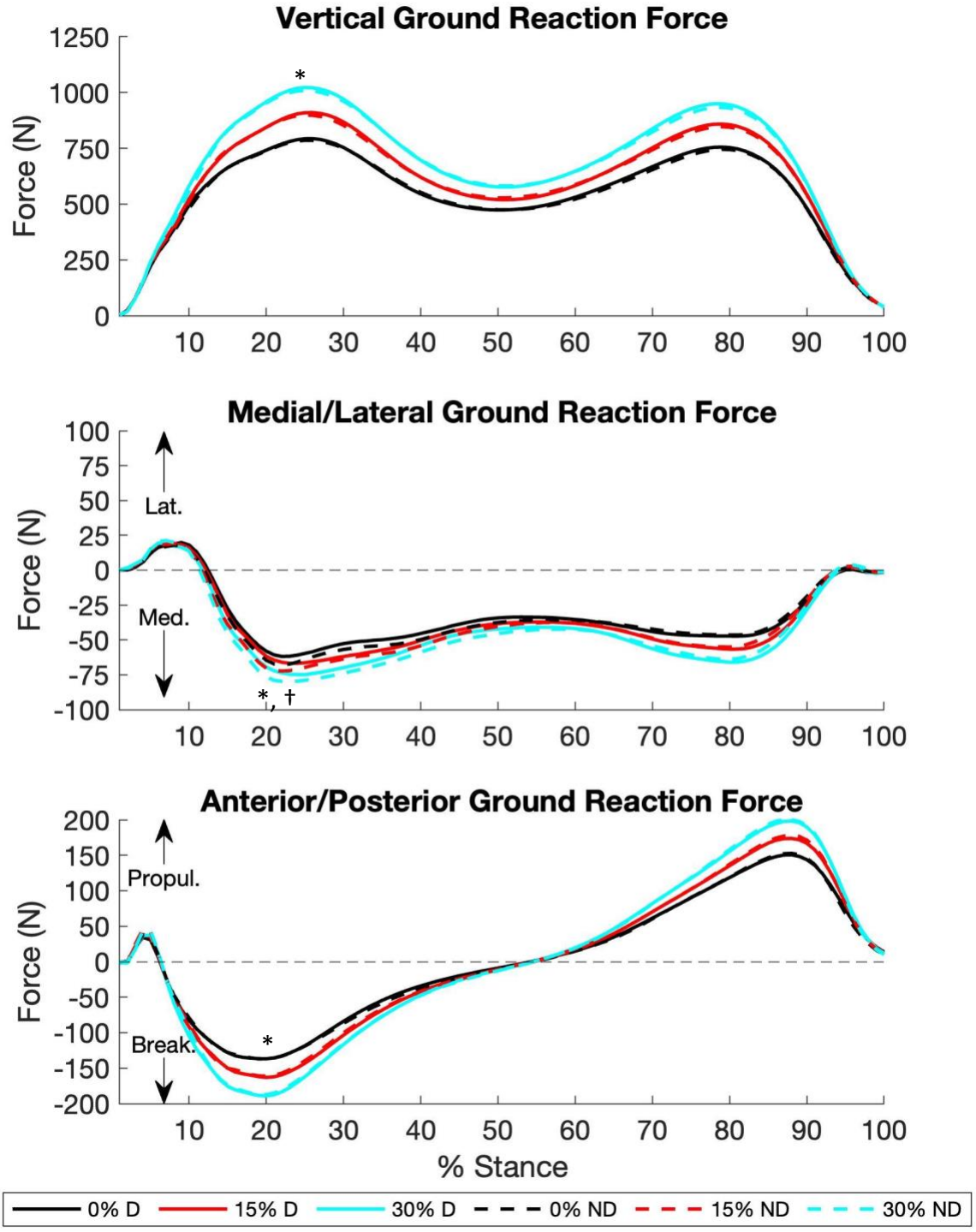

Figure 25: Time Series Dominant and NonDominant TFJ Force Across Loading Conditions
Dominant and nondominant hamstrings and quadriceps forces over percent stance during load carriage of 0% BW, 15% BW, and 30% BW. Lines represent the means across all participants. Impulse determined over nonnormalized time. #$p < 0.05$ for Interaction, *$p < 0.05$ for load effect, †$p < 0.05$ for leg dominance effect.

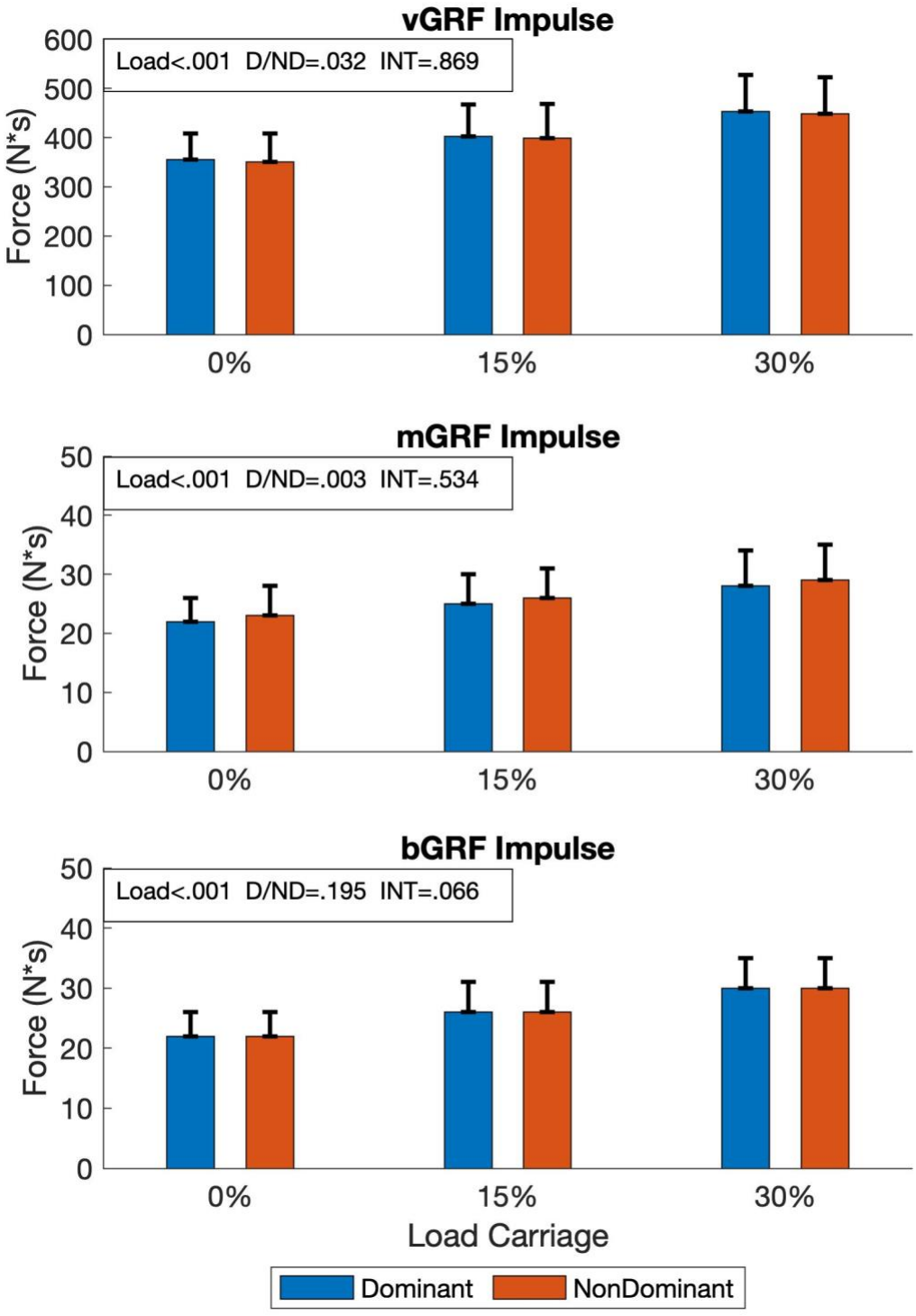

Figure 26: Dominant and NonDominant GRF Impulse Across Loading Conditions
Peak vertical, medial, and breaking dominant and nondominant ground reaction impulses during load carriage of 0% BW, 15% BW, and 30% BW. Each bar represents mean impulse at the corresponding load carriage condition. The error bar is one standard deviation above the mean. N: Newtons. s: seconds.

Load Carriage Effects on D vs ND Spatiotemporal Parameters and Kinematics

No interactions were present between load and limb dominance for step length (p = .606, η_p^2 = .022), stance time (p = .917, η_p^2 = .004), peak lower extremity sagittal plane angles (Peak Hip Flexion p = .204, η_p^2 = .067; Peak Knee Flexion p = .446, η^2 = .034; Peak Ankle Dorsiflexion p = .152, η^2 = .079), peak lower extremity frontal plane angles (Peak Hip Adduction p = .161, η_p^2 = .076; Peak Knee Adduction p = .577, η_p^2 = .020), or leg stiffness (p = .989, η_p^2 =.000), **Table 13** & **Figure 31** & **32**. There were no significant changes for step length with increasing load (p = .494, η_p^2 = .026), and no differences between dominant and nondominant step length (p = .313, η_p^2 = .044). Stance time increased with increasing load (p < .001, η_p^2 = .454) but there was no difference between limbs (p = .184, η_p^2 = .074). Lower extremity peak sagittal plane angles all increased with load (Peak Hip Flexion p = .006, η_p^2 = .223; Peak Knee Flexion p < .001, η_p^2 = .504; Peak Ankle Dorsiflexion p < .001, η_p^2= .338), **Table 13** & **Figure 31**. Peak lower extremity frontal plane angles did not change with increasing load (Peak Hip Adduction p = .593, η_p^2 = .022; Peak Knee Adduction p = .111, η_p^2= .091) nor was there a difference between limbs (Peak Hip Adduction p = .639, η_p^2= .011; Peak Knee Adduction p = .392, η_p^2= .032), **Table 13** & **Figure 32**. Leg stiffness decreased with increasing load (p < .001, η_p^2= .856), but there was no difference between the dominant and nondominant limb (p = .686, η_p^2= .007), **Table 13**.

Table 12: Dominant and NonDominant Spatiotemporal Parameters and Kinematics Mean (SD)

Variable		0%	15%	30%	Load	D vs ND	Interaction
Step Length (m)	D	0.73 (0.03)	0.72 (0.03)	0.72 (0.03)	p = .494	p = .313	p = .606
	ND	0.72 (0.03)	0.72 (0.03)	0.72 (0.03)	η_p^2 = .026	η_p^2 = .044	η_p^2 = .022
Stance Time (ms)	D	644 (26)	650 (30)	659 (31)	**p < .001**	p = .184	p = .917
	ND	642 (30)	648 (32)	657 (33)	**η_p^2 = .454**	η_p^2 = .074	η_p^2 = .004
Peak Hip Flexion (°)	D	25.9 (10.1)	27.2 (11.2)	27.8 (12.5)	**p = .006**	P = .530	p = .204
	ND	25.6 (10.2)	26.7 (11.1)	27.7 (12.5)	**η_p^2 = .223**	η_p^2 = .017	η_p^2 = .067
Peak Knee Flexion (°)	D	-18.9 (4.4)	-19.9 (4.5)	-20.9 (5.3)	**p < .001**	p = .315	p = .446
	ND	-18.3 (4.8)	-18.9 (4.3)	-20.3 (5.2)	**η_p^2 = .504**	η_p^2 = .044	η_p^2 = .034
Peak Ankle Plantar Flexion (°)	D	-7.2 (4.2)	-8.1 (3.7)	-8.7 (3.9)	**p < .001**	p = .219	p = .152
	ND	-8.0 (3.4)	-8.7 (3.1)	-9.0 (3.4)	**η_p^2 = .338**	η_p^2 = .065	η_p^2 = .079
Peak Hip Adduction (°)	D	5.2 (2.5)	5.3 (2.6)	4.8 (3.0)	p = .593	p = .639	p = .161
	ND	5.3 (3.2)	5.5 (3.2)	5.6 (3.2)	η_p^2 = .022	η_p^2 = .010	η_p^2 = .076
Peak Knee Adduction (°)	D	2.3 (2.5)	2.6 (2.6)	2.5 (3.0)	p = .111	p = .392	p = .577
	ND	1.8 (3.2)	2.2 (3.2)	2.3 (3.2)	η_p^2 = .091	η_p^2 = .032	η_p^2 = .020
Leg Stiffness ($N \cdot mm^{-1}$)	D	7.1 (1.2)	6.5 (1.0)	5.2 (0.8)	**p < .001**	p = .686	p = .989
	ND	7.1 (1.3)	6.5 (1.0)	5.2 (0.8)	**η_p^2 = .856**	η_p^2 = .007	η_p^2 = .000

Averages (SD) for step length, stance time, peak sagittal plane and frontal plane lower extremity kinematics, and leg stiffness. 2x3 repeated measures ANOVA results for main effects and interactions.

No-Load is walking with an unloaded weighted vest, 15% Load is walking with the weighted vest loaded at 15% bodyweight, 30% Load is walking with the weighted vest loaded at 30% bodyweight.

η_p^2: Partial eta. Squared. N: Newtons. s: seconds.

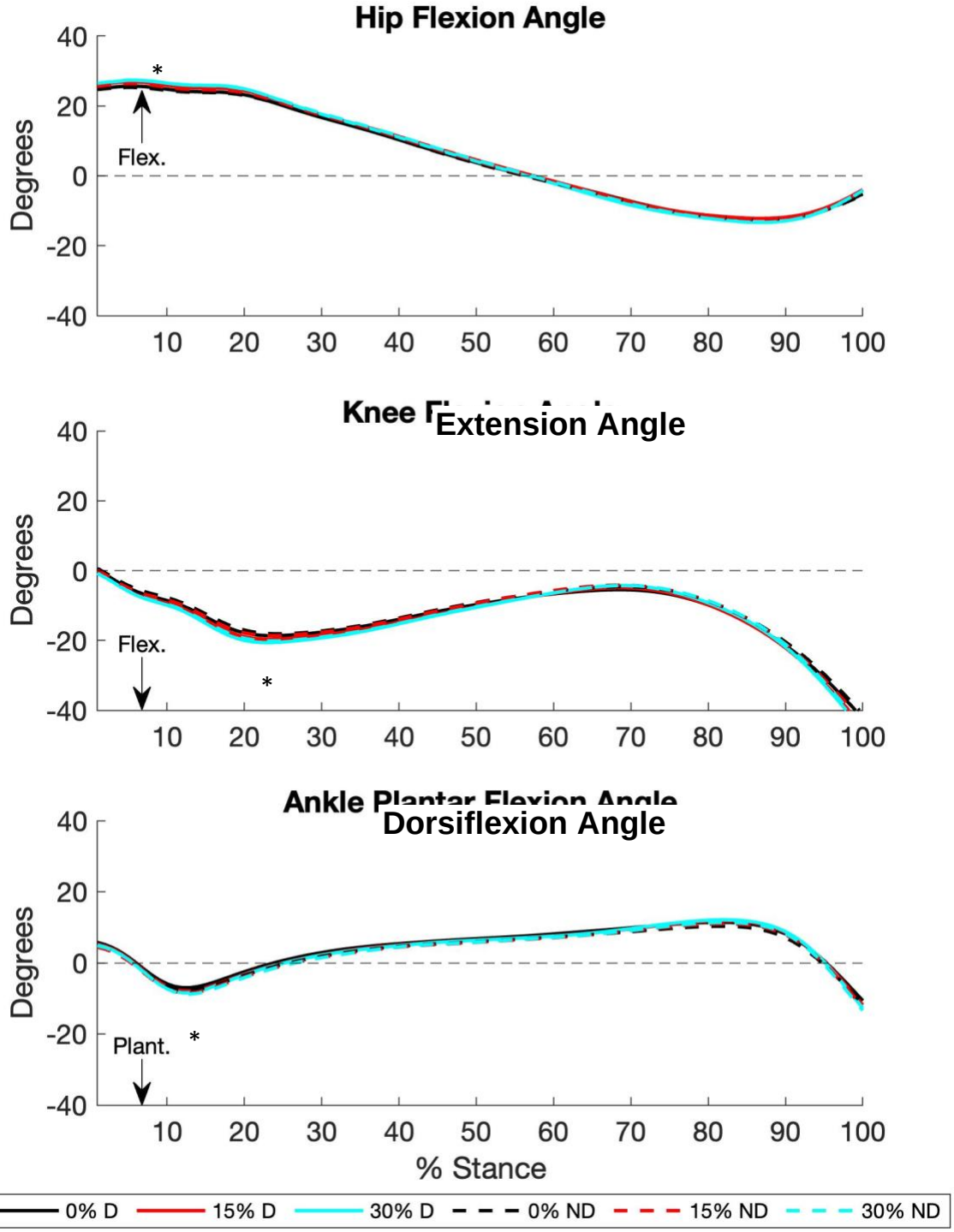

Figure 27: Time Series D and ND Sagittal Plane Kinematics Across Loading Conditions
Dominant and nondominant hip extension angle, knee extension angle, and ankle plantarflexion angle over percent stance during load carriage of 0% BW, 15% BW, and 30% BW. Line represents the mean across all participants. #$p < 0.05$ for Interaction, *$p < 0.05$ for load effect, †$p < 0.05$ for leg dominance effect.

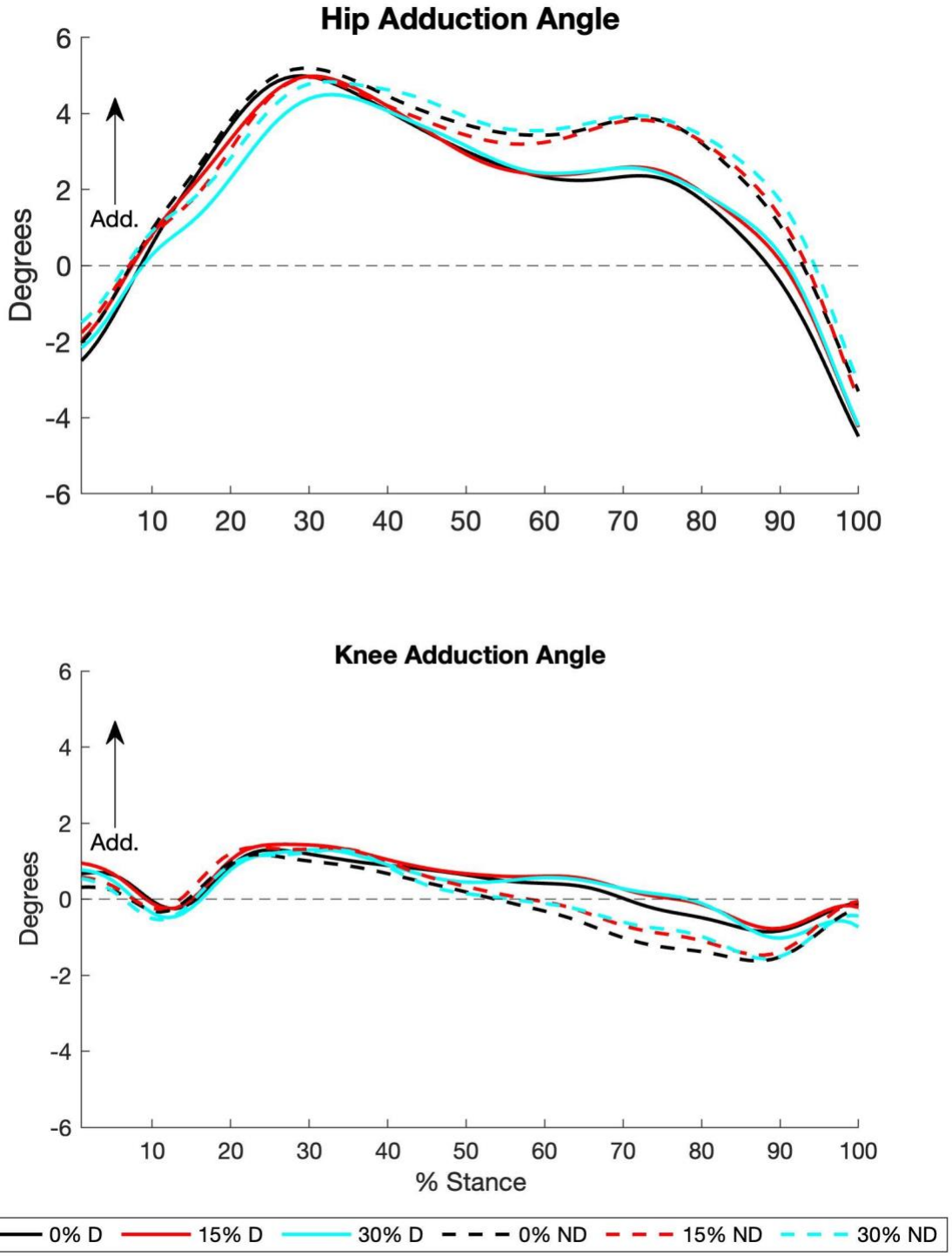

Figure 28: Time Series D and ND Frontal Plane Kinematics Across Loading Conditions
Dominant and nondominant hip adduction and knee adduction over percent stance during load carriage of 0% BW, 15% BW, and 30% BW. Line represents the mean across all participants. #p < 0.05 for Interaction, *p < 0.05 for load effect, †p < 0.05 for leg dominance effect.

Summary

Peak total, medial, and lateral TFJ contact forces and impulses increased with increasing load. Peak muscle forces and impulses all increased significantly with load. Stance time increased significantly with load. Peak knee flexion increased with load but there was no difference between the two loading conditions. Leg stiffness decreased disproportionately, therefore the participants compressed their lower extremities to a greater extent during the 30% condition as compared to the 15% condition. The medial compartment loads responded in a linear fashion while the lateral compartment impulses increased disproportionately. There was a lack of change in internal knee abduction moment and minimal change in knee abduction angular impulse between the two-loading condition.

There were no interactions between the two limbs and increasing load carriage for TFJ forces and impulses. However, the dominant and lateral compartment both exhibited greater peak TFJ force and TFJ impulse than the nondomain, while the nondominant medial compartment TFJ forces and impulse were greater than the dominant. Peak quadriceps force and impulse was greater in the dominant limb as compared to the nondominant. This same observation was present for gastrocnemius impulse. Peak hamstrings force and impulse was greater in the nondominant limb as compared to the dominant. Peak internal knee abduction moment and knee abduction angular impulse was greater in the nondominant limb as compared to the dominant. Peak medial ground reaction force was greater in the nondominant limb as compared to the dominant limb. There were no differences between the limbs for frontal and sagittal plane kinematics.

Chapter 5: Discussion

Introduction

The purposes of this study were 1: to compare tibiofemoral joint loads and gait patterns when walking on an instrumented treadmill while unloaded vs. loaded with a weighted vest at 15% and 30% bodyweight, and 2: to compare the dominant and nondominant limb's tibiofemoral joint contact forces and impulses in correspondence with increasing load carriage. We hypothesized 1: vest-borne loads relative to bodyweight will cause an increase in total, medial, and lateral tibiofemoral joint contact forces and impulses in healthy young adults during gait, but this increase will be attenuated at the 30% condition due to gait adaptations, and 2: tibiofemoral joint contact forces and impulses will be greater in the dominant limb as compared to the non-dominant limb as vest-borne loads are added. This chapter is divided into two parts based on the two purposes. In the scope of purpose 1 we discussed changes in peak TFJ contact force magnitude and distribution, changes in TFJ impulse magnitude and distribution, factors contributing to the magnitude and distribution observations. In the scope of purpose 2 we discussed asymmetries in peak TFJ contact force and impulse magnitude and distribution with load, and factors contributing to the asymmetry observations.

Changes in Peak TFJ Contact Force Magnitude and Distribution with Load

Present TFJ contact forces were similar in shape and magnitude to those reported in the literature.[4,13,28,96] We found that first peak TFJ contact forces significantly increased with increasing load. First peak TFJ contact forces were at 3.01, 3.50, and 4.08 bodyweights (BW) at no load, 15% BW load, and 30% BW load respectively. However, Lenton et al. (2016), [15] did not find first peak total TFJ contact forces to increase significantly with load. Lenton et al.[15] reported

total TFJ contact forces of 3.83, 3.99, and 4.30 BW at no load, 15 kg load (~18.3% BW), and 30 kg load (~36.4% BW) respectively. This may be attributed to musculoskeletal model differences, as Lenton et al. used an EMG driven model that predicted 1.0 BW greater baseline total contact forces than our model. Because we did find a significant increase, and because or pairwise comparisons revealed significant differences between each condition, it is important to examine how each loading condition impacted the total contact forces. Specifically, absolute ratios of increased TFJ contact forces to weight added was the mechanism of interpretation we used to discuss these data. This mechanism has been used previously,[13,28,63] such as Willy et al. (2019),[28] when they explained that there was a 2 kg increase in first peak medial TFJ contact forces for every 1 kg of load added, establishing a 2:1 ratio.

When examining the change from the no load to the two loading conditions, load carriage of 15% and 30% bodyweight induced 3.2:1 and 3.6:1 ratio increases in absolute first peak total TFJ contact forces to weight added, which were greater than the 2:1 ratio of reduced total TFJ contact forces relative to weight loss in obese adults reported by DeVita et al.,[13] but less than the 4:1 of reduced total TFJ contact forces relative to weight loss in obese adults with osteoarthritis reported by Messier et al. (2011).[63] It seems that the 30% loading condition induced a disproportionate increase in our participants' ratio as compared to the 15% condition. However, there was not a significant quadratic trend component for peak total TFJ contact force, therefore, we cannot confidently say that the increase was disproportionate, although, a medium effect size was present for the quadratic trend.

When parsing the total contact forces to the medial compartment of the knee, we found that first peak medial TFJ contact force increased with increasing load, which is similar to the results of Willy et al. (2019).[28] and Lenton et al. (2016).[15] A 2:1 ratio increase in first peak medial TFJ

contact forces to weight added was present for both loading conditions, which is the same as the ratio reported by Willy et al. during load carriage of 20 kg (~26% BW). We are confident that the increasing load from increasing load carriage 15% to 30% does not induce a disproportionate increase in peak medial TFJ contact forces due to the consistency in absolute ratios, relative percent increases close to the percentage of load added, and very large *p*-values and negligible effect sizes for the quadratic trend ($p = .602$, $\eta_p^2 = .012$). When parsing the total contact forces to the lateral compartment of the knee, we found that first peak lateral TFJ contact forces increased with increasing load. A 1.1:1 and 1.3:1 ratio increase in peak lateral TFJ force to weight added at the 15% and 30% condition, respectively, were present. Lenton et al. (2016)[15] reported lateral TFJ contact forces, but their model did not demonstrate a lateral TFJ contact force first peak, therefore, we do not have literature to compare out first lateral peak during load carriage to. Despite the seemingly disproportionate increase in our participant's peak lateral TFJ contact forces at the 30% loading condition, the quadratic trend component was not significant, but there was a medium effect size. However, these data suggests that peak lateral TFJ contact forces respond differently than the peak medial TFJ contact forces.

Changes in Peak TFJ Impulse Magnitude and Distribution with Load

The increases in peak TFJ contact forces provide only one perspective on knee joint loading. Stance time increased 5 and 14 ms with increasing load in concordance with the increasing peak TFJ forces, thus, both affecting cumulative loading. TFJ impulse provides us that perspective on cumulative loading, which is important considering loading exposure is a primary factor in the development of knee OA.[97] Absolute ratios of increased TFJ impulse to increased GRF standing impulse was the mechanism used to discuss these data. We found that total TFJ impulse increased

significantly with increasing load with a significant difference between each condition, but there were no load carriage or weight studies to compare our values and ratios to. Load carriage of 15% and 30% bodyweight induced 1.8:1 and a 2:1 ratio increases in total TFJ impulse compared to the standing impulse. Total TFJ impulse responded in similar fashion as peak total TFJ contact force, but for the impulse, there was a significant quadratic trend component indicating that as the relative load increased, there was a disproportionate increase in the impulse for our participants.

When parsed to the medial compartment, we found that medial TFJ impulse increased with increasing load, similar to the findings of Willy et al. (2019).[28] A 1.2:1 ratio increase in medial TFJ impulse to standing impulse was present for both loading conditions. This linearity was similar to what we found for peak medial TFJ contact forces. The lateral TFJ impulses, on the other hand, responded in a similar fashion as the peak lateral TFJ contact forces regarding to changing ratios with increasing load. A 0.6:1 and 0.8:1 ratio increases in lateral TFJ impulse to standing impulse increase was present for the two loading conditions. Unlike peak lateral TFJ contact force, lateral TFJ impulse exhibited a significant quadratic trend component. As the relative load increased, there was a disproportionate increase in our participants lateral TFJ impulse driven by the 30% condition, which was the same relationship we saw for total TFJ impulse.

Factors Contributing to the TFJ Contact Force and Impulse Observations

We also examined estimated hamstrings and quadriceps muscle forces as they are the primary muscle contributors to first peak TFJ contact forces. Hamstrings and quadriceps force estimates over the stance phase were consistent in shape with the literature.[13,63] Neither hamstring nor quadriceps peak force exhibited significant quadratic trends, but large and medium effect sizes were present for both respectively. For peak quadriceps force we did see a 1.7:1 and a 2.1:1

increase in force to weight added, with the 30% condition inducing a large 40% increase in peak quadriceps force. The quadriceps exhibited 2-3 times greater peak force than the hamstrings, subsequently providing a greater contribution to first peak total TFJ contact force, which is consistent with the literature.[2,13,63] Therefore, the peak quadriceps force was a contributing factor that helps explain the change in peak total TFJ contact force ratio from 3.2:1 to 3.6:1.

Gastrocnemius impulse did exhibit a significant quadratic trend, but only with ratios of 0.4:1 and 0.5:1 for gastrocnemius impulse to standing impulse increase. The disproportionate increase likely played a small role in the dipropionate increase of total TFJ impulse. Neither hamstring nor quadriceps impulse exhibited quadratic trends, but there was a medium effect size for the quadriceps. Quadriceps impulse was approximately 2-3 times greater than the hamstrings, but the ratios of quadriceps impulse to standing impulse was only 0.6:1 and 0.7:1. Qualitatively, when we exam the quadriceps time series in Figure 11, we see that the width of the quadriceps peak at the 30% loading condition appears to be wider than the other two conditions, potentially contributing to the disproportionate increase in total TFJ impulse at the 30% condition. The significant increase in knee flexion with increasing load corresponded with the increase in peak quadriceps impulse because greater knee flexion over increasing stance time induces a longer eccentric action of the quadriceps.

The increase in knee flexion during load carriage is consistent with the literature,[17,18,25,27,28] and is likely taking the role of shock/energy absorption through the quadriceps mechanism mentioned above; the increase energy absorption idea is corroborated by the significant increase in the negative power at K1S with increasing load (**Appendix F: Figure 32).** While knee flexion did significantly increase with increasing load, pairwise comparisons revealed that there was no significant difference between the no load and 15% load condition, but there was a significant

difference between 30% load and the other two conditions. The significant increase in peak knee flexion only occurring at the 30% condition suggest that the external GRF lever arm did not increase due to knee flexion at the 15% condition. Therefore, the weight of the external load alone was potentially the driving factor in the change in contact forces, which is why peak TFJ contact forces and quadriceps force all increased approximately 15% at the loading condition. The significant increase in knee flexion at the 30% condition likely did increase the external GRF lever arm from the knee joint center, which explains why we saw the change in the absolute ratio and why the relative increase in total TFJ contact force and quadriceps force were greater than 30%.

Modeling the leg as a spring is appropriate to measure leg stiffness during stance phase for gait.[98] Leg stiffness may provide a better representation of kinematic adaptations and shock/energy absorption during load carriage because leg stiffness includes all the lower extremity sagittal plane angle changes in one metric over a stance phase, whereas peak flexion only gives us one point in time for one joint. Therefore, leg stiffness can act as a kinematic correspondence to impulse. Leg stiffness decreased 8% and 27% with increasing load carriage and exhibited a significant quadratic trend component, suggesting that as load carriage increased, leg stiffness disproportionately decreased. This was driven by the small decrease at the 15% condition and the large decrease at the 30% condition, as seen in **Figure 14**. The participants adapted to increasing load carriage by increasing compression of their lower extremity during stance phase, especially during the 30% load condition. This is potentially a contributing factor to the significant quadratic trend component of total TFJ impulse.

Peak knee flexion nor leg stiffness explain why the medial and lateral compartment responded differently to increased load. To answer this, we examined the internal knee abduction moment, which influences how the total TFJ contact forces are parsed to the medial compartment. Pairwise

comparisons revealed that there was no significant difference in peak KAM between the 15% and 30% condition. If peak KAM is not significantly increasing between the two loading conditions, then the peak total TFJ contact force that is used to account for the peak knee internal abduction moment by acting through the medial compartment contact point does not significantly change. Therefore, the factor that drives the disproportionate medial force distribution is not significantly greater at the 30% condition. This occurrence is why there was no change in the peak medial TFJ contact force between the 15% and 30% loading condition. After accounting for the frontal plane moment, the remaining TFJ forces are equally parsed to the medial and lateral compartments, but the lack of significant change in peak KAM coupled with ratio increase of peak total TFJ contact force means that there is a disproportionately larger remaining force at the 30% loading condition as compared to the 15% condition. The lateral compartment gets half of that remaining force, which is why we saw increases in lateral TFJ contact forces from 15% to 30% load carriage at approximately 25% stance. It should be noted that peak lateral TFJ forces occurred at approximately 15% stance, which is not when peak medial TFJ forces occurred, meaning that lack of difference in peak KAM between the loading is not driving the increase in ratio for peak TFJ lateral force, but rather the lack of change in KAM at 15% stance as seen in **Figure 12.**

Similarly, KAM angular impulse was examined to explore its role in the stagnant medial TFJ impulse ratio and the disproportionate increase in the lateral TFJ impulse ratio. KAM angular impulse increased with increasing load. Unlike peak KAM, there was a significant difference between the 15% condition and the 30% condition. If we applied the logic of peak KAM not changing between the 15% and 30% condition resulting in the observed medial and lateral TFJ peak force distribution to KAM angular impulse and medial and lateral TFJ impulse, it would not seem to hold. But upon closer visual inspection of the difference between of KAM angular impulse

at the 15% and 30% condition via **Figure 12**, we see that the 15% and 30% KAM time series curves have a large quantity of overlap throughout stance. The only visual difference is at first peak, but we know first peak KAM 30% load is not significantly greater than first peak KAM at 15% load. The pairwise comparison p-value between the two loading conditions was $p = .035$, which while significant, is not as extreme as $p < .001$ for comparisons of no load to 15% and 30% load. This leads us to believe that KAM angular impulse might not have increased enough between the 15% and 30% to critically influence medial lateral distribution, which is why the medial TFJ impulse ratio did not change between the two loading conditions, while the lateral disproportionately increased.

Purpose 1: Summary and Implications

Present data partially confirmed our first hypothesis; total, medial, and lateral TFJ contact forces and impulse significantly increased with increasing load, but variables were not attenuated at the 30% loading condition. Total impulse disproportionately increased at the 30% condition due to lower extremity compression throughout stance, along with quadriceps and gastrocnemius contributions. It is evident that our participants' lateral peak TFJ contact forces and impulses, responded differently than the medial forces and impulses with increasing load relative to bodyweight. Within our sample, the medial compartment responds in a linear fashion to increasing load carriage due to no changes in KAM between the 15% and 30% condition, while the lateral impulses disproportionately increased with the 30% loading condition. These finding provide a basis for examining knee joint contact force distribution during gait studies along with various other activities.

The disproportionate increase in total TFJ impulse is a sign that long periods of heavy load carriage may put the knee at risk. The cumulative overloading could initiate the maladaptive mechanical transduction pathway that leads to inflammation and the activation cartilage degradation enzymes.[8,99] If these processes were to take place then there would be cartilage breakdown,[1,8] and potentially the onset of OA if this occurred on many different occasions. The medial compartment resistance to disproportionate increases with increasing load carriage is promising as a protective mechanism within healthy young adults, as the medial compartment has higher rates knee osteoarthritis.[100] However, it is unclear if the medial compartment would maintain its resistance to disproportionate increases with greater load carriage magnitudes, or how it would respond to load carriage over a long period of time. It is also possible the that the magnitude of the medial TFJ contact forces during heavy load carriage is to blame regardless of increases in ratios. The absolute loading may be lower in the lateral compartment, but if the quadratic trend were to continue and the impulses continue to disproportionally increase with greater magnitudes of load then the lateral compartment might catch up the medial from a ratio perspective. The lateral compartment's sensitivity to increasing load carriage leads to some concern. We know that lateral compartment has smaller of articular cartilage have smaller contact area during first and second peak,[101] therefore the forces are not distributed as widely as forces on the medial compartment. However, the lateral compartment does have greater cartilage volume and thickness,[102] somewhat mitigating the loading concern. The general population exhibits lower rates of isolated lateral compartment knee OA; however, it is unclear what the compartmental distribution of OA is in military populations.[100]

Asymmetries in Peak TFJ Contact Force and Impulse Magnitude and Distribution with Load Carriage

No asymmetry was present between dominant and nondominant first peak total TFJ contact force and impulse, despite asymmetries in peak quadriceps and hamstrings force, but the medial and lateral compartment both exhibited asymmetries. Interestingly, the knee compartmental asymmetries were opposite of each other, with the nondominant peak medial TFJ contact force and impulse being significantly greater than the dominant, while dominant peak lateral TFJ contact force and impulse were significantly greater than the nondominant. However, nondominant peak medial TFJ contact forces only differed approximately 102 N or 0.150 BW at each condition; the minimum detectable change threshold for the peak medial TFJ contact force is 0.246 bodyweights, as defined by Barrios and Willson (2017).[103] Therefore, the first peak medial contact force did not meet the minimum detectable change when comparing the dominant and nondominant limb. Medial TFJ impulses differed approximately 62 N·s or 0.085 BW·s, which is greater than the medial TFJ impulse minimum detectable change threshold of 0.0385.[103] This gives us confidence that the nondominant medial TFJ impulse is significantly greater than the dominant.

There is not an established minimum detectable threshold for the lateral TFJ peak contact forces or impulses to provide a basis for comparison, but the differences observed in our sample were large. Dominant peak lateral TFJ contact forces were approximately 162 N or 0.25 BW greater than nondominant. Lateral TFJ impulse responded in a similar manner with dominant being approximately 82 N·s or 0.125 BW·s greater than nondominant. The magnitude of difference in the lateral compartment is greater than the difference observed for the medial compartment. Notably, this is interesting, considering the medial compartment experiences greater overall peak contact forces and impulses than the lateral, which exemplifies how large these differences are for

the lateral compartment. Peak lateral TFJ contact forces and impulses were approximately 20% and 29% greater in the dominant limb as compared to the nondominant limb. To better understand these knee joint load asymmetries and their contributing factors, several of the musculoskeletal model's components were investigated.

Factors Contributing to Asymmetry Observations

The asymmetries in the medial and lateral knee joint compartment lead us to examine the internal knee abduction moment due to its influence in the parsing of the total TFJ compartment forces to the medial and lateral compartment. We found that nondominant first peak KAM was not only significantly greater than dominant peak KAM, but that nondominant first peak KAM at no load was greater on average than even dominant first peak KAM at the 30% loading condition. This is visually evident in **Figure 22**. Nondominant peak KAM being significantly greater means that there will be a larger parsing of the total peak TFJ contact forces to the nondominant medial knee compartment as compared to the dominant. This is a large contributing factor to why the nondominant limb experienced greater first peak medial TFJ contact forces than the dominant.

The dominant first peak lateral TFJ contact forces being greater than the nondominant can also be partially attributed to KAM. When we examine **Figure 16**, we see that the peak lateral forces occur at approximately 15% stance; when we examine **Figure 22**, at 15% stance we see that nondominant KAM is visually greater than the dominant. If nondominant KAM is also greater than dominant at 15% stance, then there is a larger remaining total TFJ force being parsed to the lateral compartment, as compared to a smaller total TFJ force being parsed to the dominant limb's lateral compartment. At 25% stance, when peak medial TFJ contact forces and peak KAM occur, the dominant lateral forces appear to be greater than the nondominant, which would be what we

expect based on nondominant peak KAM and nondominant peak medial forces both being greater than dominant.

Differences in KAM can be attributed to differences in the KAM lever arm. Factors influencing the KAM lever arm include frontal plane kinematics and medial/lateral ground reaction forces. There were no differences in frontal plane kinematics at any of the lower extremity joints, but we did find that first peak medial GRF was greater in the nondominant limb as compared to the dominant. Larger medial GRF extends the GRF lever arm in the frontal plane, therefore, larger peak medial GRF occurring in the nondominant limb likely extended the frontal plane GRF lever arm and increased peak KAM in the nondominant limb. Subsequently, increasing the force required to act on the medial knee compartment to account for the frontal plane moment. Differences in medial GRF indicates that limbs are interacting differently with the ground. The abductors are the largest contributor to peak medial GRF, while the quadriceps attenuate this affect.[104] Our model does not estimate abductor forces, but it does estimate quadriceps force. The dominant quadriceps exhibited approximately 15% greater peak force than the nondominant. It is possible that the nondominant quadriceps was not attenuating the abductor force to the same extent as the dominant, ultimately leading to a greater peak medial GRF.

To explain the compartmental impulse asymmetries, it is necessary to examine KAM angular impulse. Nondominant KAM angular impulse was significantly greater than dominant KAM impulse. Furthermore, in **Figure 22**, nondominant KAM is visually greater than dominant KAM across the whole stance phase. When KAM angular impulse is greater, there is greater cumulative force parsed to the medial compartment. The KAM impulse difference is likely the driving factor for the nondominant medial TFJ impulse being greater than the dominant, and why dominant lateral TFJ impulse was greater than nondominant. Differences in KAM angular impulse can be

partially attributed to significantly greater nondominant medial GRF impulse. However, nondominant GRF impulse was only 1 N·s greater than the dominant. Hence, the argument for medial GRF impulse influence on KAM impulse is not a strong or direct as peak medial GRF influence on peak KAM.

There are other factors that may have influenced KAM angular impulse such as knee alignment. KAM has been shown to increase with knee varus alignment and decrease with knee valgus alignment.[105] It is also understood that knee varus alignment can influence the medial knee compartment forces[7] and is associated with medial knee OA,[106] while valgus alignment can influence the lateral knee compartment forces and is associated with lateral knee OA.[106] It is possible that there are alignment differences, with the dominant limb exhibiting a valgus alignment contributing to the lesser KAM angular impulse and medial TFJ impulse, along with greater lateral TFJ impulse. The nondominant limb might exhibit varus alignment contribution to the greater KAM angular impulse and medial TFJ impulse, along with lesser lateral TFJ impulse. However, these are only speculations as we do not have alignment data available for investigation. Furthermore, there are no studies, to our knowledge, that have investigated knee alignment differences between the dominant and nondominant limb to help support this notion.

Lateral trunk sway, on the other hand, has been shown to account for variance in KAM,[107] and lateral lean towards the grounded limb during stance has been shown to reduce the external knee adduction moment.[108] Lateral trunk sway data is not readily available to us, but since KAM was greater on the nondominant side we can speculate that participants may have exhibited greater lean toward the dominant side, which should result in smaller KAM thought the stance phase. Lateral trunk lean also reduces the internal hip abduction moment,[1] which further corroborates the lean towards the dominant side speculation, because our participants exhibited a greater dominant peak

internal hip abduction moment and angular impulse as compared to the nondominant (**Appendix F: Figure 36**). Trunk lean towards the dominant limb during nondominant stance would increase nondominant KAM.[108] Due to the nondominant KAM impulse and hip abduction angular impulse being greater than dominant, we can speculate that our participates may have maintained a trunk sway or trunk lean towards the dominant limb during nondominant stance.

Purpose 2: Summary and Implications

Present data did not confirm our second hypothesis; TFJ contact forces and impulses did not increase on the dominant side to a greater extent than the nondominant with increasing load. It is evident that the global knee joint loading environment is statistically symmetrical, but when taking a local perspective by examining the medial and lateral compartment we see asymmetries. Th asymmetries are intensified when we examine cumulative loading of the two compartments via impulse. Barrios and Willson[103] noted the heightened sensitivity of impulse to smaller magnitude changes, therefore the large differences between dominant and nondominant knee joint compartmental impulses are important to highlight. The nondominant medial TFJ impulse was significantly greater than the dominant, and dominant lateral TFJ impulse was significantly greater than the nondominant. The lateral compartment, on average, demonstrated greater differences between limbs as compared to the medial.

It is unclear, if these knee loading differences are pathological, functional, or simply a consequence of gait and muscle asymmetries. There are no studies that have investigated the prevalence of medial and lateral compartment OA in the dominant vs nondominant limb in general or military populations. There is evidence that there is no difference in dominant vs nondominant total tibial articular cartilage thickness or volume.[109] However, when examining the two knee compartments, there is some evidence that the articular cartilage is thicker in the dominant medial

and lateral compartments for right legged individuals, but this observation was not consistent for left leg dominant individuals,[109] making this relationship unclear. Increased KAM has been positively correlated with medial cartilage thickness,[102] while peak forces and impulses have been positively correlated with cartilage thickness.[101] Therefore, it is likely that cartilage does adapt to the unique loading environment in both knees.

Delimitations

The delimitations of this study should be considered. There were inclusion criteria of ages between 18 and 30 years old and BMI between 18 and 25 $kg \cdot m^{-2}$. A standard walking speed of 1.4 $m \cdot s^{-1}$ was used, which may have resulted in greater TFJ contact forces for participants who were shorter or those who walk at a slower self-selected speed. TFJ contact forces are slightly lower on treadmill walking, therefore, our analysis may represent an underestimation of TFJ contact forces during overground walking at a similar speed.[4,110] The design of the study was not counter balanced. The 15% and 30% condition were done sequentially for each participant instead of being randomized. Therefore, fatigue and learning effects may be factors in on our observations during the 30% condition. We only used 5 stance phases per limb per condition. Limb dominance was self-reported instead of using surveys or functional test. Lower limb laterality has been noted to be especially difficult to determine due to differing definitions leg dominance.[31] It is possible that self-report was not rigorous enough to accurately determine leg dominance, especially considering the different perspectives on what leg dominance means. The musculoskeletal model used in this analysis utilizes a "lumped muscle model," and therefore, does not distinguish between the different quadriceps and hamstrings.[63] The model also relies on assumptions based on previous literature, muscle physiological cross-sectional area, and muscle moment arms. However, this

model has been readily used,[13,28,48,55,63,96] and has been validated for total and medial TFJ contact forces and impulses against measured TFJ contact forces from an instrumented prothesis.[56] The model's lateral compressive force estimates have not been validated against *in-vivo* loads, although, the peaks were close to reported *in-vivo* peaks of 556-871 N from an instrumented prosthesis.[4,111] Trunk markers were placed directly on the vest, and the length of the vests caused some difficulty in pelvis marker visualization during 30% condition.

Conclusion

In conclusion, total and lateral TFJ impulses are sensitive to increasing load carriage relative to bodyweight, and load carriage does not influence knee joint loading asymmetries. At a standard speed of 1.4 $m \cdot s^{-1}$, load carriage at 30% bodyweight induces an increase in peak knee flexion and a large decrease in leg stiffness that influence changes in ratios of peak total TFJ contact force to weight added and ratios of total TFJ impulse to standing impulse increase. Increasing load carriage from 15% to 30% bodyweight does not induce disproportionate increase in ratios of peak medial TFJ contact forces to weight added and ratios of medial TFJ impulse to standing impulse increase. Lateral TFJ impulses, on the other hand, are especially sensitive to increasing load carriage as they disproportionately increase. Knee joint contact force and impulse distribution can provide valuable insight to the responses of knee joint loading environment to external variables.

Dominant and nondominant knee joint loading asymmetries are present for the medial and lateral compartments. Nondominant medial TFJ impulses are greater than dominant while dominant lateral TFJ peak forces and impulses are greater than nondominant. Internal knee abduction moment and angular impulse play a large role in the medial and lateral TFJ contact

forces and impulses response to load carriage and influences the dominant vs nondominant asymmetries. Noticeably, lateral compartmental force, which is often not the focus of knee joint loading studies, demonstrated interesting responses to load carriage and exhibited large asymmetries. Dominant and nondominant limbs exhibit interesting compartmental loading asymmetries during gait that may carry over to other activates, such as running. Lastly, TFJ impulses may be a better indicator for change in the knee joint loading environment as compared to peak TFJ contact forces.

References

1. Sanchez-Adams J, Leddy HA, McNulty AL, O'Conor CJ, Guilak F. The Mechanobiology of Articular Cartilage: Bearing the Burden of Osteoarthritis. *Curr Rheumatol Rep*. 2014;16(10):451. doi:10.1007/s11926-014-0451-6

2. Sasaki K, Neptune RR. Individual Muscle Contributions to the Axial Knee Joint Contact Force during Normal Walking. *J Biomech*. 2010;43(14):2780-2784. doi:10.1016/j.jbiomech.2010.06.011

3. D'Lima DD, Fregly BJ, Patil S, Steklov N, Colwell CW. Knee joint forces: prediction, measurement, and significance. *Proc Inst Mech Eng H*. 2012;226(2):95-102.

4. Fregly BJ, Besier TF, Lloyd DG, et al. Grand challenge competition to predict in vivo knee loads. *Journal of Orthopaedic Research*. 2012;30(4):503-513. doi:https://doi.org/10.1002/jor.22023

5. Ng KW, Mauck RL, Wang CCB, et al. Duty Cycle of Deformational Loading Influences the Growth of Engineered Articular Cartilage. *Cell Mol Bioeng*. 2009;2(3):386-394. doi:10.1007/s12195-009-0070-x

6. Takahashi I, Matsuzaki T, Yoshida S, Kitade I, Hoso M. Differences in Cartilage Repair between Loading and Unloading Environments in the Rat Knee. *J Jpn Phys Ther Assoc*. 2014;17(1):22-30. doi:10.1298/jjpta.Vol17_004

7. Wong M, Siegrist M, Cao X. Cyclic compression of articular cartilage explants is associated with progressive consolidation and altered expression pattern of extracellular matrix proteins. *Matrix Biol*. 1999;18(4):391-399. doi:10.1016/s0945-053x(99)00029-3

8. Sun HB. Mechanical loading, cartilage degradation, and arthritis. *Annals of the New York Academy of Sciences*. 2010;1211(1):37-50. doi:https://doi.org/10.1111/j.1749-6632.2010.05808.x

9. Clements KM, Bee ZC, Crossingham GV, Adams MA, Sharif M. How severe must repetitive loading be to kill chondrocytes in articular cartilage? *Osteoarthritis and Cartilage*. 2001;9(5):499-507. doi:10.1053/joca.2000.0417

10. Horisberger M, Fortuna R, Valderrabano V, Herzog W. Long-term repetitive mechanical loading of the knee joint by in vivo muscle stimulation accelerates cartilage degeneration and increases chondrocyte death in a rabbit model. *Clinical Biomechanics*. 2013;28(5):536-543. doi:10.1016/j.clinbiomech.2013.04.009

11. Roemhildt ML, Coughlin KM, Peura GD, et al. Effects of Increased Chronic Loading on Articular Cartilage Material Properties in the Lapine Tibio-Femoral Joint. *J Biomech*. 2010;43(12):2301-2308. doi:10.1016/j.jbiomech.2010.04.035

12. Browning RC, Kram R. Effects of obesity on the biomechanics of walking at different speeds. *Med Sci Sports Exerc*. 2007;39(9):1632-1641. doi:10.1249/mss.0b013e318076b54b

13. DeVita P, Rider P, Hortobágyi T. Reductions in knee joint forces with weight loss are attenuated by gait adaptations in class III obesity. *Gait Posture*. 2016;45:25-30. doi:10.1016/j.gaitpost.2015.12.040

14. Harding GT, Dunbar MJ, Hubley-Kozey CL, Stanish WD, Astephen Wilson JL. Obesity is associated with higher absolute tibiofemoral contact and muscle forces during gait with and without knee osteoarthritis. *Clinical Biomechanics*. 2016;31:79-86. doi:10.1016/j.clinbiomech.2015.09.017

15. Lenton GK, Bishop PJ, Saxby DJ, et al. Tibiofemoral joint contact forces increase with load magnitude and walking speed but remain almost unchanged with different types of carried load. *PLoS One; San Francisco*. 2018;13(11):e0206859. doi:http://dx.doi.org/10.1371/journal.pone.0206859

16. Messier S, Gutekunst DJ, Davis C, DeVita P. Weight loss reduces knee-joint loads in overweight and obese older adults with knee osteoarthritis. *Arthritis & Rheumatism*. 2005;52(7):2026-2032. doi:10.1002/art.21139

17. Seay JF, Fellin RE, Sauer SG, Frykman PN, Bensel CK. Lower extremity biomechanical changes associated with symmetrical torso loading during simulated marching. *Mil Med*. 2014;179(1):85-91. doi:10.7205/MILMED-D-13-00090

18. Silder A, Delp SL, Besier T. Men and women adopt similar walking mechanics and muscle activation patterns during load carriage. *J Biomech*. 2013;46(14):2522-2528. doi:10.1016/j.jbiomech.2013.06.020

19. Knapik JJ, Reynolds KL, Harman E. Soldier load carriage: historical, physiological, biomechanical, and medical aspects. *Mil Med*. 2004;169(1):45-56. doi:10.7205/milmed.169.1.45

20. Seay JF. Biomechanics of Load Carriage—Historical Perspectives and Recent Insights. *The Journal of Strength & Conditioning Research*. 2015;29:S129. doi:10.1519/JSC.0000000000001031

21. Lincoln AE, Smith GS, Amoroso PJ, Bell NS. The natural history and risk factors of musculoskeletal conditions resulting in disability among US Army personnel. *Work*. 2002;18(2):99-113.

22. Cameron KL, Hsiao MS, Owens BD, Burks R, Svoboda SJ. Incidence of physician-diagnosed osteoarthritis among active duty United States military service members. *Arthritis & Rheumatism*. 2011;63(10):2974-2982. doi:https://doi.org/10.1002/art.30498

23. Kopec JA, Rahman MM, Berthelot JM, et al. Descriptive epidemiology of osteoarthritis in British Columbia, Canada. *The Journal of Rheumatology*. 2007;34(2):386-393.

24. Harman E, Han KH, Frykman P, Johnson M, Russell F, Rosenstein M. The effects on gait timing, kinetics, and muscle activity of various loads carried on the back. *Medicine & Science in Sports & Exercise*. 1992;24(Supplement):S129. doi:10.1249/00005768-199205001-00775

25. Kinoshita H. Effects of different loads and carrying systems on selected biomechanical parameters describing walking gait. *Ergonomics*. 1985;28(9):1347-1362. doi:10.1080/00140138508963251

26. Birrell SA, Haslam RA. The effect of military load carriage on 3-D lower limb kinematics and spatiotemporal parameters. *Ergonomics*. 2009;52(10):1298-1304. doi:10.1080/00140130903003115

27. Attwells RL, Birrell SA, Hooper RH, Mansfield NJ. Influence of carrying heavy loads on soldiers' posture, movements and gait. *Ergonomics*. 2006;49(14):1527-1537. doi:10.1080/00140130600757237

28. Willy RW, DeVita P, Meardon SA, Baggaley M, Womble CC, Willson JD. Effects of Load Carriage and Step Length Manipulation on Achilles Tendon and Knee Loads. *Mil Med*. 2019;184(9-10):e482-e489. doi:10.1093/milmed/usz031

29. DeVita P, Hortobágyi T. Obesity is not associated with increased knee joint torque and power during level walking. *Journal of Biomechanics; Kidlington*. 2003;36(9):1355-1362. doi:http://dx.doi.org/10.1016/S0021-9290(03)00119-2

30. Gundersen LA, Valle DR, Barr AE, Danoff JV, Stanhope SJ, Snyder-Mackler L. Bilateral Analysis of the Knee and Ankle During Gait: An Examination of the Relationship Between Lateral Dominance and Symmetry. *Physical Therapy*. 1989;69(8):640-650. doi:10.1093/ptj/69.8.640

31. Sadeghi H, Allard P, Prince F, Labelle H. Symmetry and limb dominance in able-bodied gait: a review. *Gait & Posture*. 2000;12(1):34-45. doi:10.1016/S0966-6362(00)00070-9

32. Sadeghi H, Allard P, Duhaime M. Functional gait asymmetry in able-bodied subjects. *Human Movement Science*. 1997;16(2):243-258. doi:10.1016/S0167-9457(96)00054-1

33. Sadeghi H. Local or global asymmetry in gait of people without impairments. *Gait & Posture*. 2003;17(3):197-204. doi:10.1016/S0966-6362(02)00089-9

34. Gregg RD, Dhaher YY, Degani A, Lynch KM. On the Mechanics of Functional Asymmetry in Bipedal Walking. *IEEE Transactions on Biomedical Engineering*. 2012;59(5):1310-1318. doi:10.1109/TBME.2012.2186808

35. Fox AJS, Bedi A, Rodeo SA. The Basic Science of Human Knee Menisci: Structure, Composition, and Function. *Sports Health*. 2012;4(4):340-351. doi:10.1177/1941738111429419

36. D'Lima DD, Fregly BJ, Patil S, Steklov N, Colwell CW. Knee joint forces: prediction, measurement, and significance. *Proc Inst Mech Eng H*. 2012;226(2):95-102.

37. Sasaki K, Neptune RR. Individual muscle contributions to the axial knee joint contact force during normal walking. *Journal of Biomechanics*. 2010;43(14):2780-2784. doi:10.1016/j.jbiomech.2010.06.011

38. Winby CR, Lloyd DG, Besier TF, Kirk TB. Muscle and external load contribution to knee joint contact loads during normal gait. *J Biomech*. 2009;42(14):2294-2300. doi:10.1016/j.jbiomech.2009.06.019

39. Manske SL, Lorincz CR, Zernicke RF. Bone Health. *Sports Health*. 2009;1(4):341-346. doi:10.1177/1941738109338823

40. Snow CM, Shaw JM, Winters KM, Witzke KA. Long-term Exercise Using Weighted Vests Prevents Hip Bone Loss in Postmenopausal Women. *J Gerontol A Biol Sci Med Sci*. 2000;55(9):M489-M491. doi:10.1093/gerona/55.9.M489

41. Sutton S, Clutterbuck A, Harris P, et al. The contribution of the synovium, synovial derived inflammatory cytokines and neuropeptides to the pathogenesis of osteoarthritis. *Vet J*. 2009;179(1):10-24. doi:10.1016/j.tvjl.2007.08.013

42. Hales CM, Carroll MD, Fryar CD, Ogden CL. Prevalence of Obesity and Severe Obesity Among Adults: United States, 2017-2018. *NCHS Data Brief*. 2020;(360):1-8.

43. Sturm R, Hattori A. Morbid Obesity Rates Continue to Rise Rapidly in the US. *Int J Obes (Lond)*. 2013;37(6):889-891. doi:10.1038/ijo.2012.159

44. Fletcher E, Lewis-Fanning E. Chronic Rheumatic Diseases—Part IV. *Postgrad Med J*. 1945;21(235):176-185.

45. King LK, March L, Anandacoomarasamy A. Obesity & osteoarthritis. *Indian J Med Res*. 2013;138(2):185-193.

46. Grotle M, Hagen KB, Natvig B, Dahl FA, Kvien TK. Obesity and osteoarthritis in knee, hip and/or hand: An epidemiological study in the general population with 10 years follow-up. *BMC Musculoskelet Disord*. 2008;9(1):132. doi:10.1186/1471-2474-9-132

47. King LK, March L, Anandacoomarasamy A. Obesity & osteoarthritis. *Indian J Med Res*. 2013;138(2):185-193.

48. DeVita P, Hortobágyi T. Functional Knee Brace Alters Predicted Knee Muscle and Joint Forces in People with ACL Reconstruction during Walking. *Journal of Applied Biomechanics*. 2001;17(4):297-311. doi:10.1123/jab.17.4.297

49. Dumas R, Barré A, Moissenet F, Aissaoui R. Can a reduction approach predict reliable joint contact and musculo-tendon forces? *Journal of Biomechanics; Kidlington*. 2019;95. doi:http://dx.doi.org/10.1016/j.jbiomech.2019.109329

50. Komistek RD, Kane TR, Mahfouz M, Ochoa JA, Dennis DA. Knee mechanics: a review of past and present techniques to determine in vivo loads. *Journal of Biomechanics*. 2005;38(2):215-228. doi:10.1016/j.jbiomech.2004.02.041

51. Nisell R, Ericson MO, Nemeth G, Ekholm J. Tibiofemoral joint forces during isokinetic knee extension. *Am J Sports Med*. 1989;17(1):49-54. doi:10.1177/036354658901700108

52. Pandy MG, Sasaki K, Kim S. A Three-Dimensional Musculoskeletal Model of the Human Knee Joint. Part 1: Theoretical Construction. *Computer Methods in Biomechanics and Biomedical Engineering*. 1997;1(2):87-108. doi:10.1080/01495739708936697

53. Dempster W. Space requirements of the seated operator, geometrical, kinematic, and mechanical aspects of the body with special reference to the limbs. *Dayton OH, Wright Patterson Air Force Base*. Published online 1959.

54. Taylor WR, Schütz P, Bergmann G, et al. A comprehensive assessment of the musculoskeletal system: The CAMS-Knee data set. *J Biomech*. 2017;65:32-39. doi:10.1016/j.jbiomech.2017.09.022

55. Willy RW, Meardon SA, Schmidt A, Blaylock NR, Hadding SA, Willson JD. Changes in tibiofemoral contact forces during running in response to in-field gait retraining. *Journal of Sports Sciences*. 2016;34(17):1602-1611. doi:10.1080/02640414.2015.1125517

56. Thakkar B, Willson JD, Harrison K, Tickes R, Blaise Williams DS. Tibiofemoral Joint Forces in Female Recreational Runners Vary with Step Frequency. *Med Sci Sports Exerc*. 2019;51(7):1444-1450. doi:10.1249/MSS.0000000000001915

57. Lai PPK, Leung AKL, Li ANM, Zhang M. Three-dimensional gait analysis of obese adults. *Clinical Biomechanics*. 2008;23:S2-S6. doi:10.1016/j.clinbiomech.2008.02.004

58. McMillan AG, Pulver AME, Collier DN, Williams DSB. Sagittal and frontal plane joint mechanics throughout the stance phase of walking in adolescents who are obese. *Gait & Posture*. 2010;32(2):263-268. doi:10.1016/j.gaitpost.2010.05.008

59. Spyropoulos P, Pisciotta JC, Pavlou KN, Cairns MA, Simon SR. Biomechanical gait analysis in obese men. *Arch Phys Med Rehabil*. 1991;72(13):1065-1070.

60. Lerner ZF, Board WJ, Browning RC. Effects of obesity on lower extremity muscle function during walking at two speeds. *Gait & Posture*. 2014;39(3):978-984. doi:10.1016/j.gaitpost.2013.12.020

61. Browning RC, Baker EA, Herron JA, Kram R. Effects of obesity and sex on the energetic cost and preferred speed of walking. *Journal of Applied Physiology*. 2006;100(2):390-398. doi:10.1152/japplphysiol.00767.2005

62. DeVita P, Hortobágyi T. Obesity is not associated with increased knee joint torque and power during level walking. *Journal of Biomechanics*. 2003;36(9):1355-1362. doi:10.1016/S0021-9290(03)00119-2

63. Messier S, Legault C, Loeser RF, et al. Does high weight loss in older adults with knee osteoarthritis affect bone-on-bone joint loads and muscle forces during walking? *Osteoarthritis and Cartilage*. 2011;19(3):272-280. doi:10.1016/j.joca.2010.11.010

64. Ding C, Cicuttini F, Scott F, Cooley H, Jones G. Knee structural alteration and BMI: a cross-sectional study. *Obes Res*. 2005;13(2):350-361. doi:10.1038/oby.2005.47

65. Messier S, Resnik AE, Beavers DP, et al. Intentional Weight Loss in Overweight and Obese Patients With Knee Osteoarthritis: Is More Better? *Arthritis Care & Research*. 2018;70(11):1569-1575. doi:10.1002/acr.23608

66. Ghori GM, Luckwill RG. Responses of the lower limb to load carrying in walking man. *Eur J Appl Physiol Occup Physiol*. 1985;54(2):145-150. doi:10.1007/BF02335921

67. Martin PE, Nelson RC. The effect of carried loads on the walking patterns of men and women. *Ergonomics*. 1986;29(10):1191-1202. doi:10.1080/00140138608967234

68. Silder A, Delp SL, Besier T. Men and women adopt similar walking mechanics and muscle activation patterns during load carriage. *Journal of Biomechanics*. 2013;46(14):2522-2528. doi:10.1016/j.jbiomech.2013.06.020

69. Polk JD, Stumpf RM, Rosengren KS. Limb dominance, foot orientation and functional asymmetry during walking gait. *Gait & Posture*. 2017;52:140-146. doi:10.1016/j.gaitpost.2016.11.028

70. Iannetta D, Passfield L, Qahtani A, MacInnis MJ, Murias JM. Interlimb differences in parameters of aerobic function and local profiles of deoxygenation during double-leg and counterweighted single-leg cycling. *American Journal of Physiology-Regulatory, Integrative and Comparative Physiology*. 2019;317(6):R840-R851. doi:10.1152/ajpregu.00164.2019

71. Barbieri FA, Gobbi LTB, Santiago PRP, Cunha SA. Dominant–non-dominant asymmetry of kicking a stationary and rolling ball in a futsal context. *Journal of Sports Sciences*. 2015;33(13):1411-1419. doi:10.1080/02640414.2014.990490

72. Peters M. Footedness: Asymmetries in foot preference and skill and neuropsychological assessment of foot movement. *Psychological Bulletin*. 1988;103(2):179-192. doi:10.1037/0033-2909.103.2.179

73. Irving D, Rebeiz JJ, Tomlinson BE. The numbers of limb motor neurones in the individual segments of the human lumbosacral spinal cord. *Journal of the Neurological Sciences*. 1974;21(2):203-212. doi:10.1016/0022-510X(74)90072-0

74. Gardinier ES, Manal K, Buchanan TS, Snyder-Mackler L. Altered loading in the injured knee after ACL rupture. *Journal of Orthopaedic Research*. 2013;31(3):458-464. doi:10.1002/jor.22249

75. van Melick N, Meddeler BM, Hoogeboom TJ, Nijhuis-van der Sanden MWG, van Cingel REH. How to determine leg dominance: The agreement between self-reported and observed performance in healthy adults. *PLoS One*. 2017;12(12):e0189876. doi:10.1371/journal.pone.0189876

76. Hanavan EP. A MATHEMATICAL MODEL OF THE HUMAN BODY. AMRL-TR-64-102. *AMRL TR*. Published online October 1964:1-149.

77. Klein P, Mattys S, Rooze M. Moment arm length variations of selected muscles acting on talocrural and subtalar joints during movement: an in vitro study. *J Biomech*. 1996;29(1):21-30. doi:10.1016/0021-9290(95)00025-9

78. Ward SR, Eng CM, Smallwood LH, Lieber RL. Are Current Measurements of Lower Extremity Muscle Architecture Accurate? *Clin Orthop Relat Res*. 2009;467(4):1074-1082. doi:10.1007/s11999-008-0594-8

79. Németh G, Ohlsén H. In vivo moment arm lengths for hip extensor muscles at different angles of hip flexion. *Journal of Biomechanics*. 1985;18(2):129-140. doi:10.1016/0021-9290(85)90005-3

80. Herzog W, Read LJ. Lines of action and moment arms of the major force-carrying structures crossing the human knee joint. *J Anat*. 1993;182(Pt 2):213-230.

81. Spoor CW, van Leeuwen JL, Meskers CG, Titulaer AF, Huson A. Estimation of instantaneous moment arms of lower-leg muscles. *J Biomech*. 1990;23(12):1247-1259. doi:10.1016/0021-9290(90)90382-d

82. Spoor CW, van Leeuwen JL. Knee muscle moment arms from MRI and from tendon travel. *J Biomech*. 1992;25(2):201-206. doi:10.1016/0021-9290(92)90276-7

83. Visser JJ, Hoogkamer JE, Bobbert MF, Huijing PA. Length and moment arm of human leg muscles as a function of knee and hip-joint angles. *Eur J Appl Physiol Occup Physiol*. 1990;61(5-6):453-460. doi:10.1007/BF00236067

84. van Eijden TM, Kouwenhoven E, Weijs WA. Mechanics of the patellar articulation. Effects of patellar ligament length studied with a mathematical model. *Acta Orthop Scand*. 1987;58(5):560-566. doi:10.3109/17453678709146400

85. Ward SR, Eng CM, Smallwood LH, Lieber RL. Are Current Measurements of Lower Extremity Muscle Architecture Accurate? *Clin Orthop Relat Res*. 2009;467(4):1074-1082. doi:10.1007/s11999-008-0594-8

86. Draganich LF, Andriacchi TP, Andersson GB. Interaction between intrinsic knee mechanics and the knee extensor mechanism. *J Orthop Res*. 1987;5(4):539-547. doi:10.1002/jor.1100050409

87. Schipplein OD, Andriacchi TP. Interaction between active and passive knee stabilizers during level walking. *Journal of Orthopaedic Research*. 1991;9(1):113-119. doi:https://doi.org/10.1002/jor.1100090114

88. Giffin JR, Vogrin TM, Zantop T, Woo SLY, Harner CD. Effects of increasing tibial slope on the biomechanics of the knee. *Am J Sports Med*. 2004;32(2):376-382. doi:10.1177/0363546503258880

89. Bezodis NE, Salo AIT, Trewartha G. Excessive fluctuations in knee joint moments during early stance in sprinting are caused by digital filtering procedures. *Gait Posture*. 2013;38(4):653-657. doi:10.1016/j.gaitpost.2013.02.015

90. Kristianslund E, Krosshaug T, van den Bogert AJ. Effect of low pass filtering on joint moments from inverse dynamics: implications for injury prevention. *J Biomech*. 2012;45(4):666-671. doi:10.1016/j.jbiomech.2011.12.011

91. Greenhouse SW, Geisser S. On methods in the analysis of profile data. *Psychometrika*. 1959;24:95-112. doi:10.1007/BF02289823

92. Cohen J. Eta-Squared and Partial Eta-Squared in Fixed Factor Anova Designs. *Educational and Psychological Measurement*. 1973;33(1):107-112. doi:10.1177/001316447303300111

93. Cohen J. *Statistical Power Analysis for the Behavioral Sciences*. 2nd ed. Routledge; 1988. doi:10.4324/9780203771587

94. Richardson JTE. Eta squared and partial eta squared as measures of effect size in educational research. *Educational Research Review*. 2011;6(2):135-147. doi:10.1016/j.edurev.2010.12.001

95. Sawilowsky S. New Effect Size Rules of Thumb. *Journal of Modern Applied Statistical Methods*. 2009;8(2). doi:10.22237/jmasm/1257035100

96. Messier SP, Gutekunst DJ, Davis C, DeVita P. Weight loss reduces knee-joint loads in overweight and obese older adults with knee osteoarthritis. *Arthritis & Rheumatism*. 2005;52(7):2026-2032. doi:10.1002/art.21139

97. Maly MR. Abnormal and cumulative loading in knee osteoarthritis. *Current Opinion in Rheumatology*. 2008;20(5):547-552. doi:10.1097/BOR.0b013e328307f58c

98. Butler RJ, Crowell HP, Davis IM. Lower extremity stiffness: implications for performance and injury. *Clin Biomech (Bristol, Avon)*. 2003;18(6):511-517. doi:10.1016/s0268-0033(03)00071-8

99. Sanchez-Adams J, Leddy HA, McNulty AL, O'Conor CJ, Guilak F. The Mechanobiology of Articular Cartilage: Bearing the Burden of Osteoarthritis. *Curr Rheumatol Rep*. 2014;16(10):451. doi:10.1007/s11926-014-0451-6

100. Stoddart JC, Dandridge O, Garner A, Cobb J, van Arkel RJ. The compartmental distribution of knee osteoarthritis – a systematic review and meta-analysis. *Osteoarthritis and Cartilage*. 2021;29(4):445-455. doi:10.1016/j.joca.2020.10.011

101. Rossom SV, Smith CR, Zevenbergen L, et al. Knee Cartilage Thickness, T1ρ and T2 Relaxation Time Are Related to Articular Cartilage Loading in Healthy Adults. *PLOS ONE*. 2017;12(1):e0170002. doi:10.1371/journal.pone.0170002

102. Koo S, Andriacchi TP. A comparison of the influence of global functional loads vs. local contact anatomy on articular cartilage thickness at the knee. *Journal of Biomechanics*. 2007;40(13):2961-2966. doi:10.1016/j.jbiomech.2007.02.005

103. Barrios J, Willson J. Minimum Detectable Change in Medial Tibiofemoral Contact Force Parameters: Derivation and Application to a Load-Altering Intervention. *J Appl Biomech*. 2017;33(2):171-175. doi:10.1123/jab.2016-0163

104. John CT, Seth A, Schwartz MH, Delp SL. Contributions of muscles to mediolateral ground reaction force over a range of walking speeds. *J Biomech*. 2012;45(14):2438-2443. doi:10.1016/j.jbiomech.2012.06.037

105. Van Rossom S, Wesseling M, Smith CR, et al. The influence of knee joint geometry and alignment on the tibiofemoral load distribution: a computational study. *Knee*. 2019;26(4):813-823. doi:10.1016/j.knee.2019.06.002

106. Sharma L, Song J, Dunlop D, et al. Varus and Valgus Alignment and Incident and Progressive Knee Osteoarthritis. *Ann Rheum Dis*. 2010;69(11):1940-1945. doi:10.1136/ard.2010.129742

107. Hunt MA, Birmingham TB, Bryant D, et al. Lateral trunk lean explains variation in dynamic knee joint load in patients with medial compartment knee osteoarthritis. *Osteoarthritis and Cartilage*. 2008;16(5):591-599. doi:10.1016/j.joca.2007.10.017

108. Mündermann A, Asay JL, Mündermann L, Andriacchi TP. Implications of increased medio-lateral trunk sway for ambulatory mechanics. *Journal of Biomechanics*. 2008;41(1):165-170. doi:10.1016/j.jbiomech.2007.07.001

109. Eckstein F, Müller S, Faber SC, Englmeier KH, Reiser M, Putz R. Side differences of knee joint cartilage volume, thickness, and surface area, and correlation with lower limb dominance--an MRI-based study. *Osteoarthritis Cartilage*. 2002;10(12):914-921. doi:10.1053/joca.2002.0843

110. Lee SJ, Hidler J. Biomechanics of overground vs. treadmill walking in healthy individuals. *Journal of Applied Physiology*. 2008;104(3):747-755. doi:10.1152/japplphysiol.01380.2006

111. Lerner ZF, DeMers MS, Delp SL, Browning RC. How tibiofemoral alignment and contact locations affect predictions of medial and lateral tibiofemoral contact forces. *Journal of Biomechanics*. 2015;48(4):644-650. doi:10.1016/j.jbiomech.2014.12.049

Appendix A: University Internal Review Board (IRB) Approval

EAST CAROLINA UNIVERSITY
University & Medical Center Institutional Review Board
4N-64 Brody Medical Sciences Building· Mail Stop 682
600 Moye Boulevard · Greenville, NC 27834
Office **252-744-2914** · Fax **252-744 2284**
rede.ecu.edu/umcirb/

Notification of Initial Approval: Expedited

From: Biomedical IRB
To: Blake Jones
CC: Ryan Wedge
Date: 3/15/2021
Re: UMCIRB 20-002973
Knee Joint Loading with External Load and Real-Time Biofeedback

I am pleased to inform you that your Expedited Application was approved. Approval of the study and any consent form(s) occurred on 3/14/2021. The research study is eligible for review under expedited category # 4,6,7. The Chairperson (or designee) deemed this study no more than minimal risk.

As the Principal Investigator you are explicitly responsible for the conduct of all aspects of this study and must adhere to all reporting requirements for the study. Your responsibilities include but are not limited to:

1. Ensuring changes to the approved research (including the UMCIRB approved consent document) are initiated only after UMCIRB review and approval except when necessary to eliminate an apparent immediate hazard to the participant. All changes (e.g. a change in procedure, number of participants, personnel, study locations, new recruitment materials, study instruments, etc.) must be prospectively reviewed and approved by the UMCIRB before they are implemented;

2. Where informed consent has not been waived by the UMCIRB, ensuring that only valid versions of the UMCIRB approved, date-stamped informed consent document(s) are used for obtaining informed consent (consent documents with the IRB approval date stamp are found under the Documents tab in the ePIRATE study workspace);

3. Promptly reporting to the UMCIRB all unanticipated problems involving risks to participants and others;

4. Submission of a final report application to the UMICRB prior to the expected end date provided in the IRB application in order to document human research activity has ended and to provide a timepoint in which to base document retention; and

5. Submission of an amendment to extend the expected end date if the study is not expected to be completed by that date. The amendment should be submitted 30 days prior to the UMCIRB approved expected end date or as soon as the Investigator is aware that the study will not be completed by that date.

The approval includes the following items:

Name	Description
Health Survey	Surveys and Questionnaires
Informed Consent	Consent Forms
PAR-Q	Standardized/Non-Standardized Instruments/Measures
Recruitment Flyer	Recruitment Documents/Scripts
Study Protocol	Study Protocol or Grant Application

For research studies where a waiver or alteration of HIPAA Authorization has been approved, the IRB states that each of the waiver criteria in 45 CFR 164.512(i)(1)(i)(A) and (2)(i) through (v) have been met. Additionally, the elements of PHI to be collected as described in items 1 and 2 of the Application for Waiver of Authorization have been determined to be the minimal necessary for the specified research.

The Chairperson (or designee) does not have a potential for conflict of interest on this study.

Appendix B: Heath Survey

Biomechanics of Load Carriage
Health Survey to Determine Eligibility For Research Participants

Demographic data:

Date _____

Name _____ Phone number _____

Address _____
_

Birth date _____ Age _____

Height (ft/in) _____ Height (m) _____

Weight (lbs) _____ Mass (kg) _____

BMI (kg/m^2) _____

Leg Length Discrepancy? Yes____ No____

Medical:

Do you have any musculoskeletal problems such as previous knee injury or arthritis, joint replacement, or other orthopedic problems? Yes____ No ____

Do you have any short term or persistent pain? Yes____ No ____. If Yes, where is this pain _____?

Do you have any neurological problems such as stroke or Parkinson's disease? Yes____ No ____

Do you have any problems with your heart such as atrial fibrillation, pacemaker, coronary artery disease, or congestive heart failure? Yes____ No ____

Do you have any pulmonary diseases such as difficulty in breathing, asthma or emphysema? Yes___ No ____

Do you have any peripheral artery disease? Yes____ No ____

Do you have high blood pressure (>160/90 mm Hg)? Yes____ No ____

Do you take medication to control your blood pressure? Yes____ No_____

Please list the medications you are currently taking

_____
_____

_____
_____

Do you have any loss of vision? Yes____ No ____

If yes, do you have eyeglasses or contact lenses that correct your vision? Yes____ No ____

Do you have any other medical problems we did not talk about? Yes____ No_____

If, "Yes," what is or are the conditions?

_____

List any surgeries you have had.

_____
_____

_____
_____

Please tell us your physician's name, telephone number, and clinic name, if you have one:

_____
_____

_____
_____

Appendix C: Physical Activity Readiness Questionnaire (PAR-Q)

Data Collection Sheet

NAME:_____ DATE:_____

HEIGHT:_____in. WEIGHT:_____ lbs. AGE:_____

PHYSICIANS NAME:_____ PHONE: _____

PHYSICAL ACTIVITY REA DINESS QUESTIONNAIRE (PAR-Q)

	Questions	Yes	No
1	Has your doctor ever said that you have a heart condition and that you should only perform physical activity recommended by a doctor?		
2	Do you feel pain in your chest when you perform physical activity?		
3	In the past month, have you had chest pain when you were not performing any physical activity?		
4	Do you lose your balance because of dizziness or do you ever lose consciousness?		
5	Do you have a bone or joint problem that could be made worse by a change in your physical activity?		
6	Is your doctor currently prescribing any medication for your blood pressure or for a heart condition?		
7	Do you know of <u>any</u> other reason why you should not engage in physical activity?		

If you have answered "Yes" to one or more of the above questions, consult your physician <u>before</u>engaging in physical activity. Tell your physician which questions you answered "Yes" to. After amedical evaluation, seek advice from your physician on what type of activity is suitable for your current condition.

Appendix D: Motion Capture Marker Locations

Trunk markers
T1
T2
T3
T4

Pelvis
RASI (Right Anterior Superior Iliac Spine)
LASI (Left Anterior Superior Iliac Spine)
RPSI (Right Posterior Superior Iliac Spine)
L5S1 (Lumbar 5/Sacrum 1)
LPSI (Left Posterior Superior Iliac Spine)

Right Thigh
TMTH (Top Medial Thigh)
TLTH (Top Lateral Thigh)
BMTH (Bottom Medial Thigh)
BLTH (Bottom Lateral Thigh)
MEKN (Medial Femoral Epicondyle)
LAKN (Lateral Femoral Epicondyle)

Left thigh
LTMT (Top Medial Thigh)
LTLT (Top Lateral Thigh)
LBMT (Bottom Medial Thigh)
LBLT (Bottom Lateral Thigh)
LMEK (Medial Femoral Epicondyle)
LLAK (Lateral Femoral Epicondyle)

Right shank
MTIB (Medial Tibial Epicondyle)
LTIB (Tibial Plateau)
TMSH (Top Medial Shank)
TLSH (Top Lateral Shank)
BMSH (Bottom Medial Shank)
BLSH (Bottom Lateral Shank)
MEMA (Medial Malleolus)
LAMA (Lateral Malleolus)

Left shank
LMTIB (Medial Tibial Epicondyle)
LLTIB (Tibial Plateau)
LTMS (Top Medial Shank)
LTLS (Top Lateral Shank)
LBMS (Bottom Medial Shank)
LBLS (Bottom Lateral Shank)

Right foot
PRHE (Proximal Heel)
DIHE (Distal Heel)
LAHE (Lateral Heel)
MTH1 (Metatarsal Head 1)
MTH5 (Metatarsal Head 5)
DIFT (Distal Great Toe)

Left foot
LPRH (Proximal Heel)
LDIH (Distal Heel)
LLAH Lateral Heel)
LMT1 (Metatarsal Head 1)
LMT5 (Metatarsal Head 5)
LDIFT (Distal Great Toe)

Right side view
Rear view

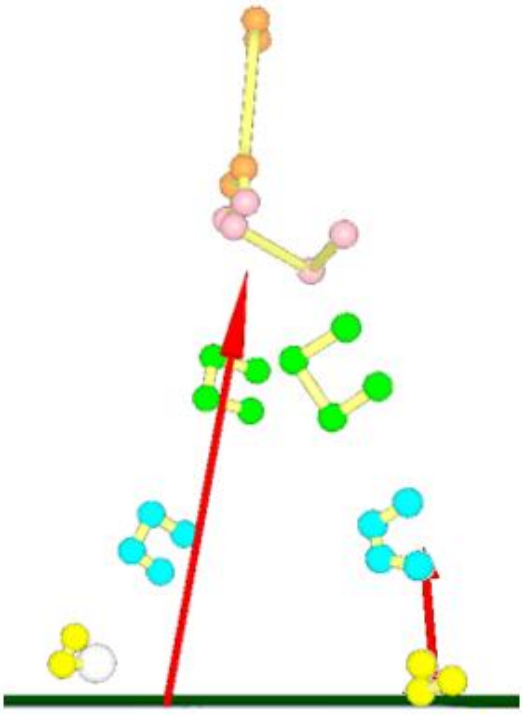

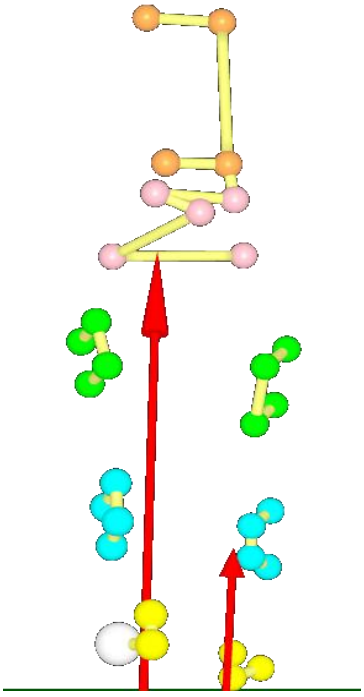

Front Standing Marker Set **Rear Standing Marker set**

Trunk

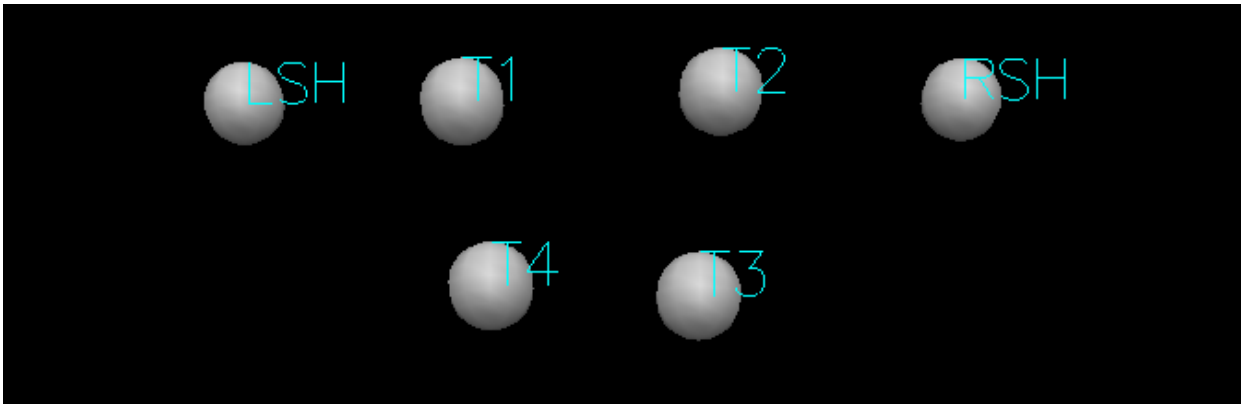

RSH
LSH
T1
T2

T3
T4

Pelvis

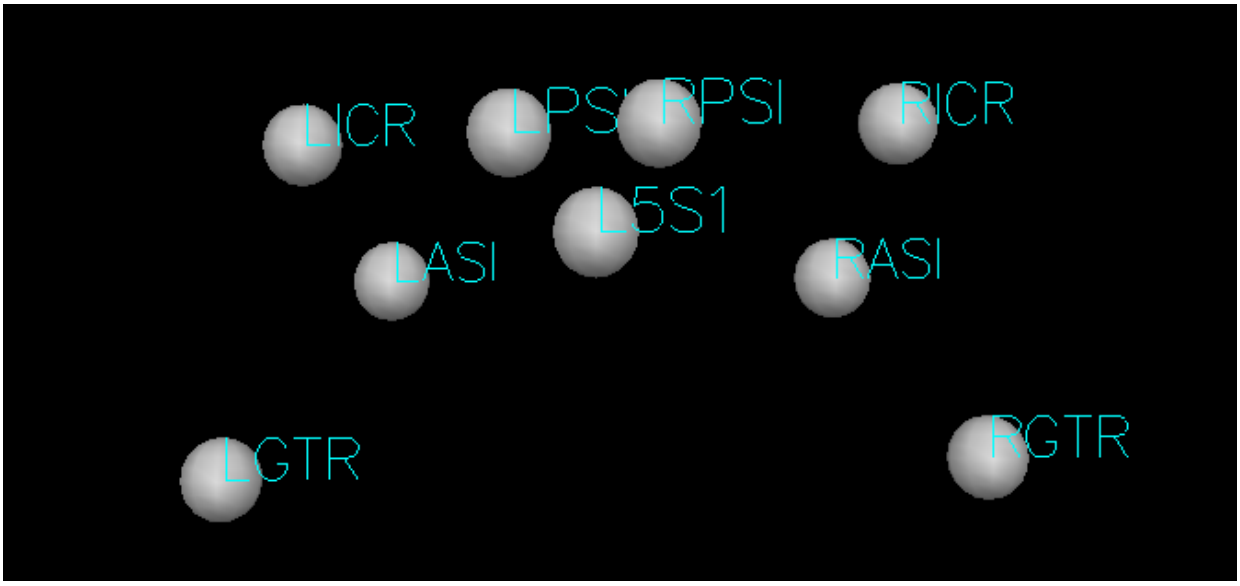

RICR
LICR
RPSI
LPSI
L5S1
RASI
LASI
RGTR
LGTR

Thighs/Knees/Shanks

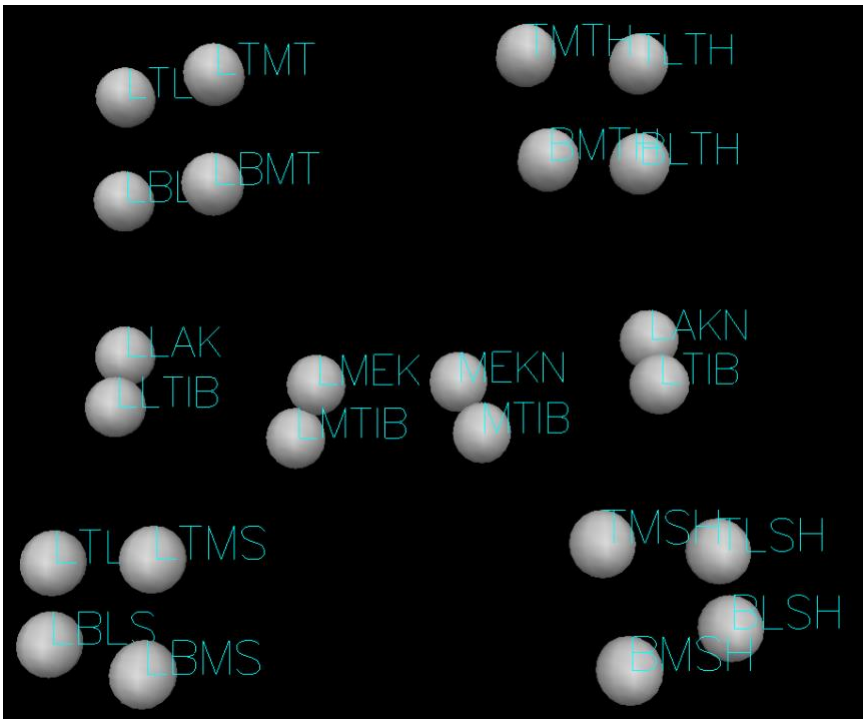

Right	Left
TMTH	LTMT
TLTH	LTLT
BMTH	LBMT
BLTH	LBLT
MEKN	**LMEK**
LAKN	**LLAK**
MTIB	**LMTIB**
LTIB	**LLTIB**
TMSH	LTLS
TLSH	LTMS
BMSH	LBMS
BLSH	LBLS

Ankles/Feet

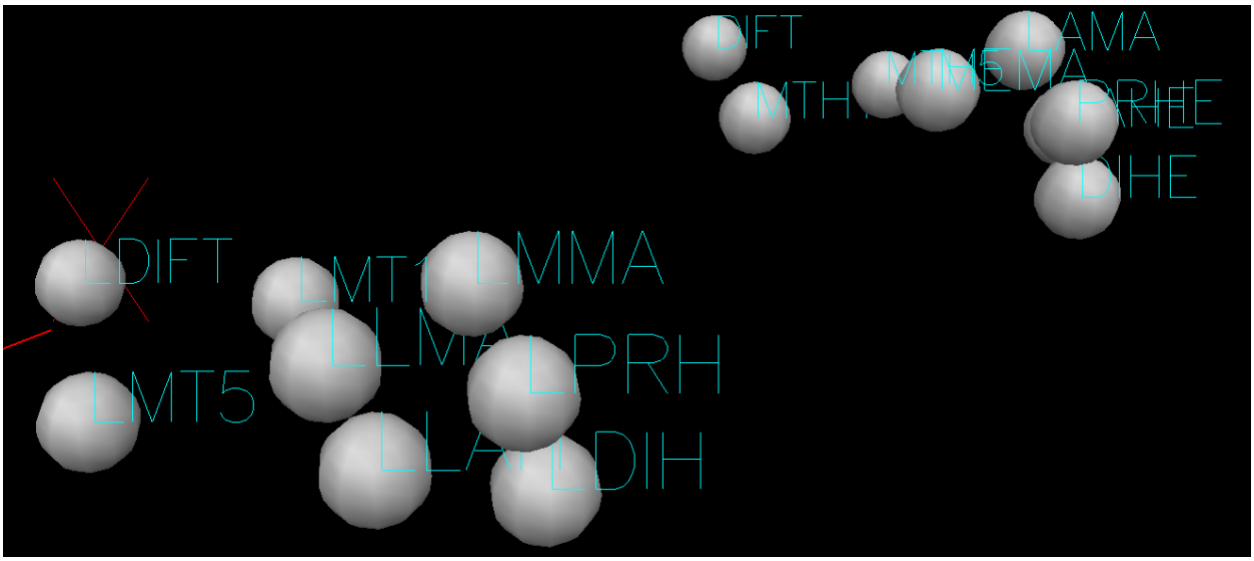

Right	Left
PRHE	LPRH
DIHE	LDIH
LAHE	LLAH
MEMA	**LMMA**
LAMA	**LLMA**
MTH1	**LMT1**
MTH5	**LMT5**
DIFT	**LDIFT**

Appendix E: Informed Consent

Informed Consent to Participate in Research
Information to consider before taking part in research that has no more thanminimal risk.

Title of Research Study: Real-time Knee Joint Loading while Walking

Principal Investigator: Blake Jones, B.S.
Co-Investigators: Dr. Ryan Wedge, PT, PhD and Dr. Paul DeVita, PhD
Institution, Department or Division: Department of Physical Therapy and Department of Kinesiology, East Carolina University Address: 2410 Health Sciences Building Telephone #: 252.744.6237

Researchers at East Carolina University (ECU) study problems in society, health problems, environmental problems, behavior problems and the human condition. Our goal is to try to find ways to improve the lives of you and others. Todo this, we need the help of volunteers who are willing to take part in research.

Why am I being invited to take part in this research?
The objectives of this study are 1) to observe changes in knee joint loading and walking mechanics when an external load of 15% and 30% bodyweight are applied via a weighted vest, and 2) to observe the changes in walking mechanics when asked to decrease knee joint loads while walking with an external load. You are being invited to takepart in this research because you are a healthy volunteer between the ages of 18 and 30 without a history of major lower extremity injury or surgery. The decision to take part in this research is yours to make. By doing this research, we hope to better understand how to best develop a method of visually displaying knee joint loads in order to assist the user in improving knee joint loads through walking modification.

If you volunteer to take part in this research, you will be one of 24 people to do so.

Are there reasons I should not take part in this research?
I understand I should not participate in this research if I have any health problems that get worse when I walk or carryheavy loads. Also, I should not participate in this research if I have had any surgeries or major injuries in my legs. I should not volunteer for this study if I am under 18 years of age or older than 30.

What other choices do I have if I do not take part in this research?
You can choose not to participate. You may stop participating at any point during the study.

Where is the research going to take place and how long will it last?

The research will take place in the Human Movement Analysis Laboratory on the Health Sciences Building of East Carolina University. You will need to come to the laboratory one time during the study. The total amount of time you will be asked to volunteer for this study is approximately 120 minutes.

What will I be asked to do?
Before the lab visit, you will complete a screening Health Survey and Physical Activity questionnaire over the phone. In the lab, your height, weight, and leg length will be measured. Then, you will have any loose- fitting clothing tucked in and secured. You will be fitted with a weighted vest, and your arms, trunk, pelvis, legs, and feet will have motion capture markers placed on bony landmarks using tape and elastic wraps. Next, you will be first fit with a mouthpiece so we can collect the oxygen you breath in and the carbondioxide you breath out. We will have you stand on the treadmill for 5 minutes for a calibration trial while measuring Energy Expenditure. You will then start to walk on the instrumented treadmill at 1.4 m/s for 5 minutes. After the first five minutes real-time visual feedback of vertical ground reaction forces will be displayed on a monitor, you will continue walking for another 5 minutes will try to adjust your walking pattern in order to decrease your knee loads.You will then step off the treadmill and will have the weighted vest loaded at either 15% or 30% of your bodyweight. The same process will be repeated for 15% or 30% bodyweight load, and then repeated a third time with remaining loading condition.

What might I experience if I take part in the research?
Risk associated with this study are minimal. Any risks that may occur with this research are no more than what you would experience during regular walking on a treadmill. To minimize risk of injury, a treadmill stop button will be available if you want to stop or are experiencing pain. There may not be any personal benefit to you, but the information gained by doing this research may help others in the future. Individuals trained in CPR, AED, and First Aid will be present in the lab during the duration of the tests. If you experience any pain or any complications occur,the test will be terminated immediately.

Will it cost me to take part in this research?
There are no costs associated with this study. If any injury occurs in the course of research, please notify the principle investigator.

Who will know that I took part in this research and learn personal information about me?
The people and organizations listed below may know that you took part in this research
and may see information about you that is normally kept private. With your permission, these people may use yourprivate information to do this research:

- The University & Medical Center Institutional Review Board (UMCIRB) and its staff, who have responsibilityfor overseeing your welfare during this research, and other ECU staff who oversee this research.
- Any agency of the federal, state, or local government that regulates human research. This includes the Department of Health and Human Services (DHHS), the North Carolina Department of health, and the Officefor Human Research Protections.
- Research assistants under direct supervision of the primary investigator

How will you keep the information you collect about me secure? How long will you keep it?
No visual record or otherwise identifiable record of your performance is kept other than marker movements, force data, inspired and expired gases, and knee load adjustment. All electronic and other information pertaining to your participation will be kept confidential through the use of number codes. Any form with your name will be stored in a locked file cabinet in the Human Movement Analysis

Laboratory, which remains locked except when in use. The onlypeople with access to the passwords or your personal information will be the researchers identified above. Motion analysis data collected during the study will not be linked with any personally identifiable information. Electronic information from this study is also password protected.
The results of this study may be published in scientific literature or presented at professional meetings. If used for thesereasons, no information that could be used to identify you will be included. We may ask to take a photograph of you during the data collection. If you consent to a photograph, it will not include your face or any other identifiable marks. The information from this study will be maintained for a minimum of three years. After a minimum of three years, hard copies of your information will be destroyed and electronic information will be archived in piratedrive (piratedrive is a secure individual folder created on an ECU server for each faculty, staff and student for data file storage).

What if I decide I don't want to continue in this research?

You can stop at any time after it has already started. There will be no consequences if you stop, and you will not be criticized. You will not lose any benefits that you normally receive.

Who should I contact if I have questions?

The people conducting this study will be available to answer any questions concerning this research, now or in the future. You may contact the Principal Investigator Blake Jones via email at jonesbl20@student.ecu.edu and Co-Investigator Dr. DeVita via email at devitap@ecu.edu and Co-Investigator Dr. Wedge via email at wedger19@ecu.edu

If you have questions about your rights as someone taking part in research, you may call the University & Medical Center Institutional Review Board (UMCIRB) at phone number 252-744-2914 (days, 8:00 am-5:00 pm). If you would like to report a complaint or concern about this research study, you may call the Director for Human Research Protections, at 252-744-2914.

Is there anything else I should know?

Identifiers might be removed from the identifiable private information or identifiable biospecimens and, after such removal, the information or biospecimens could be used for future research studies or distributed to another investigator for future research studies without additional informed consent from you or your Legally Authorized Representative (LAR). However, there still may be a chance that someone could figure out the information is aboutyou.

I have decided I want to take part in this research. What should I do now?

The person obtaining informed consent will ask you to read the following and if you agree, you should sign this form

- I have read (or had read to me) all of the above information
- I have had an opportunity to ask questions about things in this research I did not understand and have receivedsatisfactory answers
- I know that I can stop taking part in this study at any time
- By signing this informed consent form, I am not giving up any of my rights
- I have been given a copy of this consent document, and it is mine to keep

Do you consent to a photograph of your trunk and legs to be potentially used for publication purposes? The photograph will not include any identifiable information, identifiable features, andwill not include your face.
Yes ( ) No ( )

Participant's Name (PRINT)	**Signature**	**Date**

Person Obtaining Informed Consent: I have conducted the initial informed consent process. I have orally reviewedthe contents of the consent document with the person who has signed above and answered all of the person's questions about the research.

Person Obtaining Consent (PRINT)	**Signature**	**Date**

Appendix F: Supplemental Material

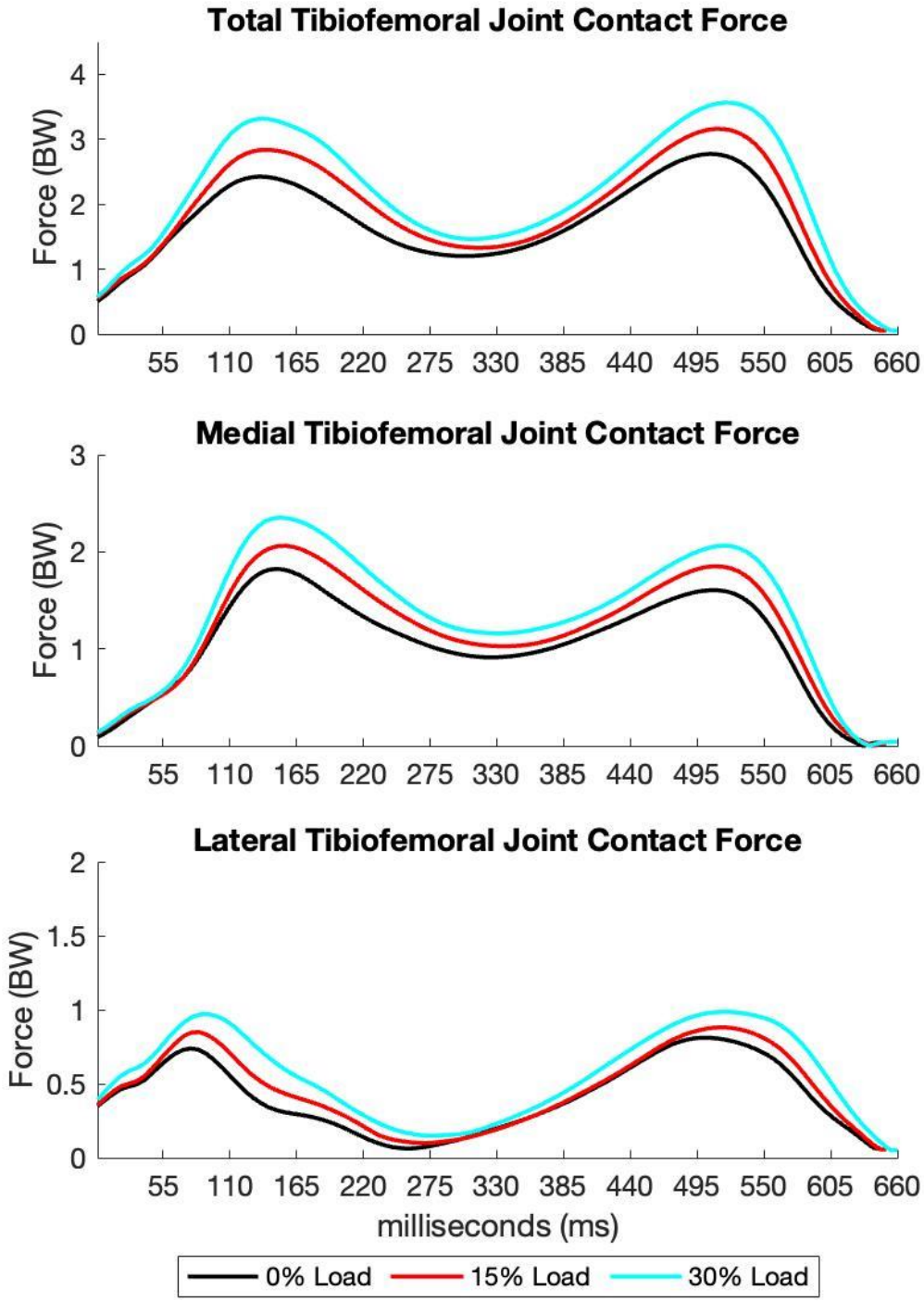

Figure 29: Tibiofemoral Joint Contact Forces Across Loading Conditions over Milliseconds Total, medial, and lateral tibiofemoral contact forces over percent stance during load carriage of 0% BW, 15% BW, and 30% BW over milliseconds. Bold line represents the mean across all

participants. The first peak of total, medial, and lateral tibiofemoral joint contact forces increased across condition ($p < .001$).

Lower extremity peak internal sagittal plane moments increased with increasing load (HEM $p < .001$, $\eta_p^2 = .694$; KEM $p < .001$, $\eta_p^2 = .614$; ADM $p = .002$, $\eta_p^2 = .234$), **Table 4** & **Figure 12**. From 0% load to 15%, and from 0% to 30%, peak hip extension moment increased on average 0.06 N·m/kg (7.6%) and 0.19 N·m/kg (20.7%); peak knee extension moment increased 0.10 N·m/kg (17.2%) and 0.24 N·m/kg (41.4%); and peak dorsiflexion moment increased 0.02 N·m/kg (6.7%) and 0.04 N·m/kg (13.3%), respectively, **Table 4**. All peak internal sagittal plane moments were described by linear trends (HEM $p < .001$, $\eta_p^2 = .794$; KEM $p < .001$, $\eta_p^2 = .670$; ADM $p = .004$, $\eta_p^2 = .313$), but no quadratic trends (HEM $p = .052$, $\eta_p^2 = .154$; KEM $p = .227$, $\eta_p^2 = .063$; ADM $p = .703$, $\eta_p^2 = .006$).

Hip and knee peak internal frontal plane moments increased with increasing load (HAM $p < .001$, $\eta_p^2 = .743$; KAM $p < .001$, $\eta_p^2 = .469$), **Table 4** & **Figure 13**. From 0% load to 15%, and from 0% to 30%, peak hip abduction moment increased on average 0.11 N·m/kg (12.6%) and 0.16 N·m/kg (17.2%); peak knee abduction moment increased 0.05 N·m/kg (11.9%) and 0.07 N·m/kg (16.7%), **Table 4**. Peak hip and knee internal abduction moments were described by linear trends (HAM $p < .001$, $\eta_p^2 = .818$; KAM $p < .001$, $\eta_p^2 = .614$). Peak hip abduction moment was also described by a quadratic trend ($p = .022$, $\eta_p^2 = .207$), while peak knee abduction moment had no quadratic trend component ($p = .183$, $\eta_p^2 = .076$).

Table 13: Internal Sagittal and Frontal Plane Moments, Mean (SD)

Variable	No Load	15% Load	30% Load	Main Effects	Trend Quadratic
				p	*p*
				η_p^2	η^2
Peak Hip Extension Moment (N·m/kg)	-0.92 (0.20)	-0.99 (0.21) *	-1.11 (0.24) **, ‡	**< .001** **.694**	.052 **.154**
Peak Knee Extension Moment (N·m/kg)	0.58 (0.25)	0.68 (0.30) **	0.82 (0.36) **, ‡	**< .001** **.614**	.227 .063
Peak Dorsiflexion Moment (N·m/kg)	0.30 (0.07)	0.32 (0.07)	0.34 (0.08) *	**.002** **.234**	.703 .006
Peak Hip Abduction Moment (N·m/kg)	-0.87 (0.14)	-0.98 (0.17) **	-1.02 (0.17) **, ‡	**< .001** **.743**	**.022** **.207**
Peak Knee Abduction Moment (N·m/kg)	-0.42 (0.14)	-0.47 (0.16) **	0.49 (0.16) **	**< .001** **.469**	.183 .076
Knee Extension Angular Impulse (N·m·s/kg)	0.07 (0.04)	0.08 (0.05) **	0.10 (0.05) **, ‡	**< .001** **.547**	.739 .005
Knee Abduction Angular Impulse (N·m·s/kg)	-0.12 (0.05)	-0.14 (0.06) **	-0.15 (0.07) **,†	**< .001** **.526**	.166 .082
Hip Abduction Angular Impulse (N·m·s/kg)	-0.31 (0.05)	-0.35 (0.06) **	-0.38 (0.07) **,†	**< .001** **.781**	.075 .131

Averages (SD) for peak hip extension, knee extension, ankle dorsiflexion, hip abduction, and knee abduction moments at each loading conditions, along with knee extension and abduction angular impulse and hip abduction angular impulse Repeated measures ANOVA results for main effects, Bonferroni pairwise comparisons, and post-hoc quadratic trend analysis. Post-hoc linear trend analysis all at $p < .005$

0% load is walking with an unloaded weighted vest, 15% load is walking with the weighted vest loaded at 15% bodyweight, and 30% load is walking with the weighted vest loaded at 30% bodyweight.

η_p^2: Partial eta. Squared. N: Newtons. m: meters. kg: kilograms

*$p < 0.05$ compared with No-Load, **$p \leq 0.005$ compared with No-Load.

†$p \leq 0.05$ compared with 15% Load, ‡$p \leq 0.005$ compared with 15% Load.

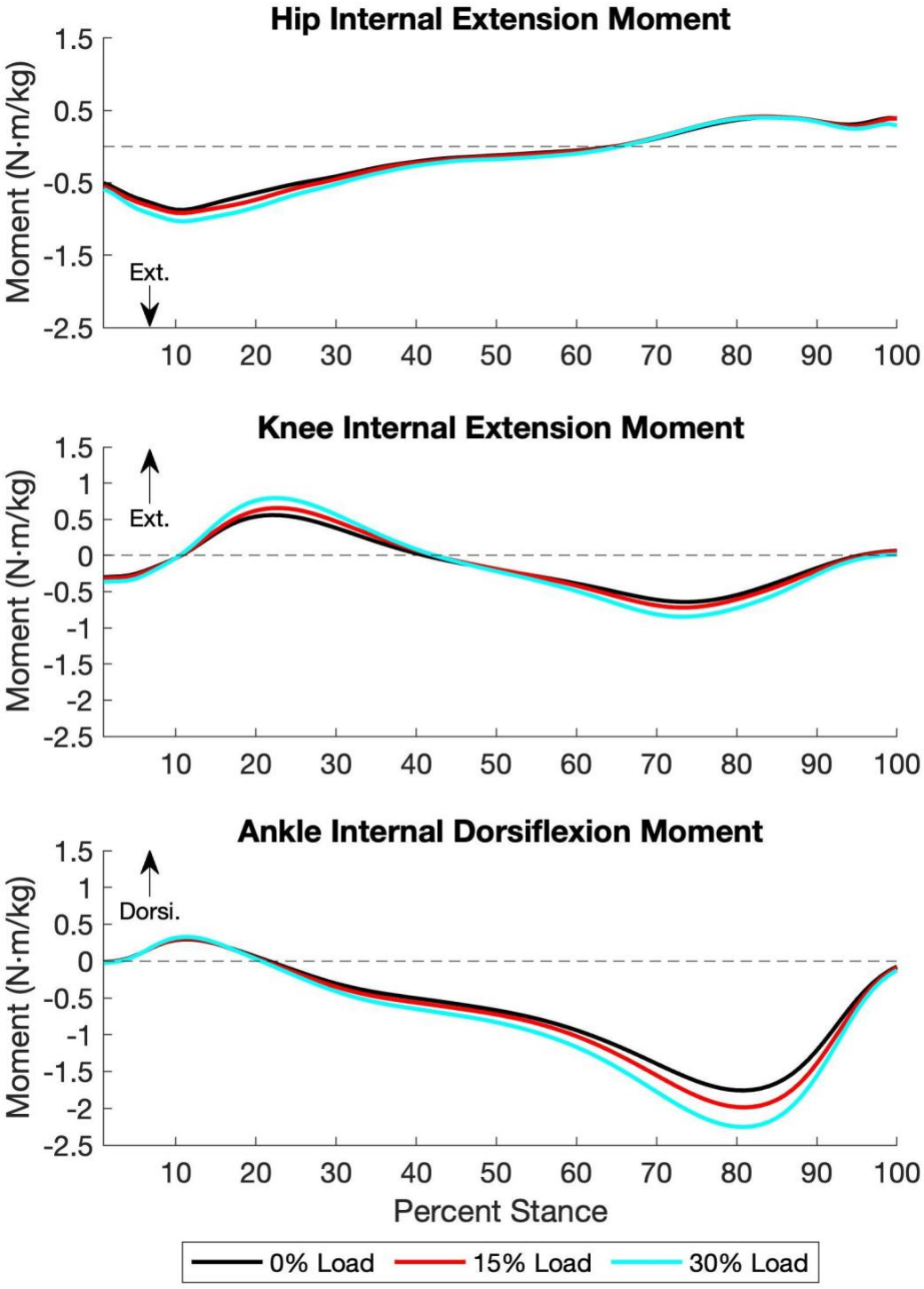

Figure 30: Lower Extremity Sagittal Plane Moments Across Loading Conditions
Peak hip extension, knee extension, and ankle dorsiflexion moments over percent stance during load carriage of 0% BW, 15% BW, and 30% BW. Bold line represents the mean across all participants. The peak of the sagittal plane moments increased across condition $p < .005$.

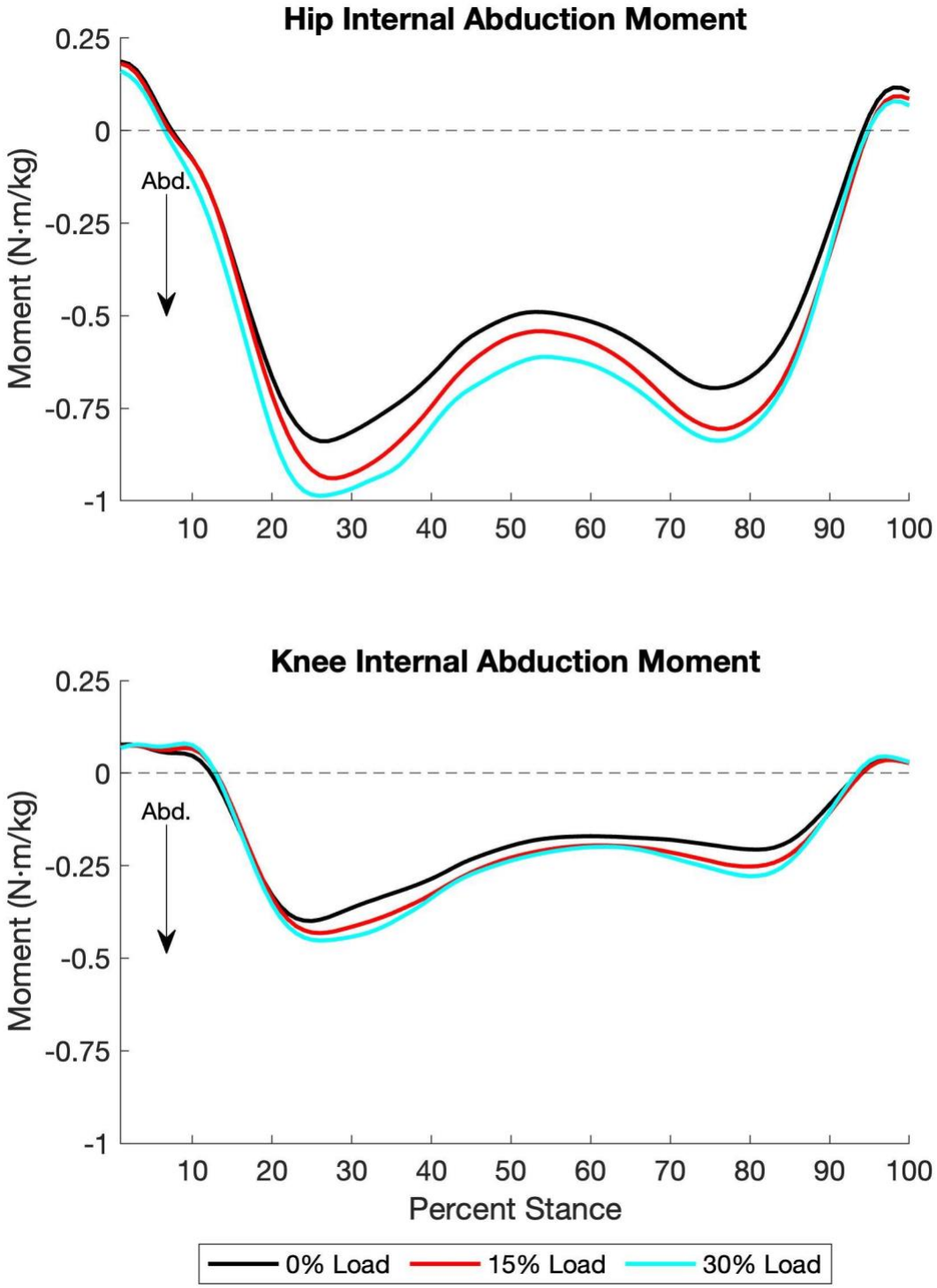

Figure 31: Lower Extremity Frontal Plane Moments Across Loading Conditions
Internal hip abduction and knee abduction moments over percent stance during load carriage of 0% BW, 15% BW, and 30% BW. Bold line represents the mean across all participants. The peak of the frontal plane moments increased across condition $p < .001$

Table 14: Sagittal Plane Knee Power And Work, Mean (SD)

Variable	No Load	15% Load	30% Load	Main Effects	Trend Quadratic
				p	*p*
				η_p^2	η^2
Peak Knee Power *K1S* (W/kg)	-0.77 (0.41)	-0.90 (0.52) *	-1.12 (0.59) **, ‡	**< .001** **.565**	.054 **.152**
Negative Knee Work *K1S* (J/kg)	-0.07 (0.02)	-0.08 (0.03) **	0.09 (0.03) **, ‡	**< .001** **.609**	.474 .023

Averages (SD) for peak knee power and negative work at K1S for each loading conditions. Repeated measures ANOVA results for main effects, Bonferroni pairwise comparisons, and post-hoc quadratic trend analysis. Post-hoc linear trend analysis all at $p < .005$

0% load is walking with an unloaded weighted vest, 15% load is walking with the weighted vest loaded at 15% bodyweight, and 30% load is walking with the weighted vest loaded at 30% bodyweight.

η_p^2: Partial eta. Squared. N: Newtons. m: meters. kg: kilograms

*$p < 0.05$ compared with No-Load, **$p \leq 0.005$ compared with No-Load.

†$p \leq 0.05$ compared with 15% Load, ‡$p \leq 0.005$ compared with 15% Load.

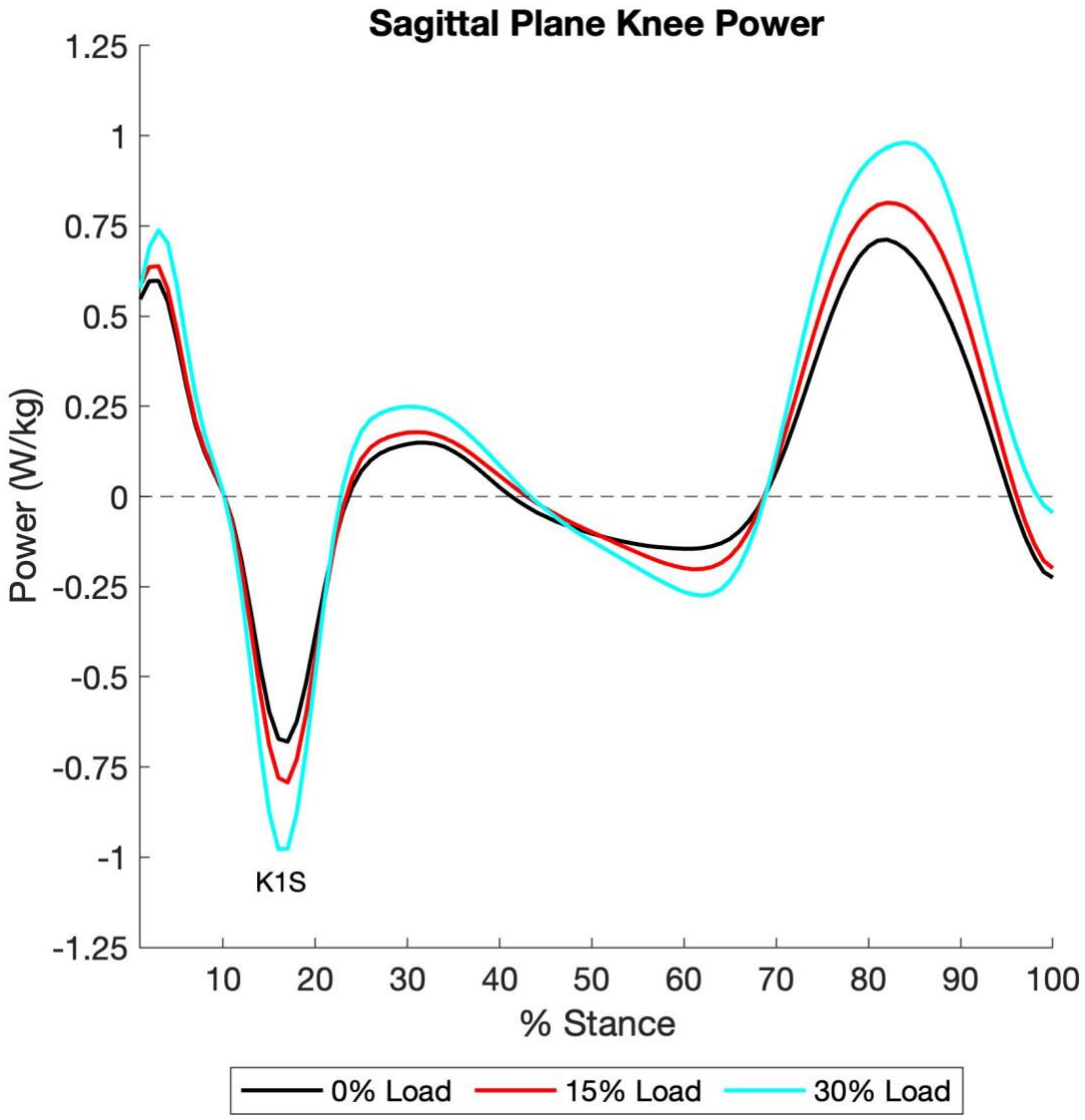

Figure 32: Sagittal Plane Knee Power Across Loading Conditions
Sagittal plane knee power over percent stance during load carriage of 0% BW, 15% BW, and 30% BW. Bold line represents the mean across all participants.

First peak vertical, first peak medial, and peak breaking ground reaction forces increased directly with increased load carriage (vGRF $p < .001$, $\eta_p^2 = .935$; mGRF $p < .001$, $\eta_p^2 = .577$; bGRF $p < .001$, $\eta_p^2 = .906$), **Table 5** & **Figure 14**. From 0% load to 15% and from 0% to 30% first peak vGRF increased on average 118 N (14.7%) and 232 N (28.6%); first peak mGRF increased 7 N (10.8%) and 16 N (24.6%), and peak bGRF increased 25 N (16.6%) and 51 N (35.1%), respectively, **Table 5**. All peak GRF forces were described by linear trends (vGRF $p < .001$, $\eta_p^2 = .950$; mGRF $p < .001$, $\eta_p^2 = .635$; bGRF $p < .001$, $\eta_p^2 = .931$), but no quadratic trends (vGRF $p = .601$, $\eta_p^2 = .012$; mGRF $p = .385$, $\eta_p^2 = .033$; bGRF $p = .555$, $\eta_p^2 = .015$).

GRF impulses responded similarly, with load carriage increasing vertical, medial, and breaking impulses (vGRF $p < .001$, $\eta_p^2 = .938$; mGRF $p < .001$, $\eta_p^2 = .644$); bGRF $p < .001$, $\eta_p^2 = .896$), **Table 5** & **Figure 14**. From 0% load to 15%, and from 0% to 30%, vGRF impulse increased 46 N·s (13.2%) and 97 N·s (27.2%); mGRF impulse increased 3 N·s (13.6%), and 6 N·s (27.3%), and bGRF impulse increased 4 N·s (18.2%) and 8 N·s (36.4%), respectively, **Table 5**. All GRF impulses were described by significant linear trends (vGRF $p < .001$, $\eta_p^2 = .943$; mGRF $p < .001$, $\eta_p^2 = .718$; bGRF $p < .001$, $\eta_p^2 = .918$). vGRF impulse exhibited a quadratic trend component with a large effect size ($p = .047$, $\eta_p^2 = .161$). No quadratic trend components were evident for mGRF or bGRF impulses ($p = .492$, $\eta_p^2 = .021$; bGRF $p = .934$, $\eta_p^2 < .001$).

Table 15: Ground Reaction Forces and Impulses, Mean (SD)

Variable	No Load	15% Load	30% Load	Main Effects	Trend Quadratic
				p	p
				η_p^2	η_p^2
First Peak vGRF (N)	810 (116)	929 (129)	1041 (156)	< **.001**	.601
		**	**, ‡	**.935**	.012
First Peak mGRF (N)	-65 (12)	-72 (14)	-81 (17)	< **.001**	.385
		**	**, ‡	**.577**	.033
Peak bGRF (N)	-145 (217)	-169 (29)	-196 (27)	< **.001**	.555
		**	**, ‡	**.906**	.015
vGRF Impulse (N·s)	356 (54)	402 (64)	453 (74)	< **.001**	**.047**
		**	**, ‡	**.938**	**.161**
mGRF Impulse (N·s)	22 (4)	25 (5)	28 (6)	< **.001**	.492
		**	**, ‡	**.644**	.021
bGRF Impulse (N·s)	22 (4)	26 (5)	30 (5)	< **.001**	.934
		**	**, ‡	**.896**	.000

Averages (SD) for first peak and impulses of the tibiofemoral joint. Repeated measures ANOVA results for main effects, Bonferroni pairwise comparisons,
and post-hoc quadratic trend analysis. Post-hoc linear trend analysis all at $p < .001$
0% load is walking with an unloaded weighted vest, 15% load is walking with the weighted vest loaded at 15% bodyweight, and 30% load is walking with the weighted vest loaded at 30% bodyweight. First peak vertical, first peak medial, and peak breaking ground reaction forces and impulse increased significantly with load and exhibited linear trends.
η^2: Partial eta. Squared. N: Newtons. s: seconds.
*p < 0.05 compared with No-Load, **p ≤ 0.005 compared with No-Load.
†p ≤ 0.05 compared with 15% Load, ‡p ≤ 0.005 compared with 15% Load.

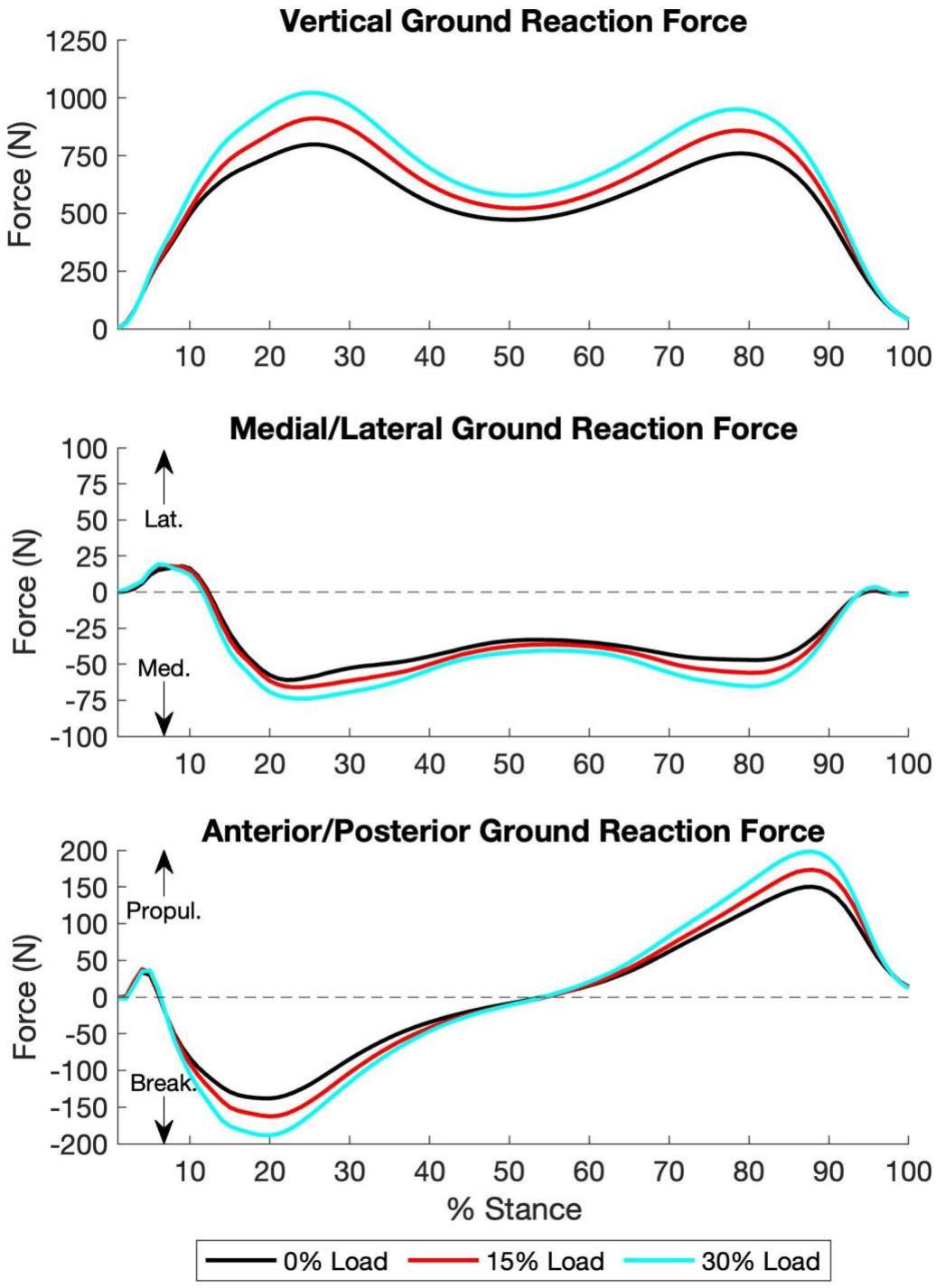

Figure 33: Ground Reaction Forces Across Loading Conditions
Vertical, medial/lateral, and anterior/posterior ground reaction forces over percent stance during load carriage of 0% BW, 15% BW, and 30% BW. Bold line represents the mean across all participants. The first peak of total, medial, and lateral tibiofemoral joint contact forces increased across condition ($p < .001$). Impulse determined over nonnormalized time.

Table 16: Spatiotemporal Parameters and Kinematics, Mean (SD)

Variable	No Load	15% Load	30% Load	Main Effects	Trend Quadratic
				p	p
				η_p^2	η_p^2
Peak Hip Adduction Angle (°)	5.1 (2.6)	5.2 (2.7)	4.8 (3.0)	.059	.055
				.125	**.151**
Peak Knee Adduction Angle (°)	2.4 (3.4)	2.6 (3.2)	2.5 (3.4)	.662	.430
				.018	.027

Averages (SD) for peak hip and knee adduction angles.. Repeated measures ANOVA results for main effects, Bonferroni pairwise comparisons, and post-hoc quadratic trend analysis. Post-hoc linear trend analysis for both frontal plane angles at $p < .005$

0% load is walking with an unloaded weighted vest, 15% load is walking with the weighted vest loaded at 15% bodyweight, and 30% load is walking with the weighted vest loaded at 30% bodyweight.

η_p^2: Partial eta. Squared. m: meters. °: degrees. N: Newtons. mm: millimeters. ms: milliseconds.

*$p < 0.05$ compared with No-Load, **$p \leq 0.005$ compared with No-Load.

†$p \leq 0.05$ compared with 15% Load, ‡$p \leq 0.005$ compared with 15% Load.

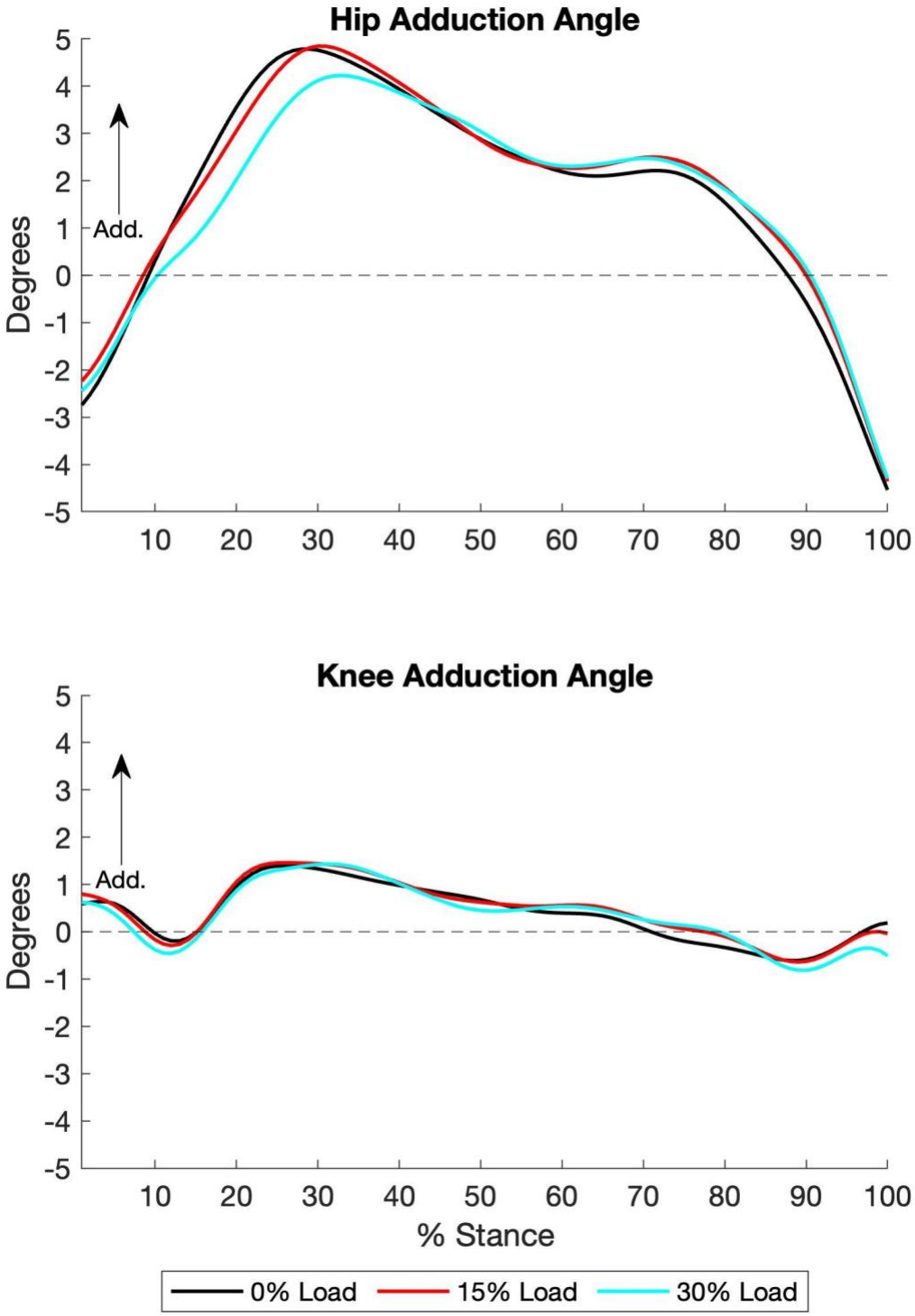

Figure 34: Lower Extremity Frontal Plane Kinematics Across Loading Conditions
Knee adduction and hip adduction over percent stance during load carriage of 0% BW, 15% BW, and 30% BW. Bold line represents the mean across all participants.

An interaction between load and limb dominance with was present for first peak hip extension moment (p = .006, η_p^2= .227), **Table 10** & **Figure 24**. Probing the interaction between the dominant and nondominant limb at each loading condition via two-tailed paired t-tests revealed that there was no significant difference between limbs at 0% load (p = .270, d = .231) and15% load (p = .089, d = .362), but at 30% load nondominant peak hip extension moment was greater than dominant (p = .039, d = .447), **Table 10**. Probing the interaction on the effect of load carriage on dominant peak hip extension moment and nondominant peak hip extension moment via one-way repeated measures ANOVAs revealed that dominant and nondominant peak hip extension moments increased with increasing load (D p < .001, η_p^2= .685; ND p < .001, η_p^2 = .802), **Table 10**. No interaction was present for peak knee extension moment (p = .170, η_p^2= .074) or first peak dorsiflexion moment (p = .474, η_p^2= .032), **Table 11 & Figure 24**. Peak knee extension moment and peak ankle dorsiflexion moment increased directly with increased load carriage (KEM p < .001, η_p^2= .656; ADM p < .001, η_p^2= .371) with dominant knee extension moment and ankle dorsiflexion moment being greater than nondominant (KEM p = .005, η_p^2= .290; ADM p = .008, η_p^2= .333), **Table 11** & **Figure 24** & **25**. At 0%, 15%, and 30%; dominant peak knee extension moment was 0.11 N·m/kg (22.2%), 0.13 N·m/kg (21.8%), and 0.15 N·m/kg (20.7%) greater than nondominant, and dominant peak dorsiflexion moment was 0.05 N·m/kg (18.9%), 0.06 N·m/kg (21.4%), and 0.06 N·m/kg (20.0%) greater than nondominant.

No interactions between load and limb dominance were present for peak hip and knee abduction moment (HAM p = .098, η_p^2= .096; KAM p = .286, η_p^2= .052) Table 12 & Figure 25). Peak hip and knee abduction moment increased with increasing load carriage (HAM p < .001, η_p^2= .835; KAM p < .001, η_p^2= .712) with nondominant hip and knee abduction moment being greater than dominant (HAM p = .002, η_p^2= .360; KAM p = .005, η_p^2= .299), **Table 11** & **Figure 26** &

27. At 0%, 15%, and 30%; nondominant peak hip abduction moment was 0.13 N·m/kg (13.8%), 0.12 N·m/kg (11.3%), and 0.16 N·m/kg (14.0%) greater than nondominant, and nondominant peak abduction moment was 0.10 N·m/kg (20.8%), 0.09N·m/kg (16.8%), and 0.11 N·m/kg (19.1%) greater than dominant.

Table 17: D vs. ND Peak Hip Extension Moment Across Load Interaction, Mean (SD)

Variable		0%	15%	30%	$\underline{p}$ η_p^2
Peak Hip Extension Moment (N·m/kg)	D	-0.94 (0.19)	-1.01 (0.19)	-1.13 (0.23)	**$p < .001$** **$\eta_p^2 = .685$**
	ND	-0.96 (0.21)	-1.06 (0.23)	-1.19 (0.24)	**$p < .001$** **$\eta_p^2 = .778$**
	$\underline{p}$	.270	.089	.039	Interaction **$p = .011$**
	d	.231	.362	.447	**$\eta_p^2 = .178$**

Averages (SD) for first peak total hamstrings force. 2 x 3 repeated measures ANOVA results for main effects and interactions. Two-tailed paired samples t-tests results for dominant vs nondominant peak hamstrings force at each loading condition, and one-way repeated measures ANOVA results for dominant peak hamstrings force across each loading condition and nondominant peak hamstrings force across each loading condition.
0% load is walking with an unloaded weighted vest, 15% load is walking with the weighted vest loaded at 15% bodyweight, and 30% load is walking with the weighted vest loaded at 30% bodyweight.
η_p^2: Partial eta. Squared. *d*: Cohen's d. N: Newtons.

Table 18: Dominant and NonDominant Peak Sagittal and Frontal Plane Moments Mean (SD)

Variable		0%	15%	30%	Load	D vs ND	Interaction
Peak Knee Extension Moment (N·m/kg)	D	0.55 (0.24)	0.66 (0.30)	0.80 (0.35)	***p* < .001**	***p* = .005**	p = .170
	ND	0.43 (0.24)	0.51 (0.23)	0.64 (0.34)	**η_p^2= .656**	**η_p^2= .294**	η_p^2= .074
Peak Dorsiflexion Moment (N·m/kg)	D	0.29 (0.07)	0.31 (0.08)	0.33 (0.09)	***p* < .001**	***p* = .008**	p = .474
	ND	0.24 (0.08)	0.25 (0.08)	0.27 (0.09)	**η_p^2 = .371**	**η_p^2 = .333**	η_p^2 = .032
Peak Hip Abduction Moment (N·m/kg)	D	-0.88 (0.15)	-1.00 (0.19)	-1.06 (0.20)	***p* < .001**	***p* = .002**	p = .098
	ND	-1.01 (0.12)	-1.12 (0.14)	-1.22 (0.17)	**η_p^2 = .835**	**η_p^2 = .360**	η_p^2 = .096
Peak Knee Abduction Moment (N·m/kg)	D	-0.43 (0.16)	-0.49 (0.19)	-0.52 (0.20)	***p* < .001**	***p* = .005**	p = .286
	ND	-0.54 (0.12)	-0.59 (0.14)	-0.64 (0.17)	**η_p^2 = .712**	**η_p^2 = .299**	η_p^2 = .052
Knee Extension Angular Impulse (N·m·s/kg)	D	0.07 (0.03)	0.08 (0.04)	0.10 (0.05)	***p* < .001**	***p* = .011**	p = .442
	ND	0.05 (0.03)	0.06 (0.04)	0.08 (0.05)	**η_p^2= .615**	**η_p^2= .248**	η_p^2= .035
Knee Abduction Angular Impulse (N·m·s/kg)	D	-0.13 (0.06)	-0.15 (0.08)	-0.16 (0.08)	***p* < .001**	***p* = .003**	p = .072
	ND	-0.16 (0.07)	-0.20 (0.06)	-0.22 (0.07)	**η_p^2 = .556**	**η_p^2 = .320**	η_p^2 = .127
Hip Abduction Angular Impulse (N·m·s/kg)	D	-0.32 (0.05)	-0.36 (0.07)	-0.40 (0.08)	***p* < .001**	***p* = .001**	p = .114
	ND	-0.37 (0.06)	-0.42 (0.05)	-0.46 (0.06)	**η_p^2 = .836**	**η_p^2 = .373**	η_p^2 = .096

Averages (SD) for first peak knee extension and abduction moment, peak dorsiflexion moment, peak hip abduction moment. And knee extension and abduction angular impulse, along with hip abduction angular impulse 2x3 repeated measures ANOVA results for main effects and interactions.

0% load is walking with an unloaded weighted vest, 15% load is walking with the weighted vest loaded at 15% bodyweight, and 30% load is walking with the weighted vest loaded at 30% bodyweight.

η_p^2: Partial eta. Squared. N: Newtons. s: seconds. m: meters kg: kilograms

N: Newtons. m: meters. kg: kilograms

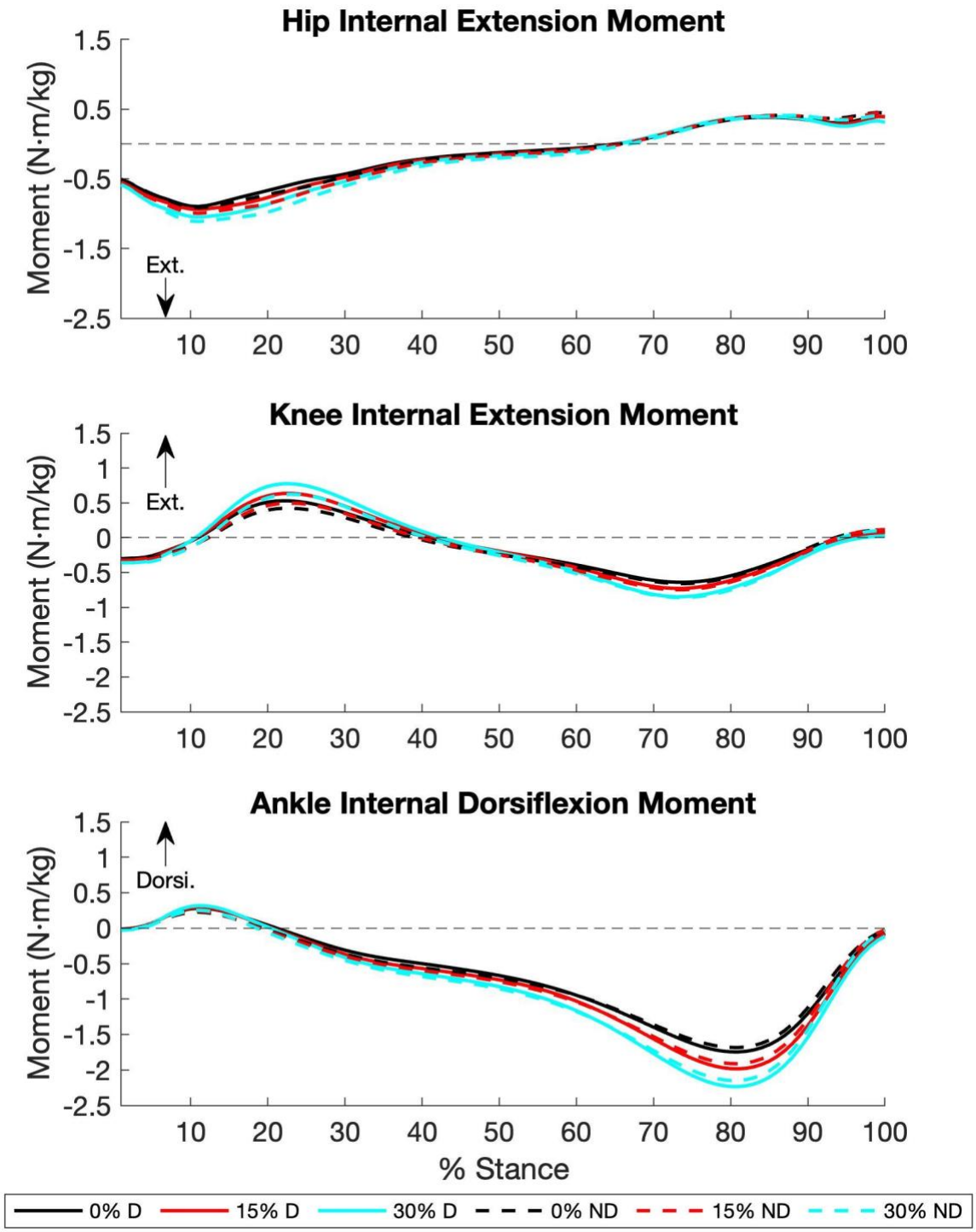

Figure 35: Time Series D vs ND Sagittal Moments Across Loading Conditions
Dominant and nondominant peak internal hip extension moment, peak internal knee extension moment, and peak ankle internal dorsiflexion moments over percent stance during load carriage of 0% BW, 15% BW, and 30% BW. Lines represent the means across all participants.
N: Newtons. m: meters. kg: kilograms

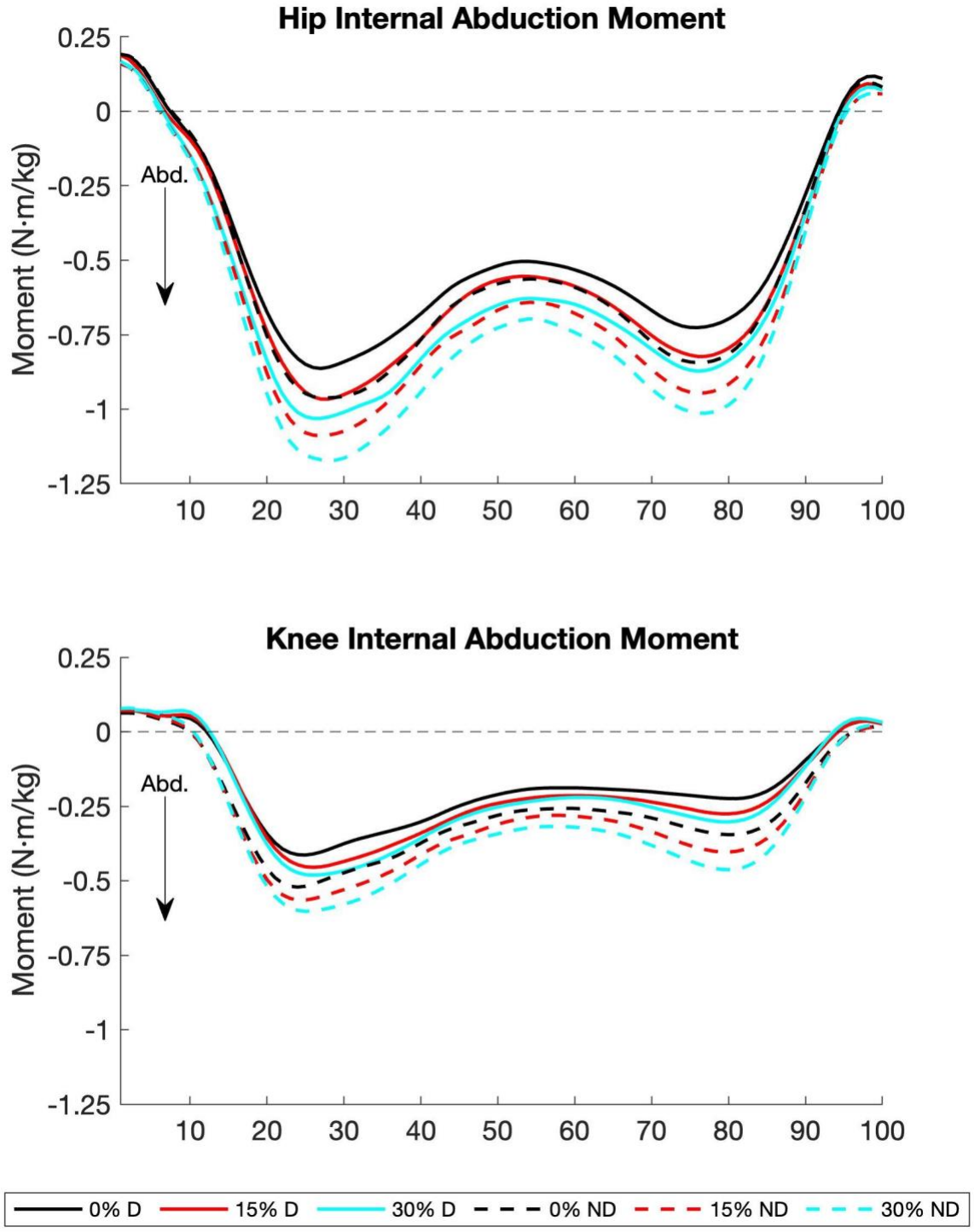

Figure 36: Time Series D vs ND Frontal Moments Across Loading Conditions
Dominant and nondominant peak internal hip abduction moment, peak internal abduction extension moment, and peak ankle internal dorsiflexion moments over percent stance during load carriage of 0% BW, 15% BW, and 30% BW. Lines represent the means across all participants.

Table 19: D vs. ND Peak Hamstrings Force Across Load Interaction, Mean (SD)

Variable		0%	15%	30%	*p* η_p^2
Peak Knee Power *K1S* (W/kg)	D	-0.72 (0.40)	-0.87 (0.52)	-1.09 (0.59)	**< .001** **.618**
	ND	-0.53 (0.31)	-0.59 (0.38)	-0.75 (0.39)	**< .001** **.520**
					Interaction
	p	**.030**	**.003**	**.001**	**.002**
	d	**.473**	**.671**	**.752**	**.240**

Averages (SD) for first peak total hamstrings force. 2x3 repeated measures ANOVA results for main effects and interactions. Two-tailed paired samples t-tests results for dominant vs nondominant peak hamstrings force at each loading condition, and one-way repeated measures ANOVA results for dominant peak hamstrings force across each loading condition and nondominant peak hamstrings force across each loading condition.
0% load is walking with an unloaded weighted vest, 15% load is walking with the weighted vest loaded at 15% bodyweight, and 30% load is walking with the weighted vest loaded at 30% bodyweight.
η_p^2: Partial eta. Squared. *d*: Cohen's d. N: Newtons.

Table 20: Dominant and NonDominant Sagittal Plane Knee Work Mean (SD)

Variable		0%	15%	30%	Load	D vs ND	Interaction
Negative Knee Work (J/kg)	D	-0.06 (0.02)	-0.07 (0.03)	-0.09 (0.03)	***p* < .001**	*p* = .767	*p* = .930
	ND	-0.06 (0.03)	-0.07 (0.02)	-0.09 (0.03)	**η_p^2 = .617**	η_p^2 = .004	η_p^2 = .001
Positive Knee Work (J/kg)	D	0.12 (0.03)	0.14 (0.04)	0.18 (0.05)	***p* < .001**	***p* = .048**	*p* = .497
	ND	0.11 (0.04)	0.13 (0.04)	0.16 (0.05)	**η_p^2= .771**	**η_p^2= .160**	η_p^2= .030

Averages (SD) for first peak and impulses of the tibiofemoral joint. 2x3 repeated measures ANOVA results for main effects and interactions.
0% load is walking with an unloaded weighted vest, 15% load is walking with the weighted vest loaded at 15% bodyweight, and 30% load is walking with the weighted vest loaded at 30% bodyweight.
η_p^2: Partial eta. Squared. N: Newtons. s: seconds. m: meters kg: kilograms

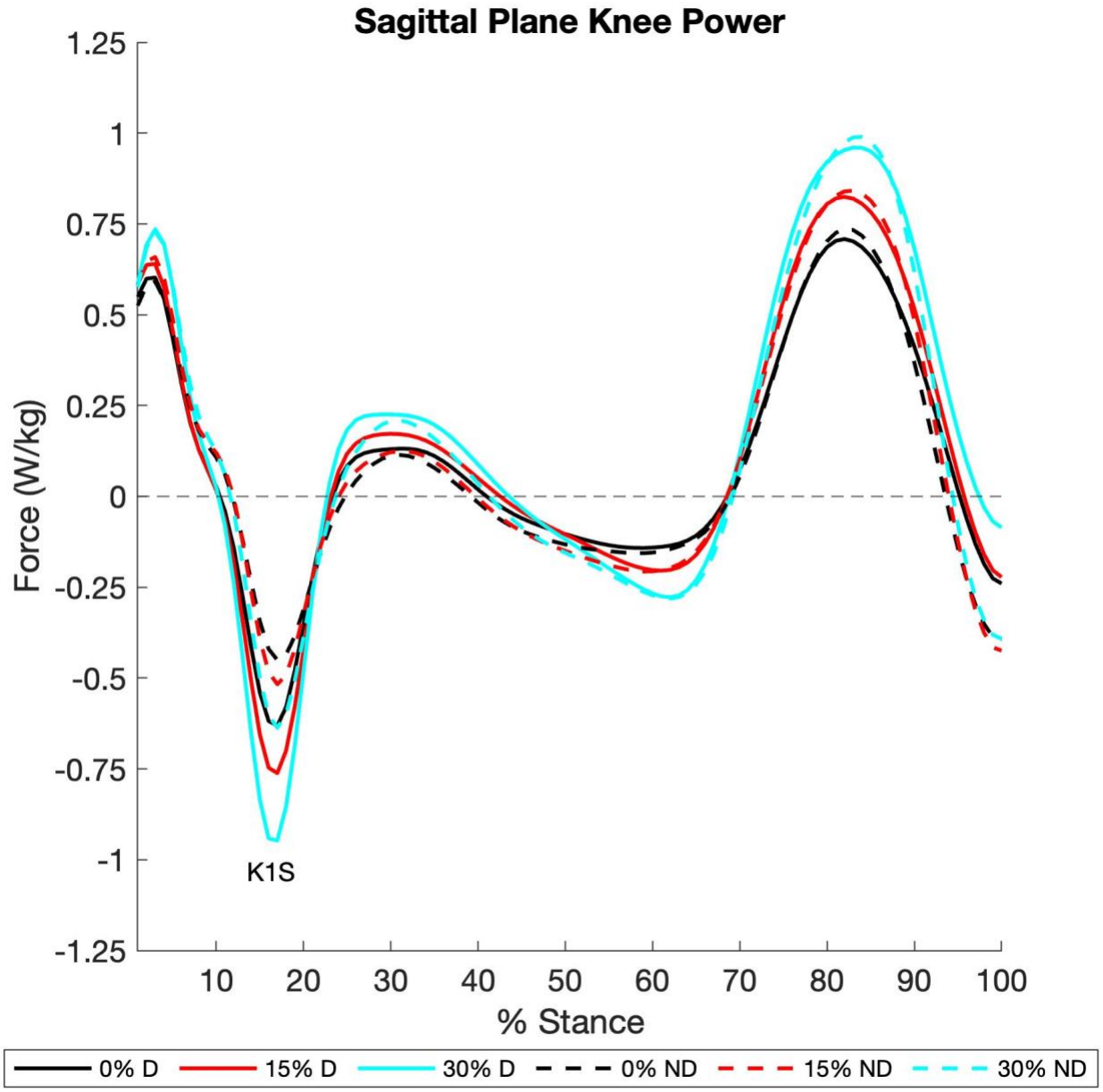

Figure 37: D vs ND Sagittal Plane Knee Power Across Loading Conditions
Dominant and nondominant sagittal plane knee power over percent stance during load carriage of 0% BW, 15% BW, and 30% BW. Bold line represents the mean across all participants.